Virtual Basophils

Oral Alpan, M.D.
Amerimmune

Disclosures

None

Learning
OBJECTIVES

Understanding:

1) functional immune tests as biosensors
2) Assay development
3) Artificial intelligence in developing virtual cells

Hypo-allergenic Infant formula approval in the United States

- **Phase 1: Testing on 30-40 infants to assess safety: that it does not create allergic reactions: 1-2 years**
- **Phase 2: Testing in 200-300 babies to assess growth and development: 2-3 years.**

What can flow cytometry tell you about a cell?

- Size (Surface area)
- Granularity (Cell Internal Complexity)
- Fluorescence (Relative intensity, 8 colors)

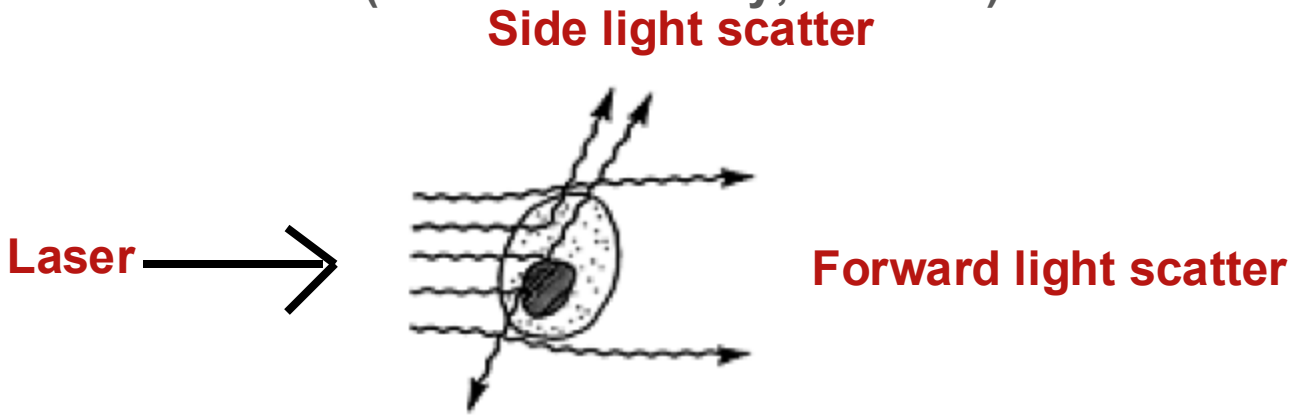

Identifying immune disease in a patient

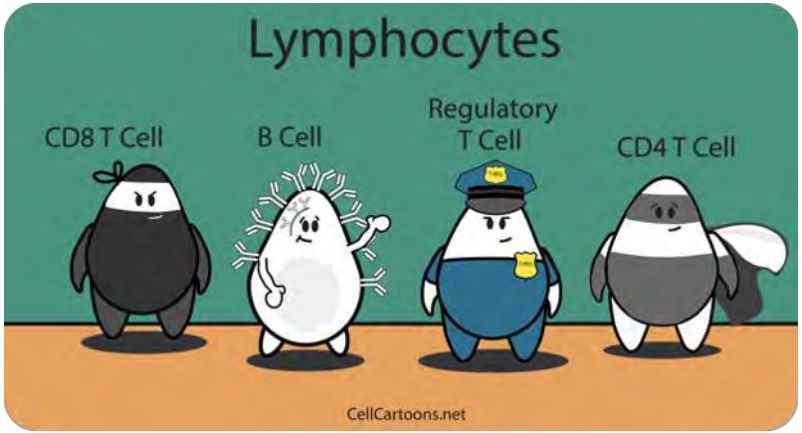

What we look at on the cells

- Presences of lymphocyte populations and sub-populations
- Cell Activation markers
- Level of maturation (naïve vs. memory cells)
- Functional characteristics (e.g. basophil activation test)

BAT is a functional assay

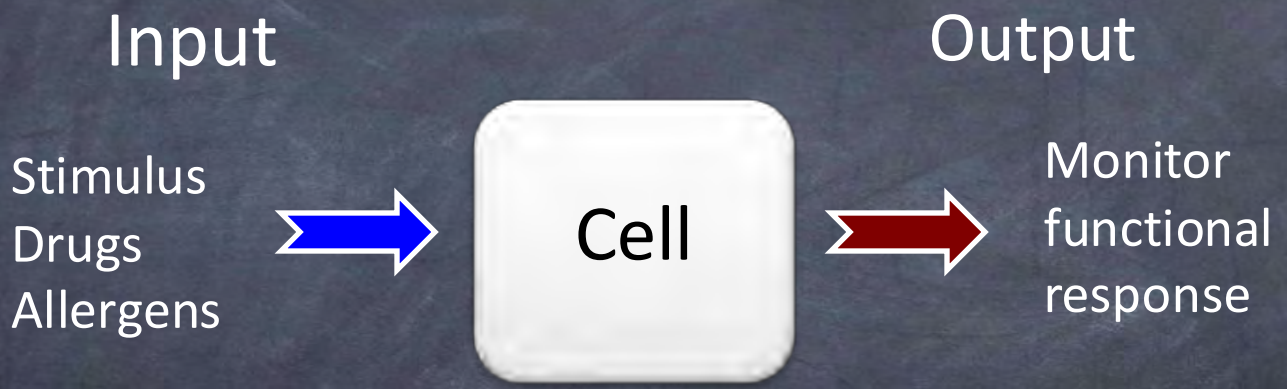

Input/output assay always more valuable than static assays in most situations

Monitoring human basophil activation via CD63 monoclonal antibody 435

Edward F. Knol, MSc,* Frederik P. J. Mul,* Hans Jansen,**
Jero Calafat, PhD, and Dirk Roos, PhD*** *Amsterdam, The Netherlands*

On activation of human basophilic granulocytes with anti-IgE or with the chemotactic peptide, formyl-methionyl-leucyl-phenylalanine, the expression of the CD63 antigen on the cell surface, detected by monoclonal antibody (MAb) 435, increased up to 100-fold. The kinetics of CD63 up regulation and histamine release were identical, and a strong correlation was found between percentage of MAb 435-binding basophils and extent of histamine release. Immunoelectronmicroscopy demonstrated that the epitope for MAb 435 in resting basophils is located on the basophilic granule membrane. After basophil activation, MAb 435 bound to the exterior of the plasma membrane. Experiments with various doses of anti-IgE demonstrated that the binding of MAb 435 to basophilic granulocytes follows an all-or-nothing–like response per cell. Basophils either do not bind the MAb at all, or they bind a maximal amount of the MAb. We also measured the up regulation of the CD11/CD18 leukocyte adhesion complex. Here, too, we noted an increase in cell-surface exposure of all subunits after activation. This increase was not as strong as increase found with MAb 435. Thus, MAb 435 is an interesting new tool for investigating the activation of human basophils, in addition to the measurement of mediator release. This MAb may be useful for the detection of basophil activation in vivo. (J ALLERGY CLIN IMMUNOL 1991;88:328-38.)

Key words: *Basophils, degranulation, activation, histamine release, CD63, CD18, CD11a,b,c, up regulation*

CD63 up-regulation

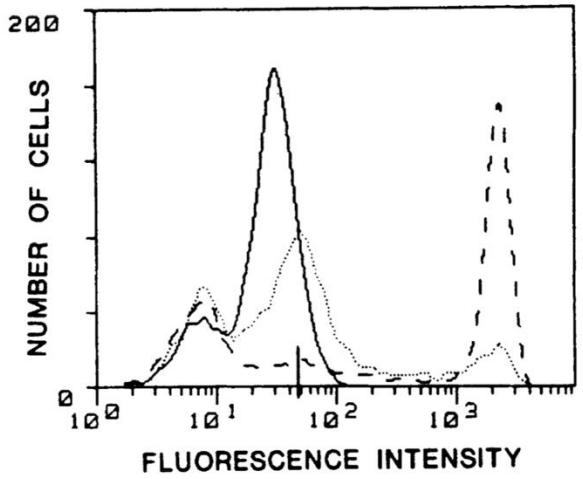

FIG. 1. Binding of MAb 435 to resting and anti-IgE–stimulated basophils. Stimulation was performed for 30 minutes at 37° C. After stimulation, the basophils were incubated with MAb 435 and FITC-labeled GAMG Ab. Binding was analyzed by flow cytofluorometry (—), resting basophils (. . .), basophils stimulated with 10 ng of anti-IgE per milliliter (resulting in 14% HR) (– – –), and basophils stimulated with 100 ng of anti-IgE per milliliter (resulting in 70% HR). Fluorescence intensity is in arbitrary units. Ninety-nine percent of the basophils demonstrated a background fluorescence with an irrelevant Ab <50 arbitrary units, indicated by the *vertical bar.* Cells with a fluorescence between 2 and 20 arbitrary units are contaminating lymphocytes. Representative experiment of six performed.

Histamine release

fmlp

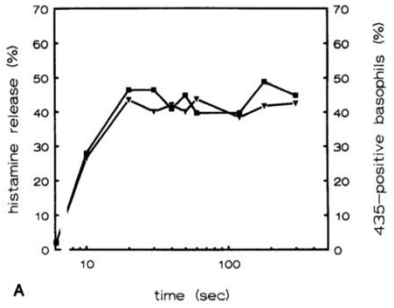

α-IgE

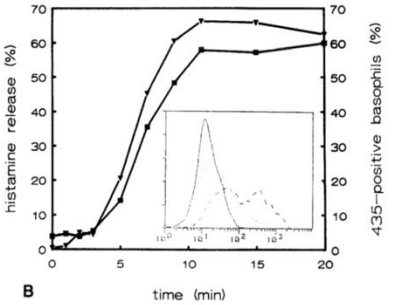

FIG. 3. Time course of HR and MAb 435 binding induced by anti-IgE or FMLP. **A,** Basophilic granulocytes were stimulated with 1 μmol/L of FMLP **B,** Basophilic granulocytes stimulated with 100 ng of anti-IgE per milliliter. After the indicated intervals, HR (■——■) and MAb 435 binding (▼——▼) were analyzed in the same samples. Histamine was measured in the cell-free supernatant and was expressed as percentage of histamine present in the cells at $t = 0$. MAb 435 binding was performed as illustrated in Fig. 1 on basophils immediately fixed with 0.5% paraformaldehyde. MAb 435 positivity was determined as the number of basophils that demonstrated more binding of MAb 435 compared to the resting basophils. **Inset, B,** MAb 435 binding to resting basophils (——), to basophils after a 5-minute stimulation with anti-IgE (●●●●), or to basophils after a 7-minute stimulation with anti-IgE (– – –). Representative experiment of seven performed.

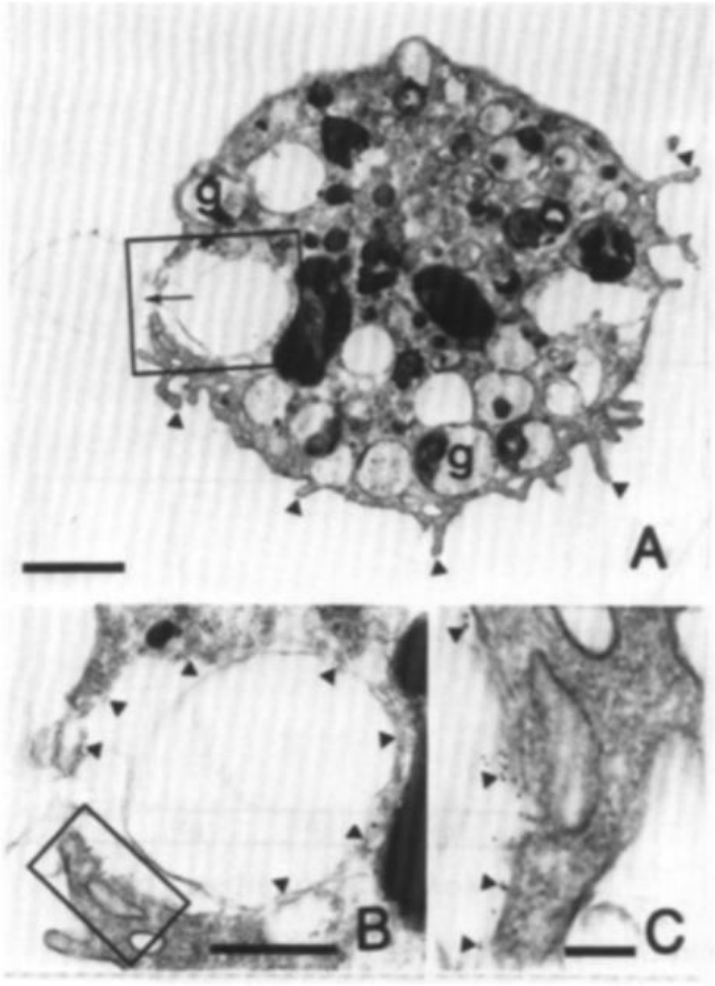
g
g
A
B
C

Basophil Activation Test Methodology

The Basophil Activation Test (BAT) is a laboratory test using flow cytometry to detect the presence of certain markers on the surface of basophils upon exposure to allergens. BAT is technically and clinically validated, in clinical use in the US, and extensively published for over 30 years. (Journal of Immunological Methods 2025; 537:113815)

Blood sample drawn from a patient

Allergen added to sample and incubated for 30 minutes

Flow cytometry used to measure the degree of activation of basophils

- ✓ Quantifies basophil degranulation (CD63) and activation(CD203c) upon exposure to allergens. (JAllergy Clin Immunol 2025;155:275-85)
- ✓ No infant exposure; non-invasive and safe for high-risk patients, no risk of severe reaction or anaphylaxis.
- ✓ High specificity while retaining sensitivity. (REF)
- ✓ More precise than allergen-specific skin prick and oral food challenges, PPV of 91% and NPV of 94%. (Clin Exp Allergy. 2019 Mar;49(3):350-356.)
- ✓ Not affected by antihistamines or steroids, allowing broader patient use.
- ✓ History of use for demonstration of hypoallergenicity in hydrolyzed formulas. (Front Allergy. 2023 Jul 21; 4:1207924.)

BAT: Testing Formula For Allergen Content With 100% Sensitivity & Specificity

Utility	Subjects/Material	Efficacy	Sensitivity & Specificity
Testing Patients for Food Allergy		80% 	Detecting Allergy: **Sensitivity: 95%** **Specificity: 94%** 15-20% of the patients have non-reactive basophils; all comers with food allergy
Testing Formula for Allergen Content		STRATIFIED 	Detecting Allergen Content: **Sensitivity: 100%** **Specificity: 100%** 0% of patient have non-reactive basophils since highly allergic and highly basophil reactive patients' cells can be used as a milk allergen detector.

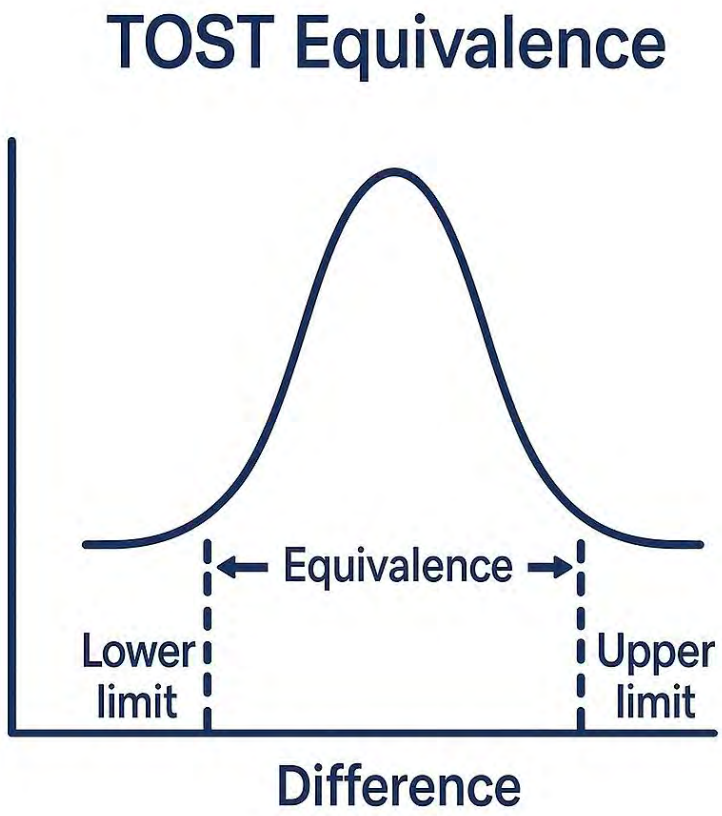

- Many samples needed
- Time consuming

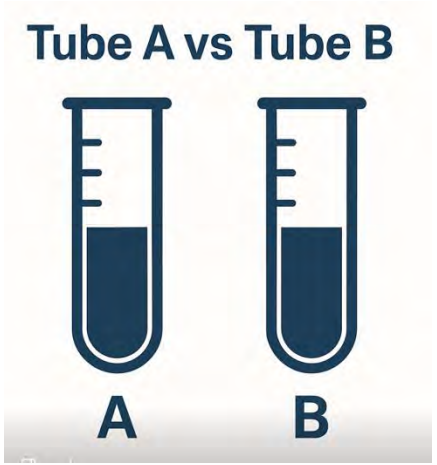

Basophil I/O Wiring Diagram

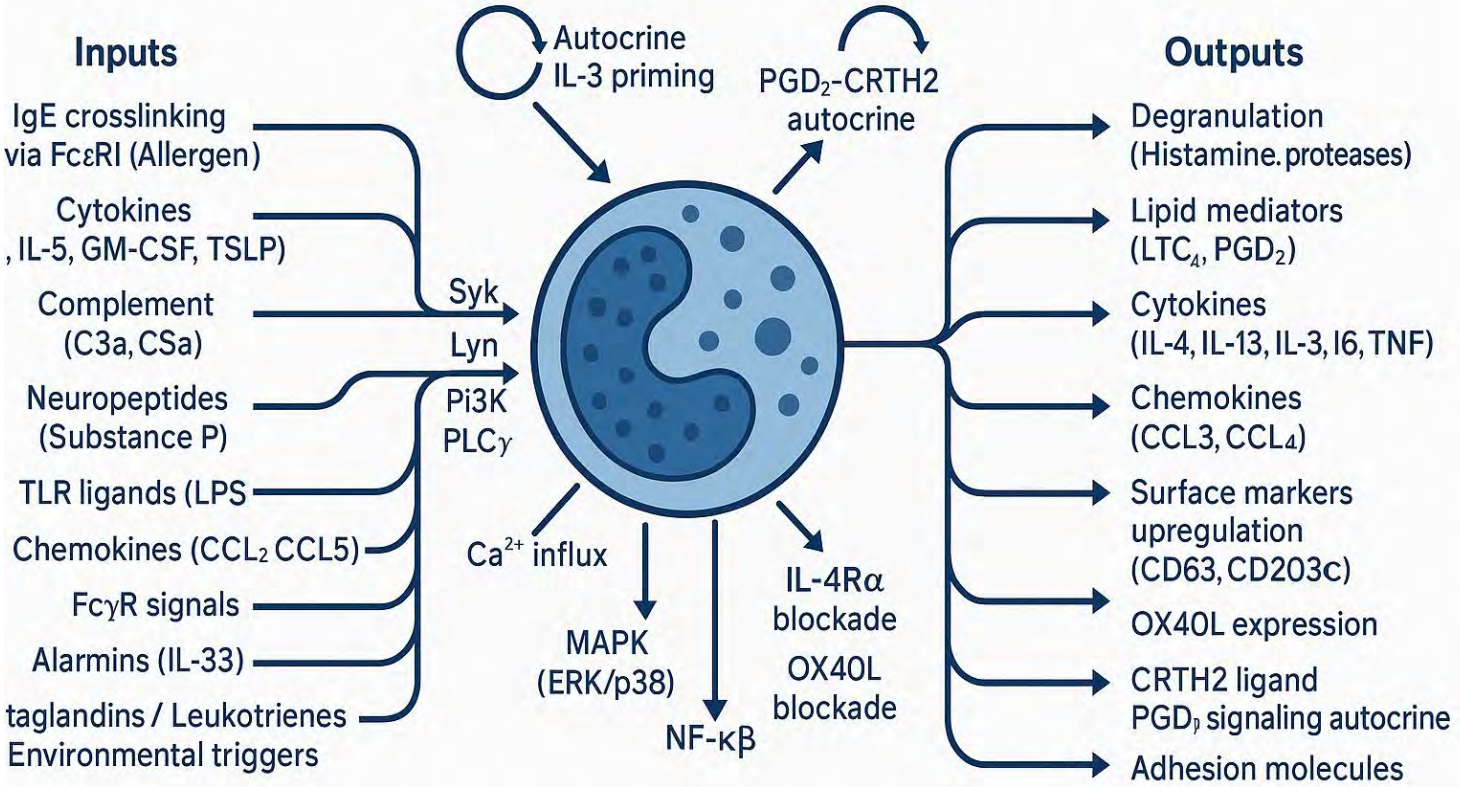

Predictive Allergen Quantification with Minimal Experiments

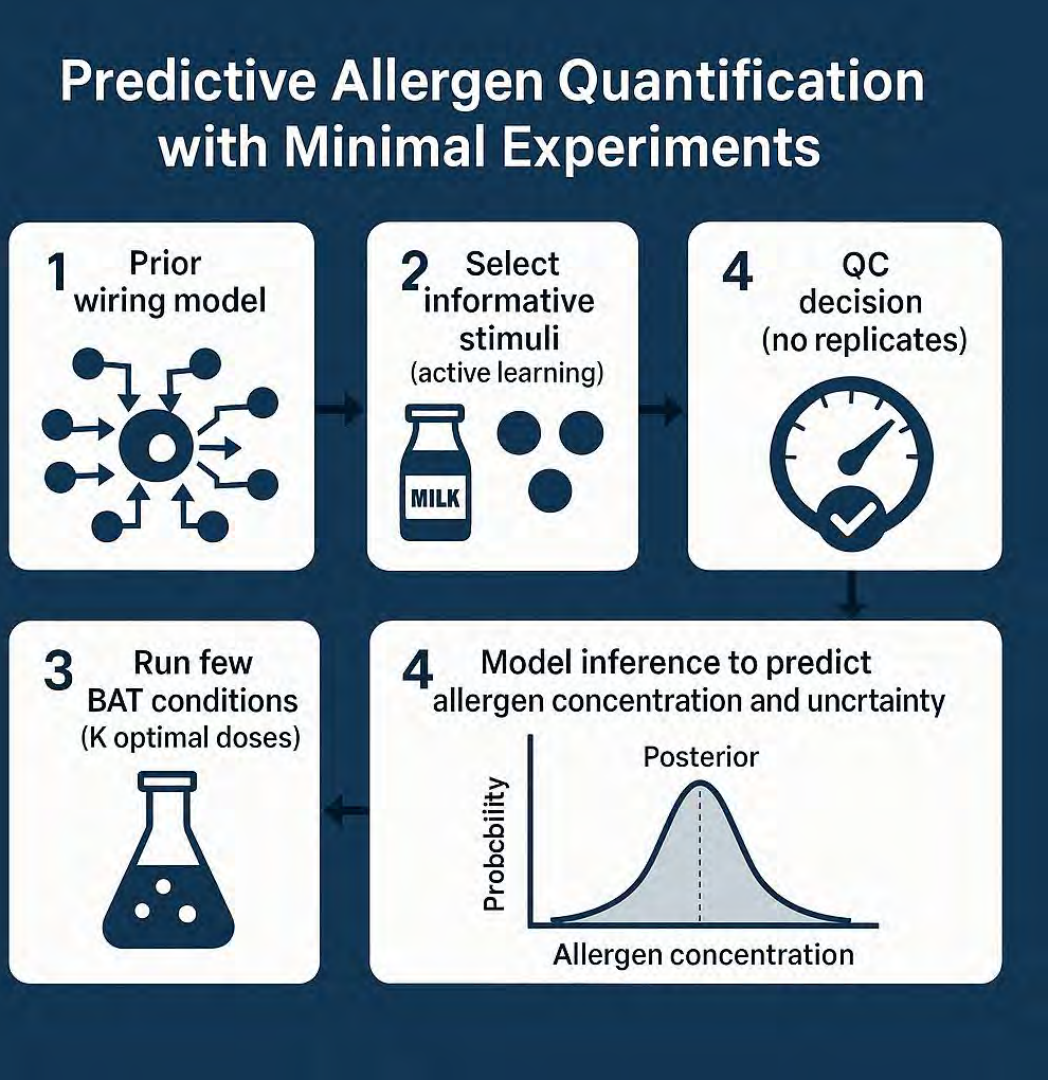

ONE-PASS ALLERGEN PREDICTION

Minimal Math

$$r = \frac{y}{n}$$

One-Pass Prediction

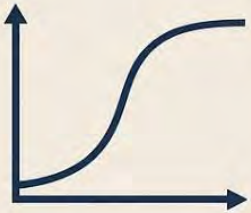

$$r = p_i(c)$$

Decision Rule

$$\Pr(c \geq c_{min}) \geq 95\%$$

PASS

Minimal Math: One-Pass Prediction

Universität Zürich[UZH]

ITINERARE
Innovative Therapies in Rare Diseases

An AI-based approach to identify lysosomal cystine export regulating mTORC1 signaling

Genetic Rare and Immune Disorder Symposium
Tysons, Virginia – November 16 and 17 2025

Svenja Keller
Institute of Physiology, University of Zurich

Disclosures

Svenja Keller has no relevant financial relationships with ineligible companies to disclose.

This continuing education activity is provided by AffinityCE, The Lysosomal and Rare Disorders Research and Treatment Center (LDRTC), and CheckRare CE. AffinityCE, CheckRare CE and LDRTC staff, planners, and reviewers, have no relevant financial relationships with ineligible companies to disclose. AffinityCE adheres to the ACCME's Standards for Integrity and Independence in Accredited Continuing Education. Any individuals in a position to control the content of a CME activity, including faculty, planners, reviewers, or others, are required to disclose all relevant financial relationships with ineligible companies. All relevant financial relationships when present, have been mitigated by the peer review of content by non-conflicted reviewers prior to the commencement of the activity.

This activity has been supported by educational grants from commercial supporters. Please see the final program for a list of all supporters.

Learning Objectives

At the conclusion of this activity, participants will be able to:

1. **Explain** how genetically engineered preclinical models of *CTNS* deficiency recapitulate early-onset phenotypes of the lysosomal storage disorder cystinosis and serve as translational platforms for therapeutic discovery and development.
2. **Describe** how artificial intelligence–driven target discovery and cross-species validation pipelines accelerate the identification of disease pathways and the development of novel therapeutic strategies.
3. **Evaluate** the biological roles of nutrient-sensing and lysosomal signaling pathways in maintaining epithelial homeostasis, and their potential as therapeutic targets in cystinosis.

Cystinosis: from Cystine Storage to Lysosome Dysfunction to Disease

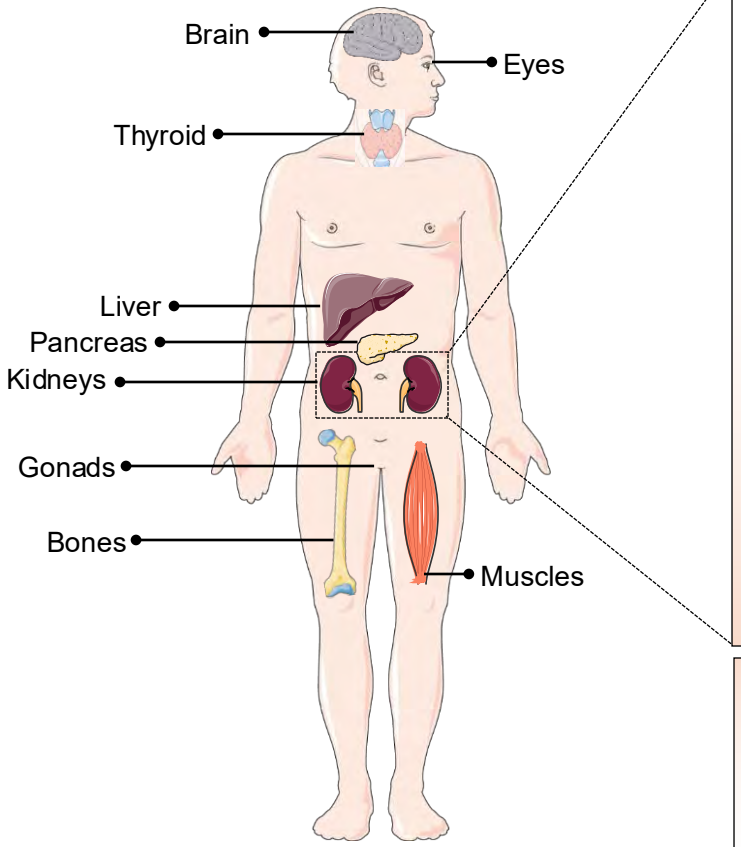

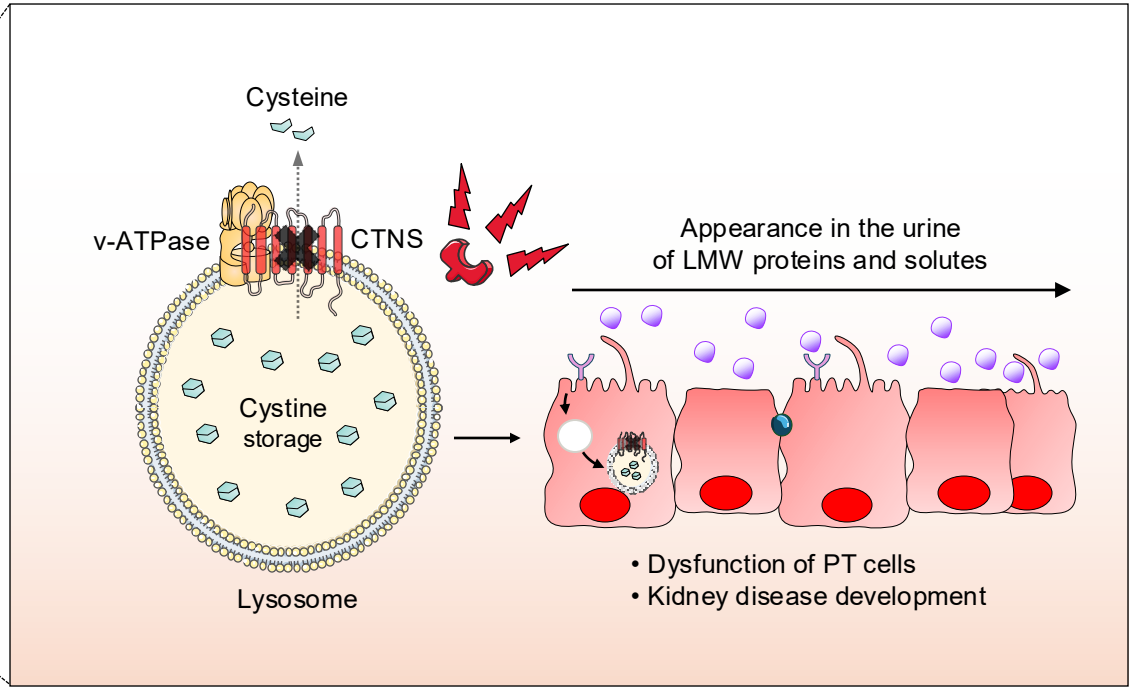

Nucleus/Lysosomes

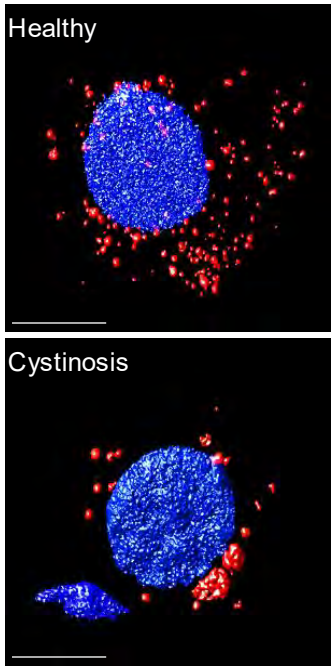

Loss-of-function mutations in the *CTNS* gene/cystinosin:

- Defective export of cystine from lysosomes
- Cystine storage in cells, organs, and tissues across the body
- Morphological and functional abnormalities of lysosomes
- Early dysfunction of PT segments and proximal tubulopathy (tubular proteinuria)
- Progressive multisystem complications (brain, eyes, liver, and muscle) later in life

Cherqui & Courtoy. Nature Reviews Nephrology, 2017

Cysteamine Treatment Neither Prevents nor Reverse Proximal Tubulopathy

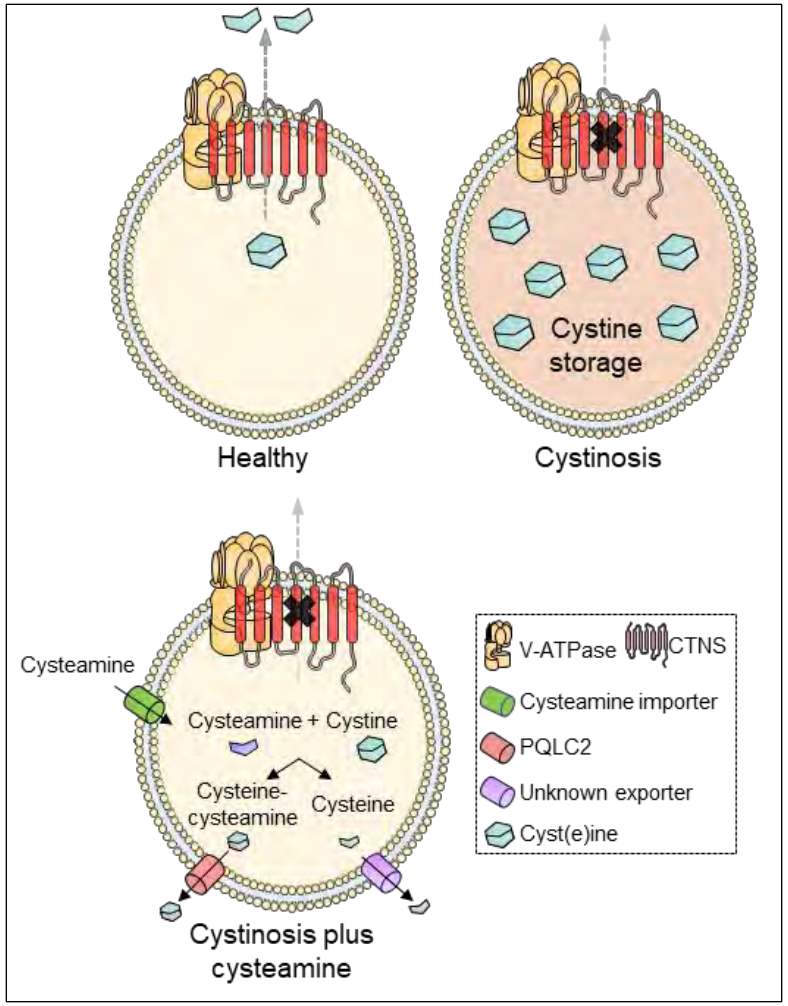

Cysteamine helps to export cystine from lysosomes

<u>Drawbacks of cysteamine</u>:

- Frequent dosing schedules
- Side effects
- Poor tolerability
- No effect on PT dysfunction

…Urgent need to develop safer, better tolerated, and effective treatments

Brodin-Sartorius et al. Kidney International, 2012

Leveraging Model Systems for Disease Biology & Therapeutic Discovery

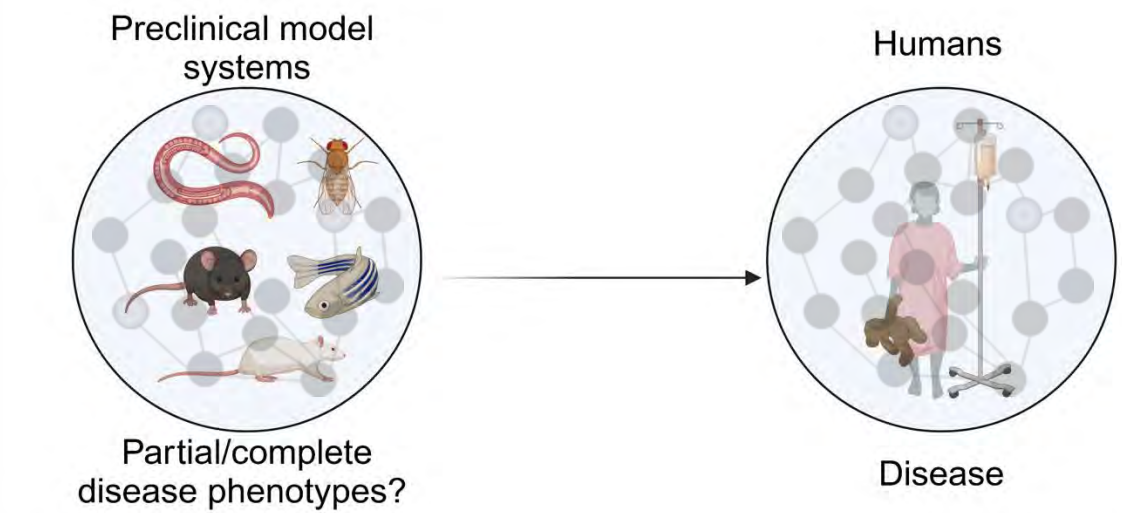

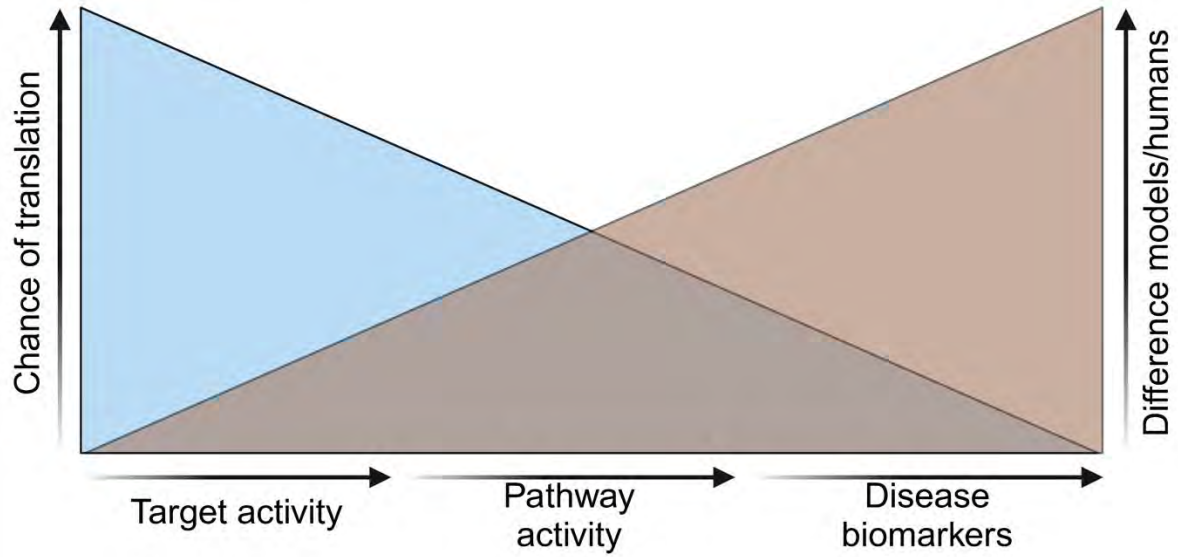

Translational Predictability:

We need preclinical model systems that closely recapitulate cystinosis phenotypes

Kimberli Scearce-Levie et al. Nature Reviews Drug Discovery, 2020

Time Course of Disease Phenotypes in the *Ctns* Knockout (KO) Mouse Model

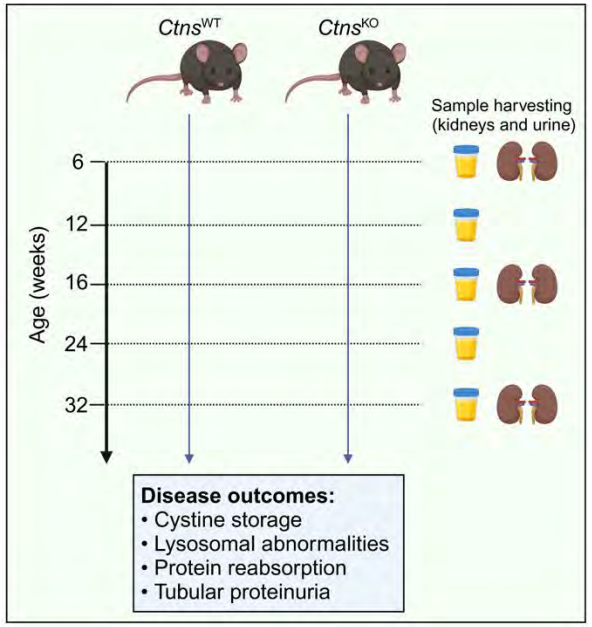

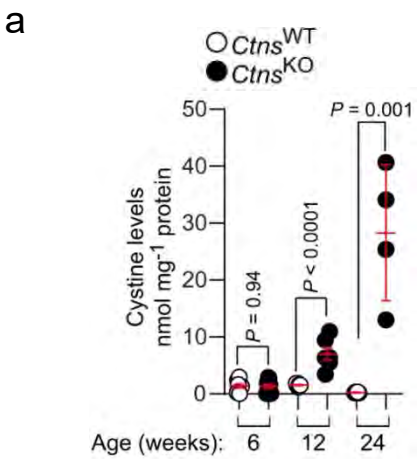

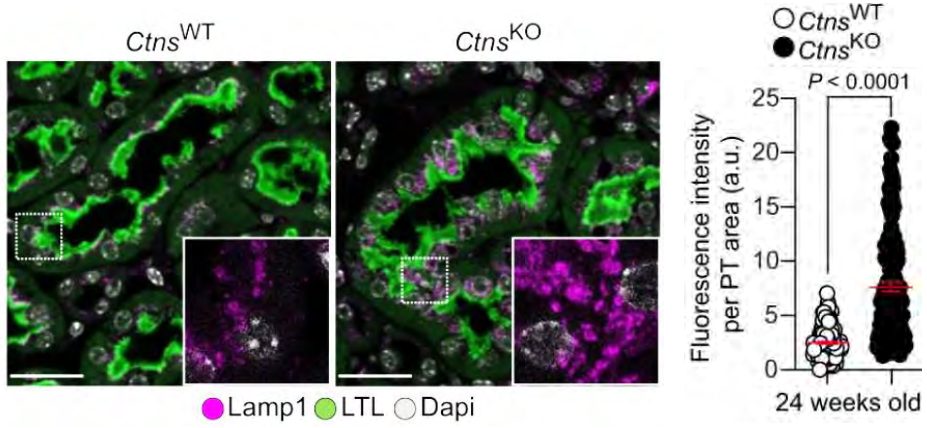

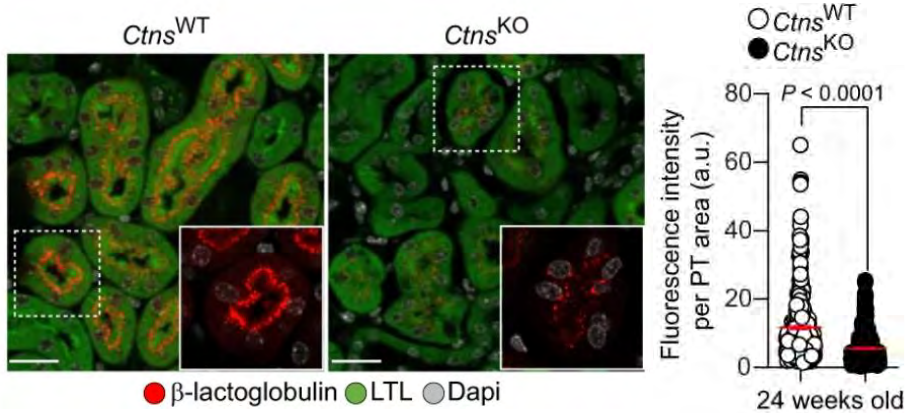

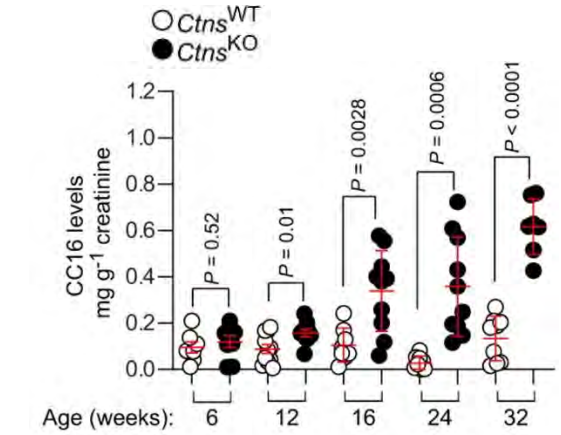

Enlarged lysosomes, defective endocytosis and proximal tubulopathy in CTNS-deficient mice

Festa et al. Nature Communications, 2018

Physiologically Relevant Cell Systems to Study Disease Mechanisms

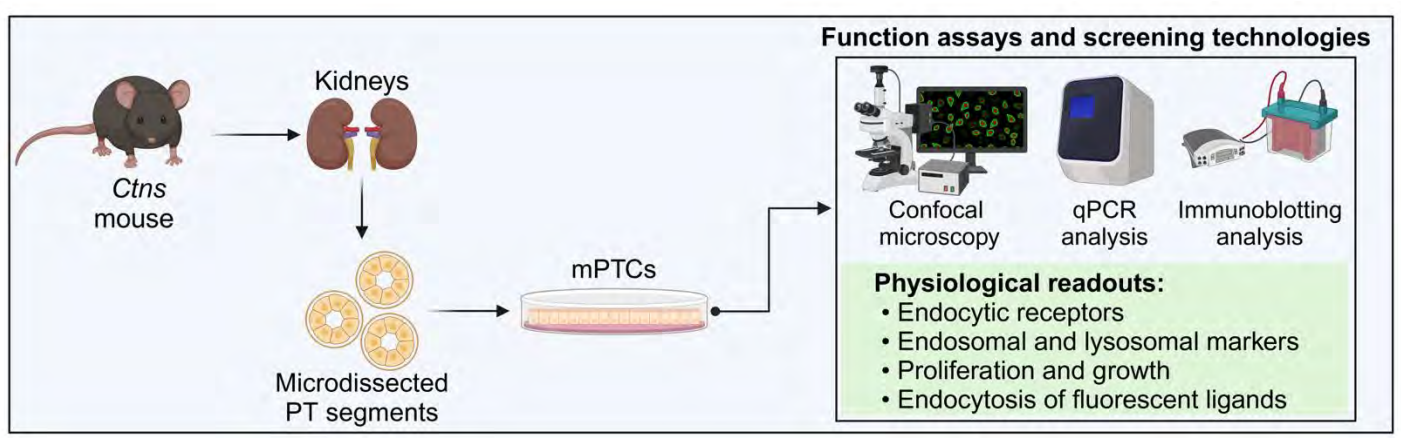

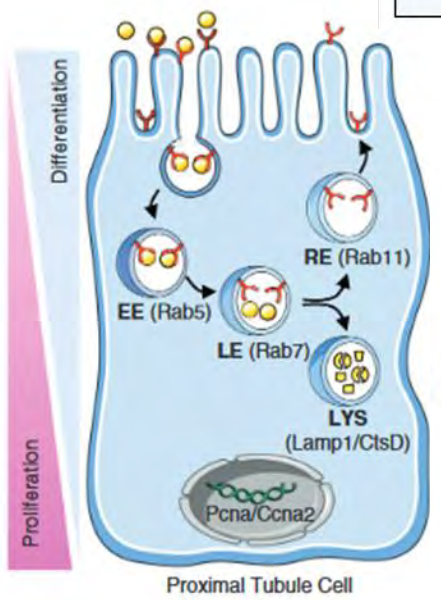

a

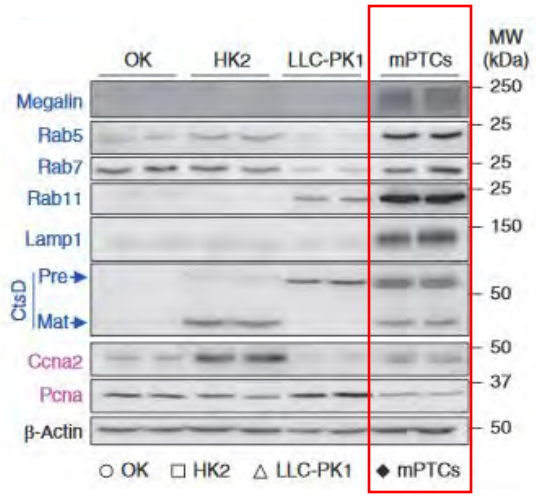

b

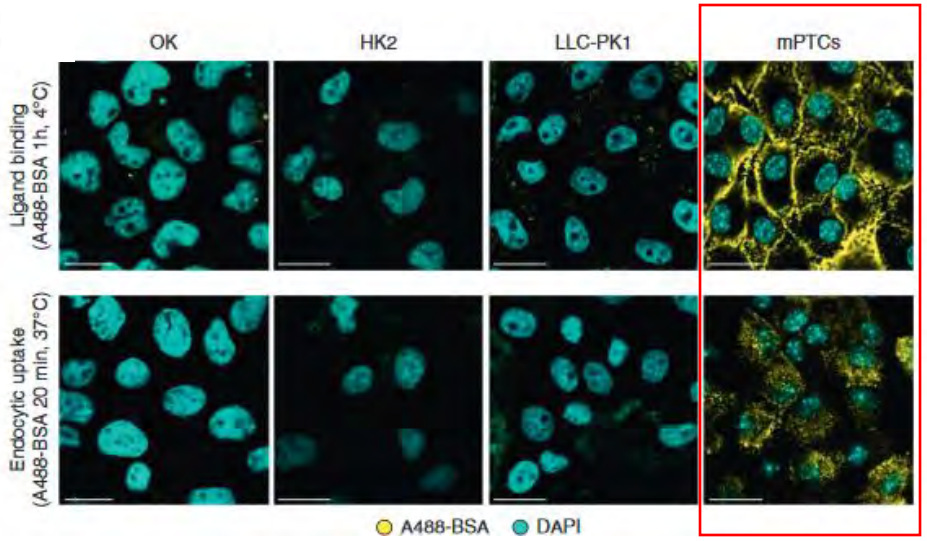

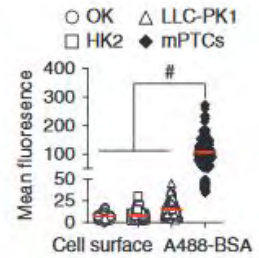

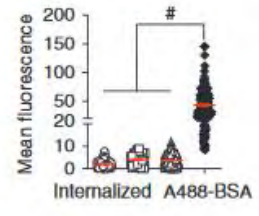

Primary PT cells adequately recapitulate physiological characteristics of their native tissue

Berquez et al. JASN, 2021

Developing Methods to Profile Lysosome Biology and Disease Pathways

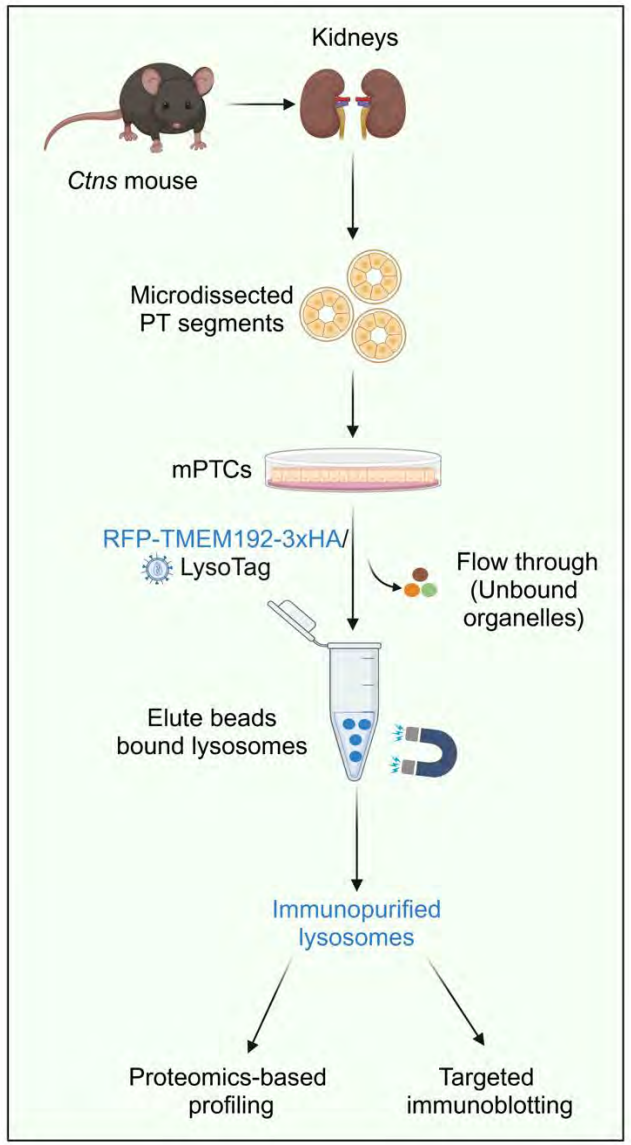

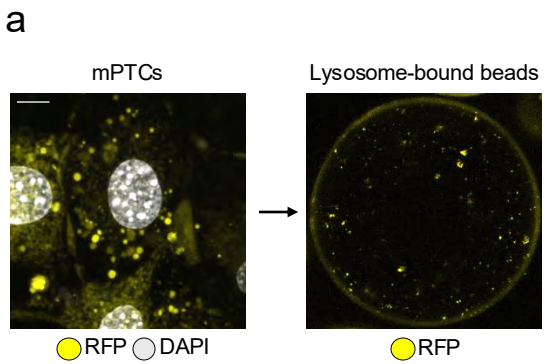

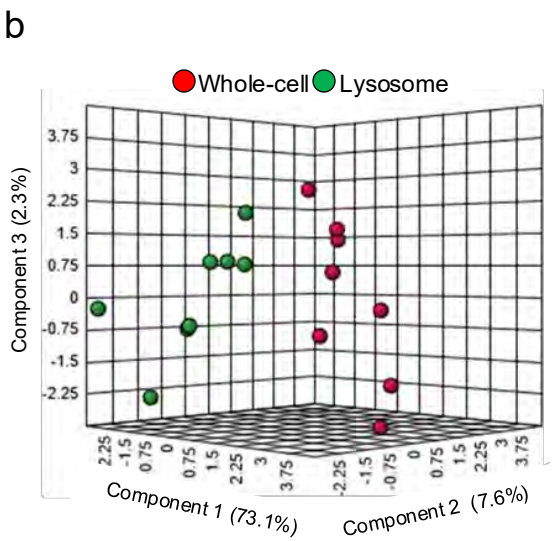

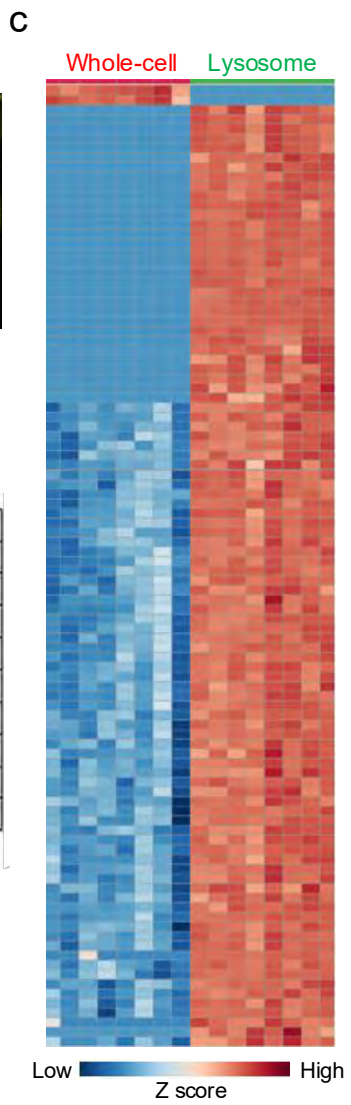

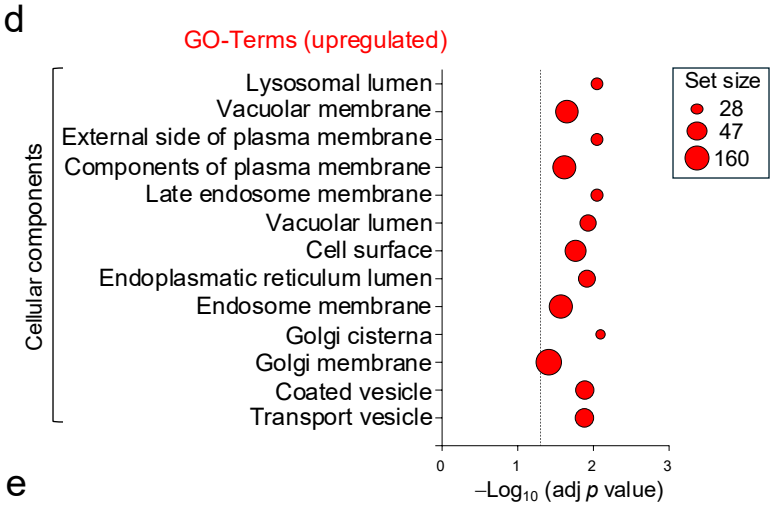

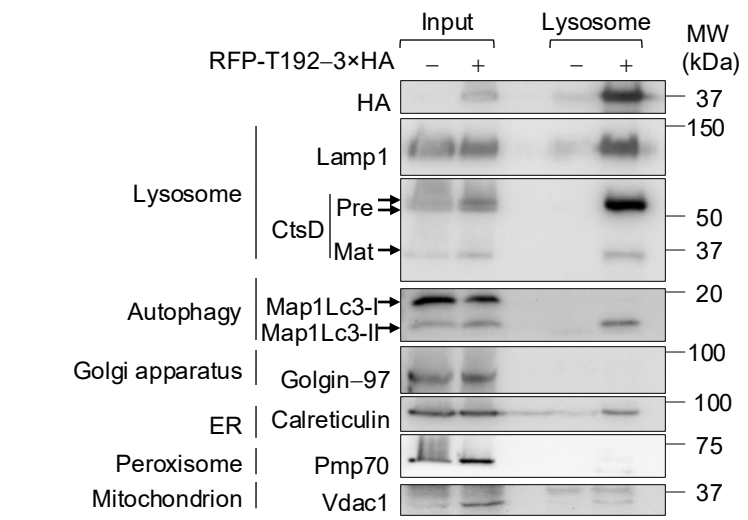

Berquez et al. Nature Communications, 2023

Dynamics and Degradative Activity of Lysosomes in Cystinosis Cells

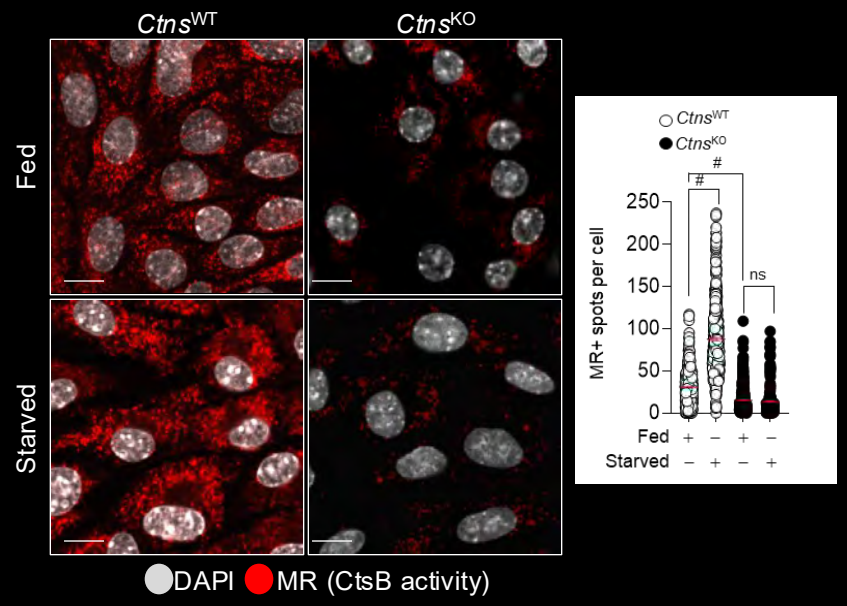

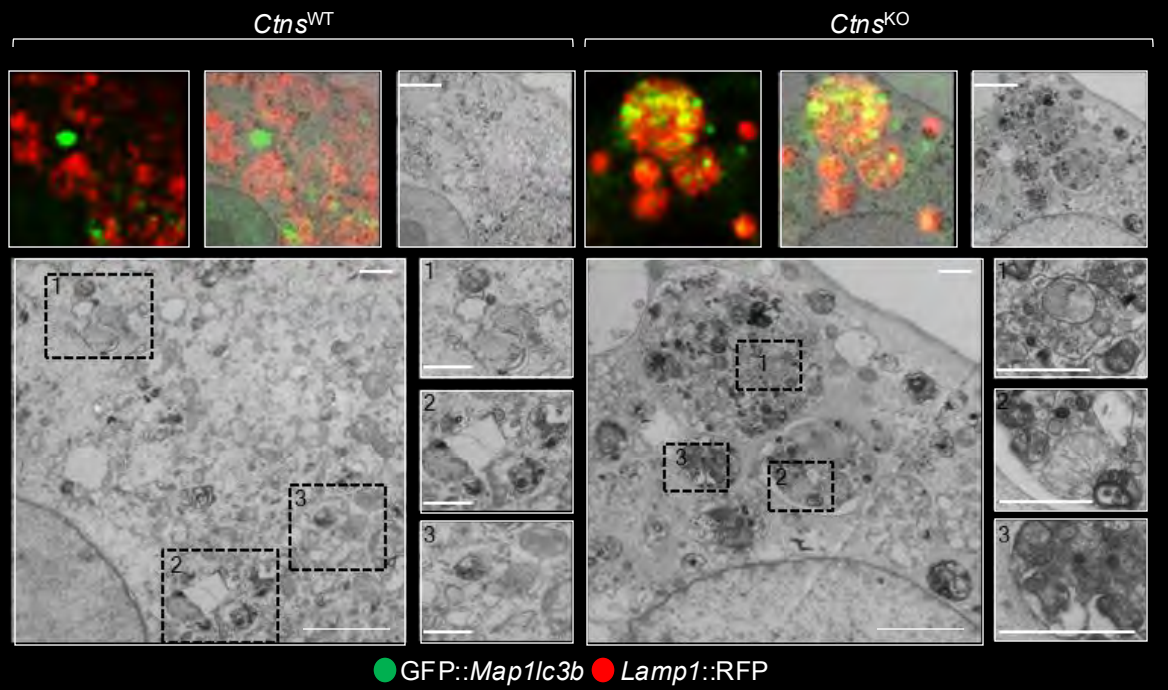

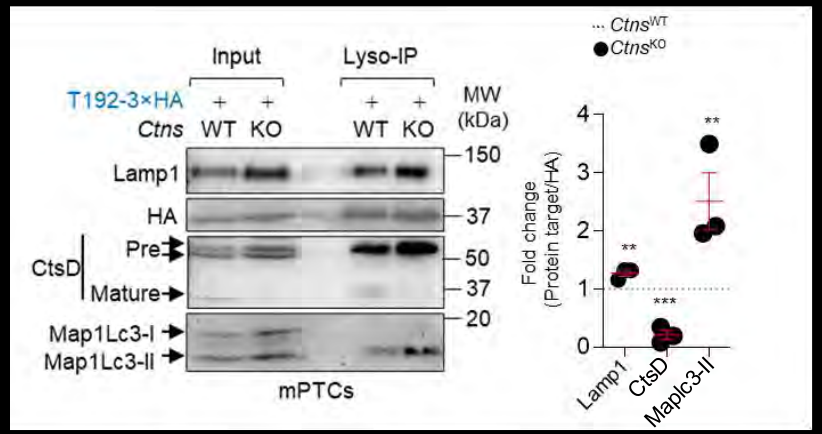

Morphologically abnormal and defective lysosomes downstream of CTNS deficiency

Festa et al. Nature Communications, 2018

CTNS Rat Model recapitulates most important Disease Hallmarks of Cystinosis

$Ctns^{WT}$
$Ctns^{KO}$

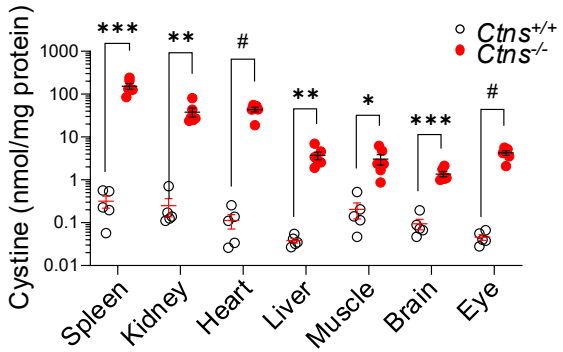

Cystine accumulation

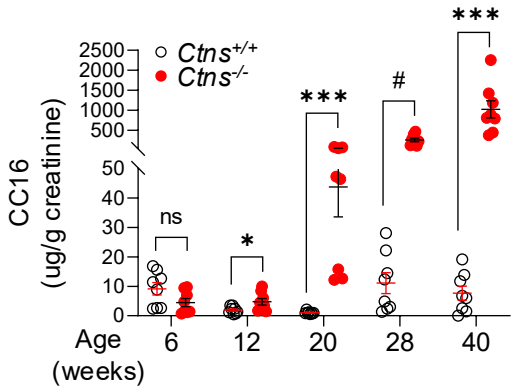

LMW proteinuria

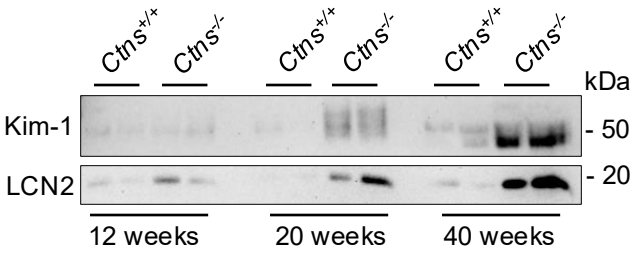

PT damage markers

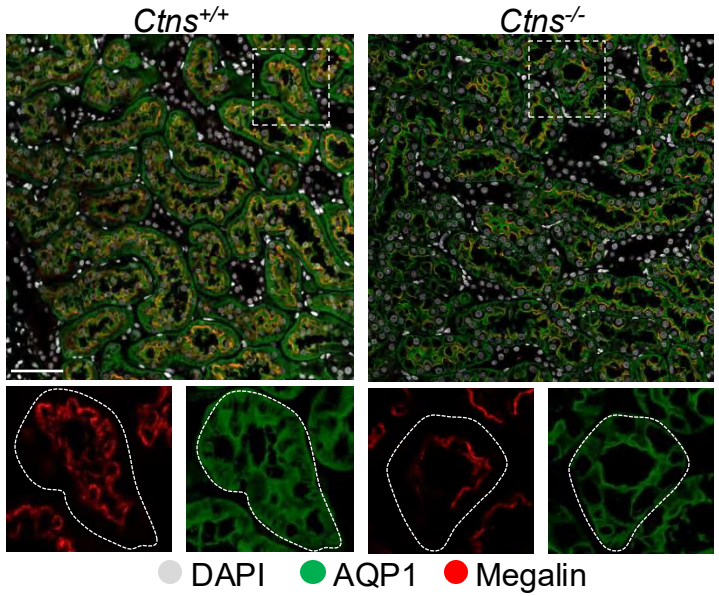

Differentiation

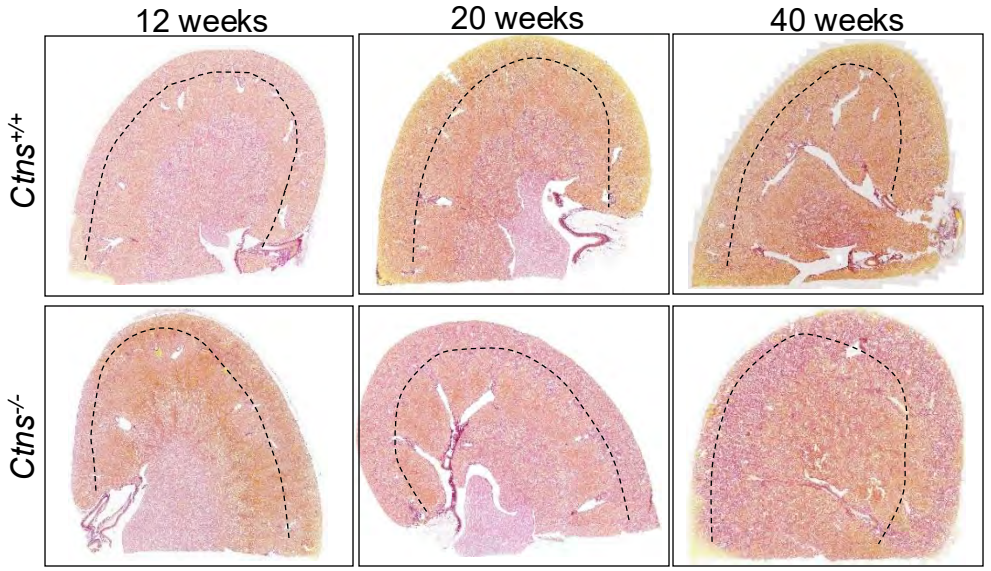

Fibrosis

Krohn *et al*, HMG, 2022

CTNS Zebrafish Line Expressing a LMW Proteinuria Biosensor

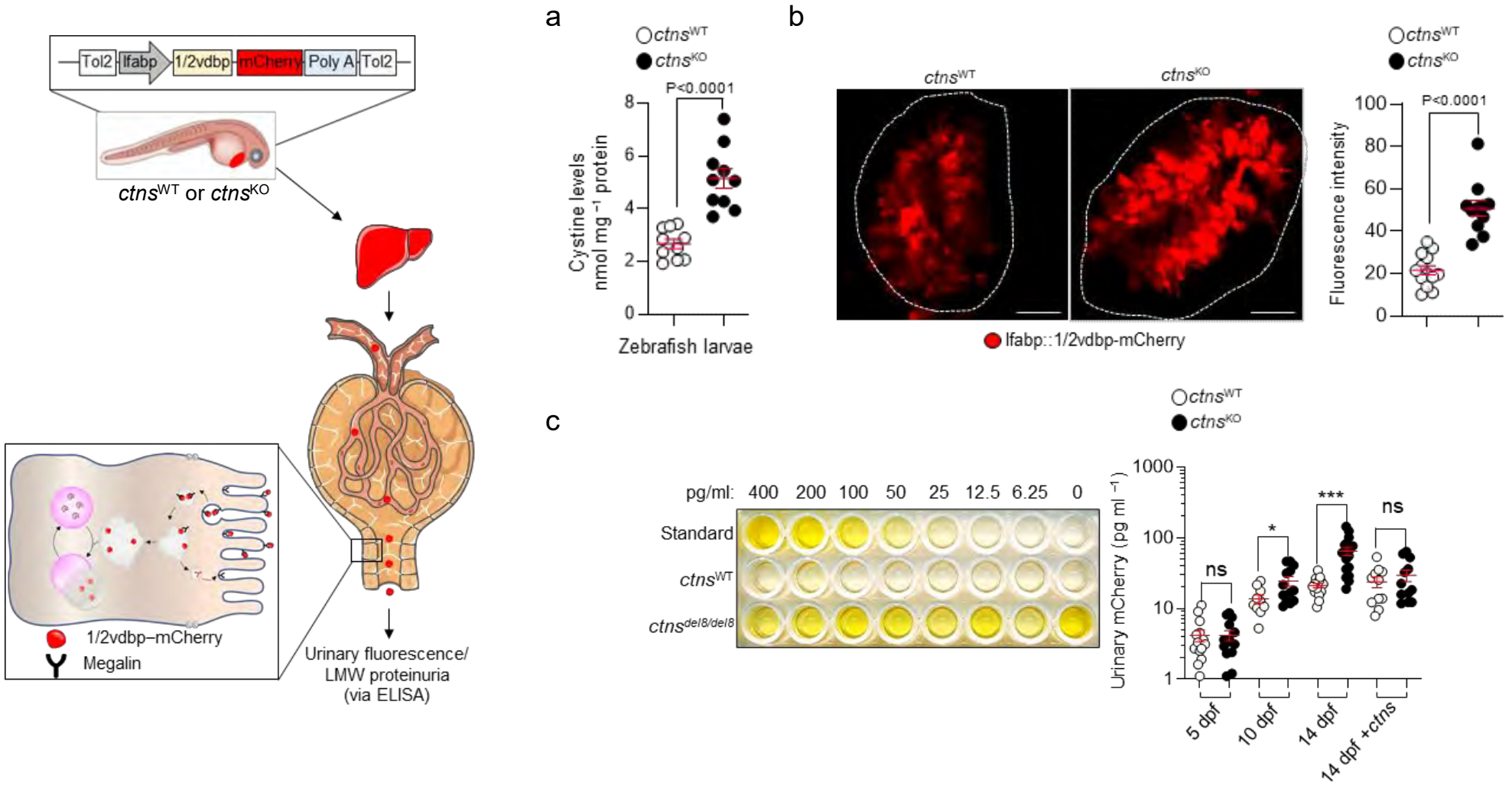

Festa et al. *Nature Communications*, 2018

Chen et al. *Kidney International*, 2020

Targeting Actionable Pathways to Restore Homeostasis in Cystinosis

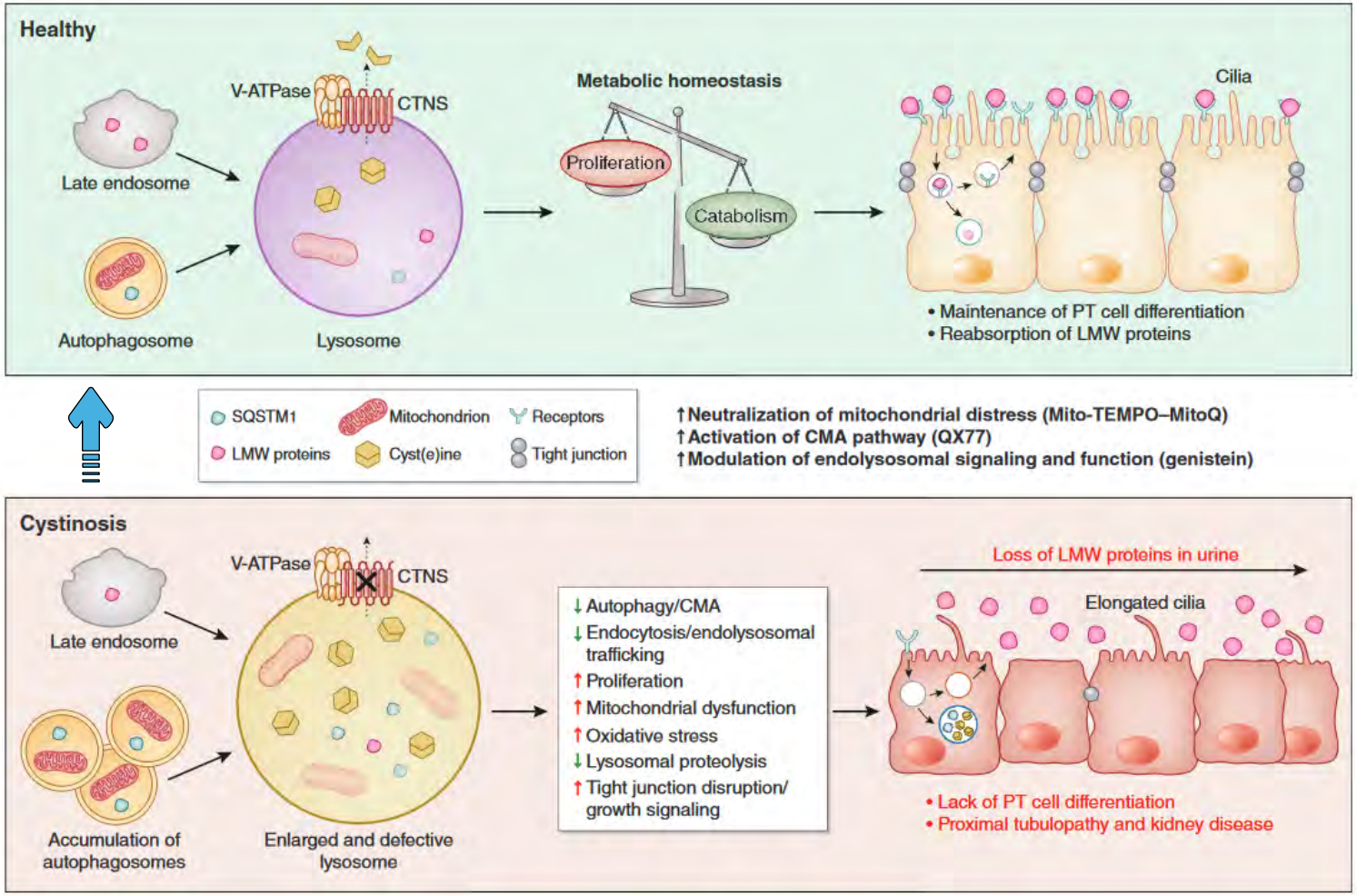

Enhancing autophagy, lysosome, or mitochondrial redox balance mitigates phenotypic changes in cystinosis cells

Keller et al. Kidney International, 2023

Leveraging Artificial Intelligence for Drug Target Discovery & Prioritization

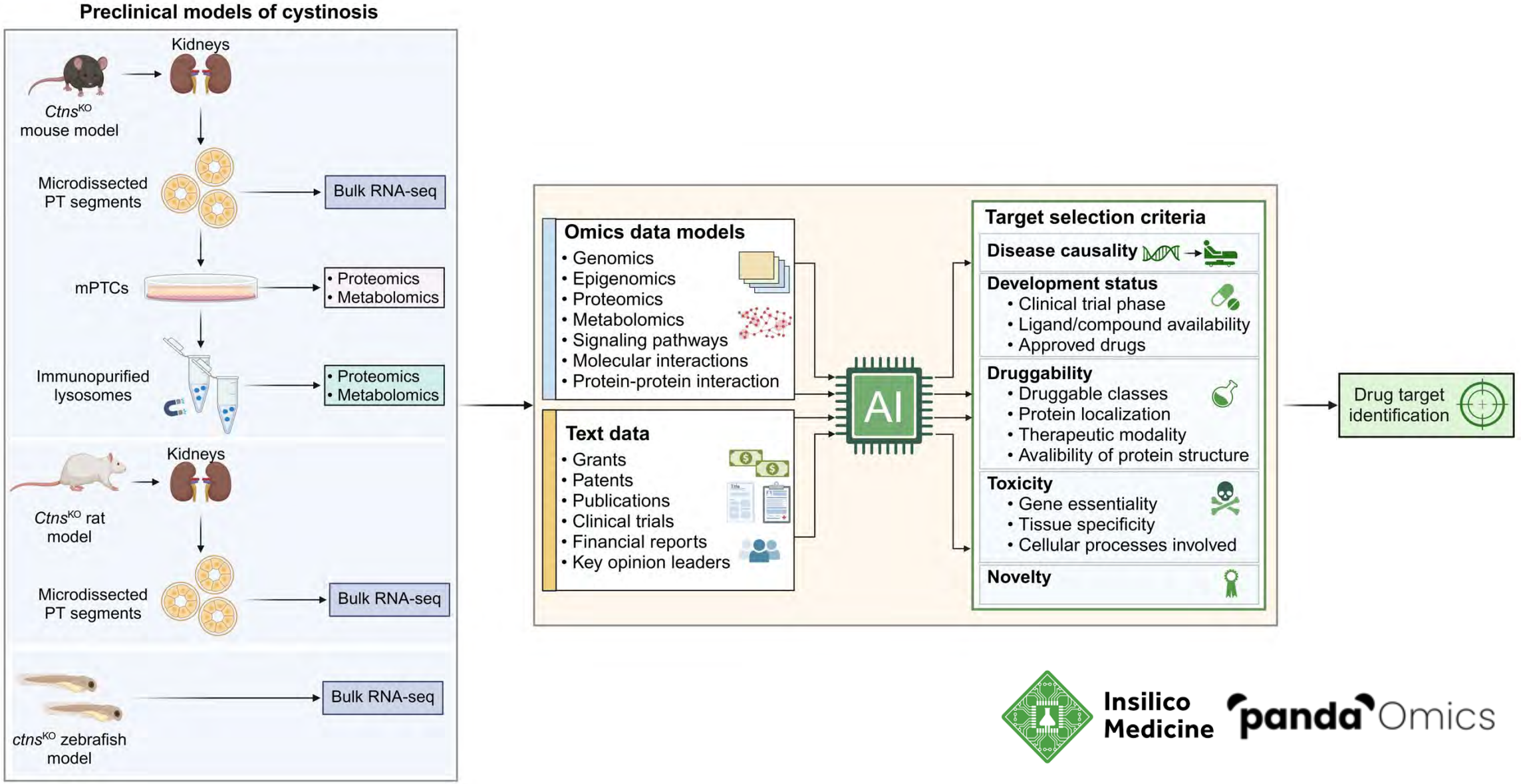

Insilico Medicine pandaOmics

Ren et al. Nature Biotechnology 2024

Actionable Targets Revealed from the AI-driven Drug Discovery Platform

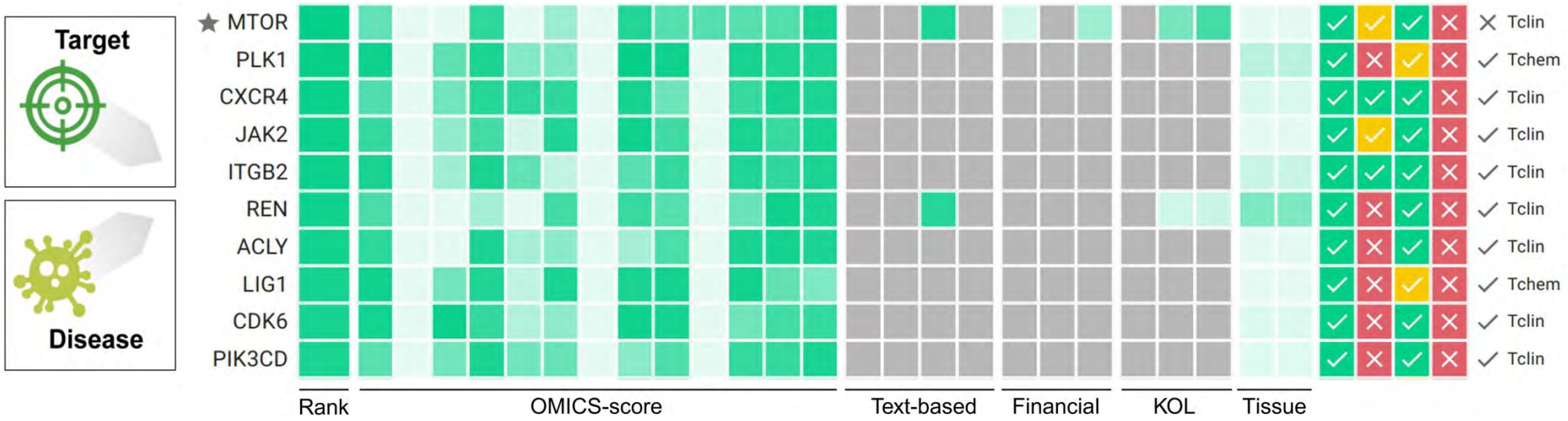

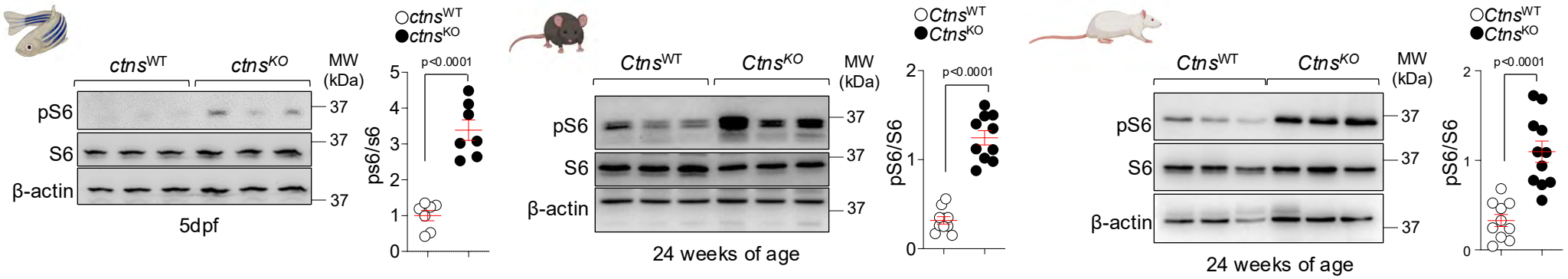

Cystine storage constitutively activates mTORC1 in an evolutionarily conserved manner

Berquez et al. Nature Communications, 2023

CTNS deficiency augments the lysosomal levels of subunits of V-ATPase and Regulator complex

mTORC1 scaffolding complex

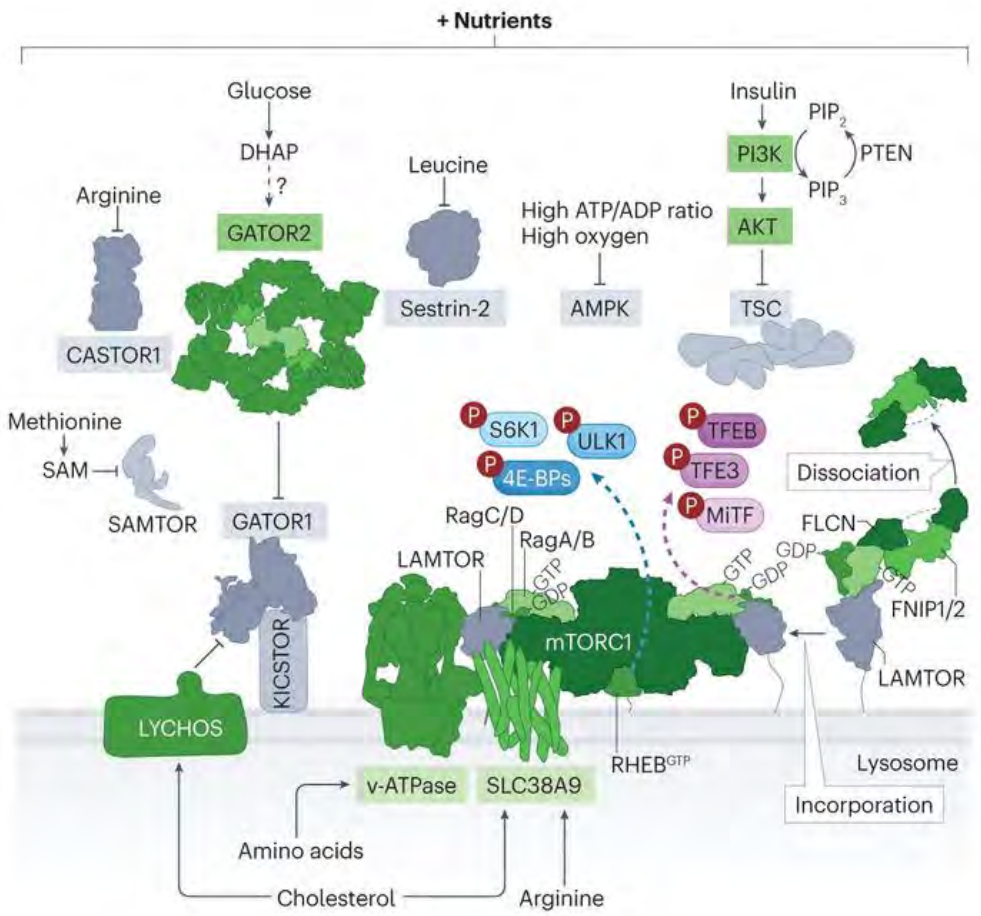

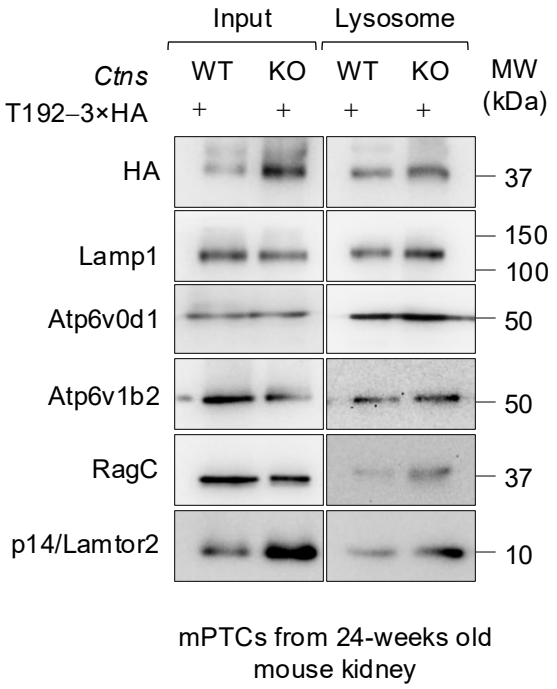

mPTCs from 24-weeks old mouse kidney

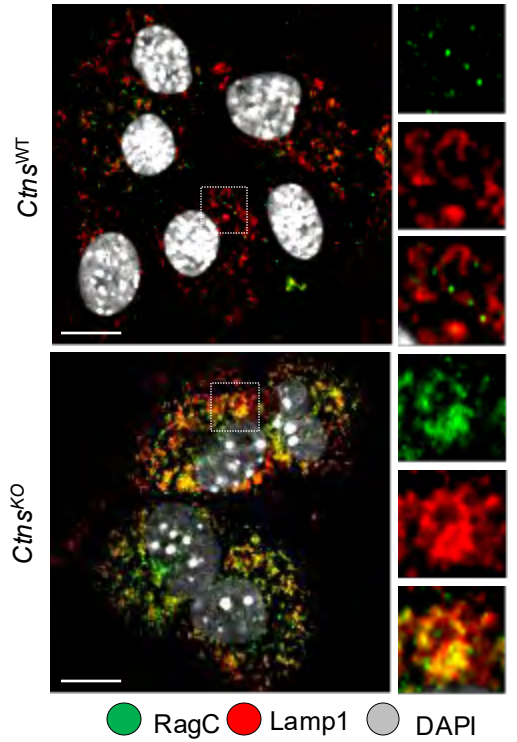

C Goul et al, *Nat Rev Mol Cell Biol*, 2023

Cystine Storage Activates mTORC1 via Ragulator-Rags Scaffold Complex

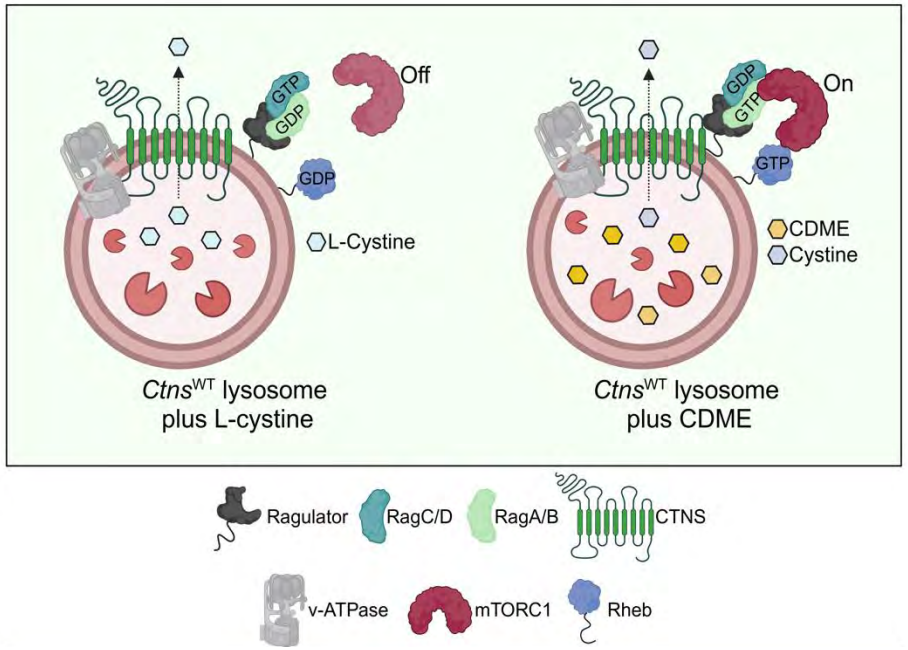

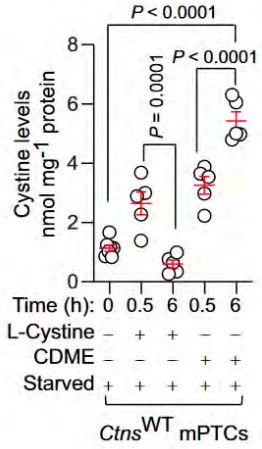

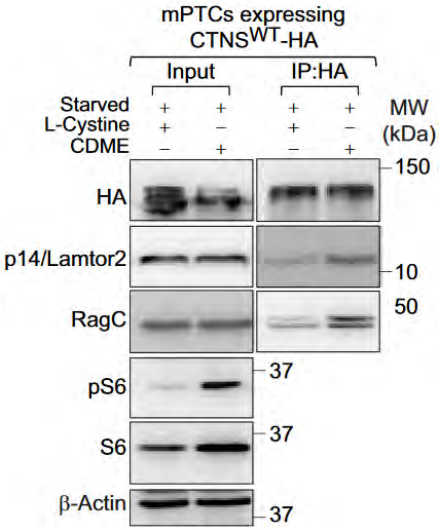

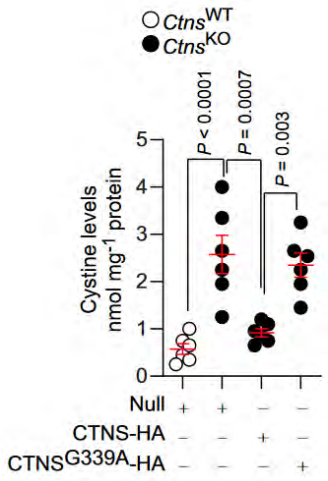

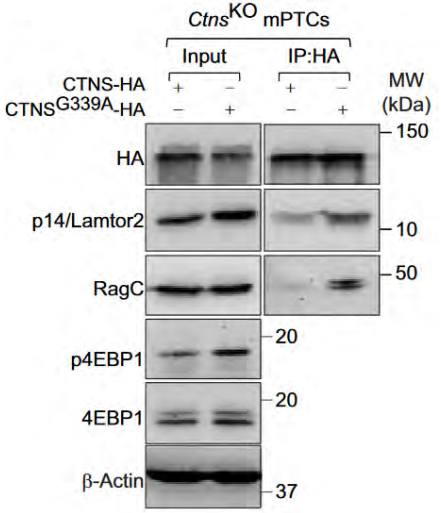

Berquez et al. Nature Communications, 2023

Lysosomal mTORC1 Signaling as a Targetable Pathway in Cystinosis

Ctns^{WT} or *Ctns*^{KO}

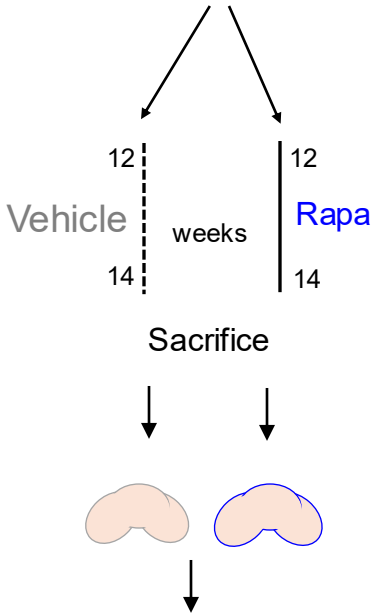

Tissue samples for:

- mTOR activity
- Lysosome
- Endocytosis
- Differentiation
- Proliferation
- PT cell height

a

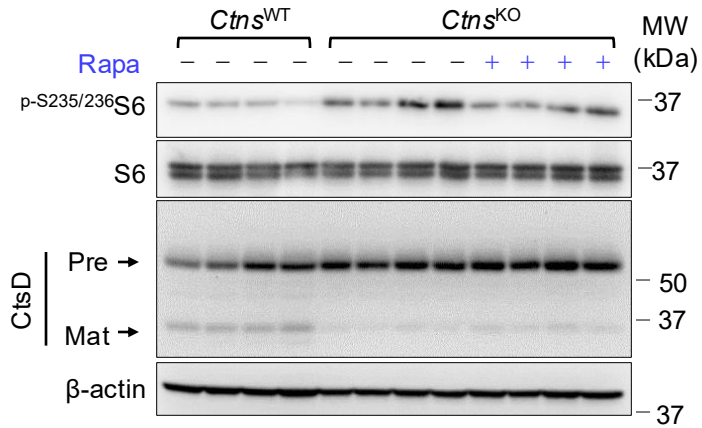

b

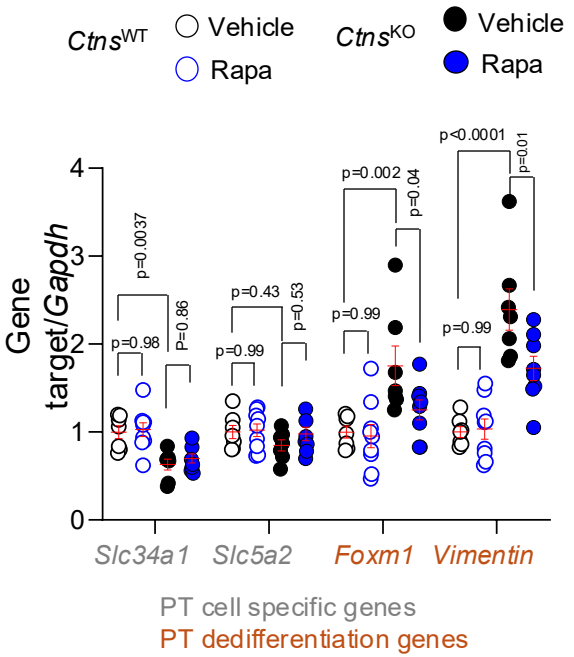

c

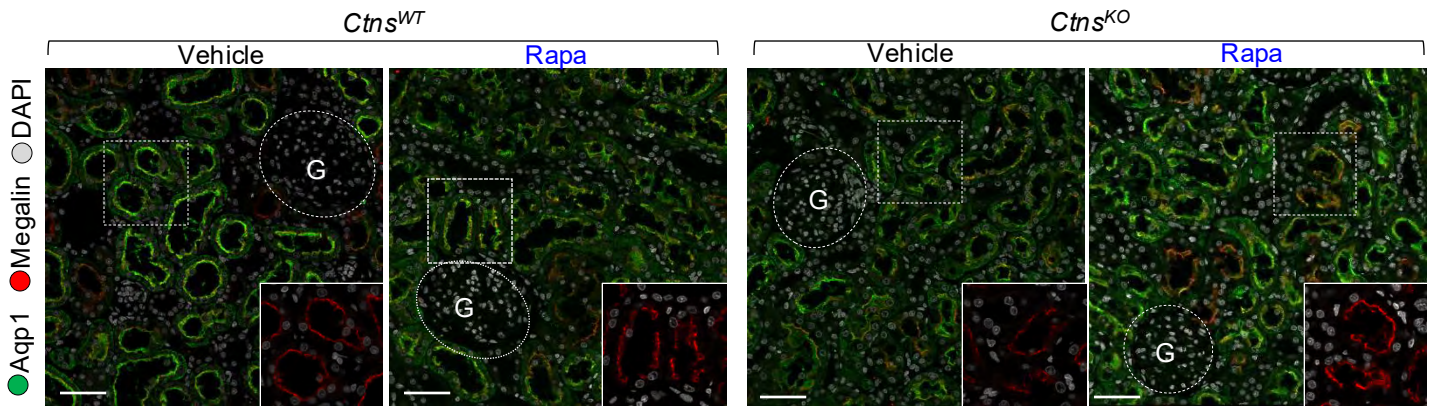

Berquez et al. Nature Communications, 2023

Rapamycin Improves Proximal Tubulopathy in a Zebrafish Model of Cystinosis

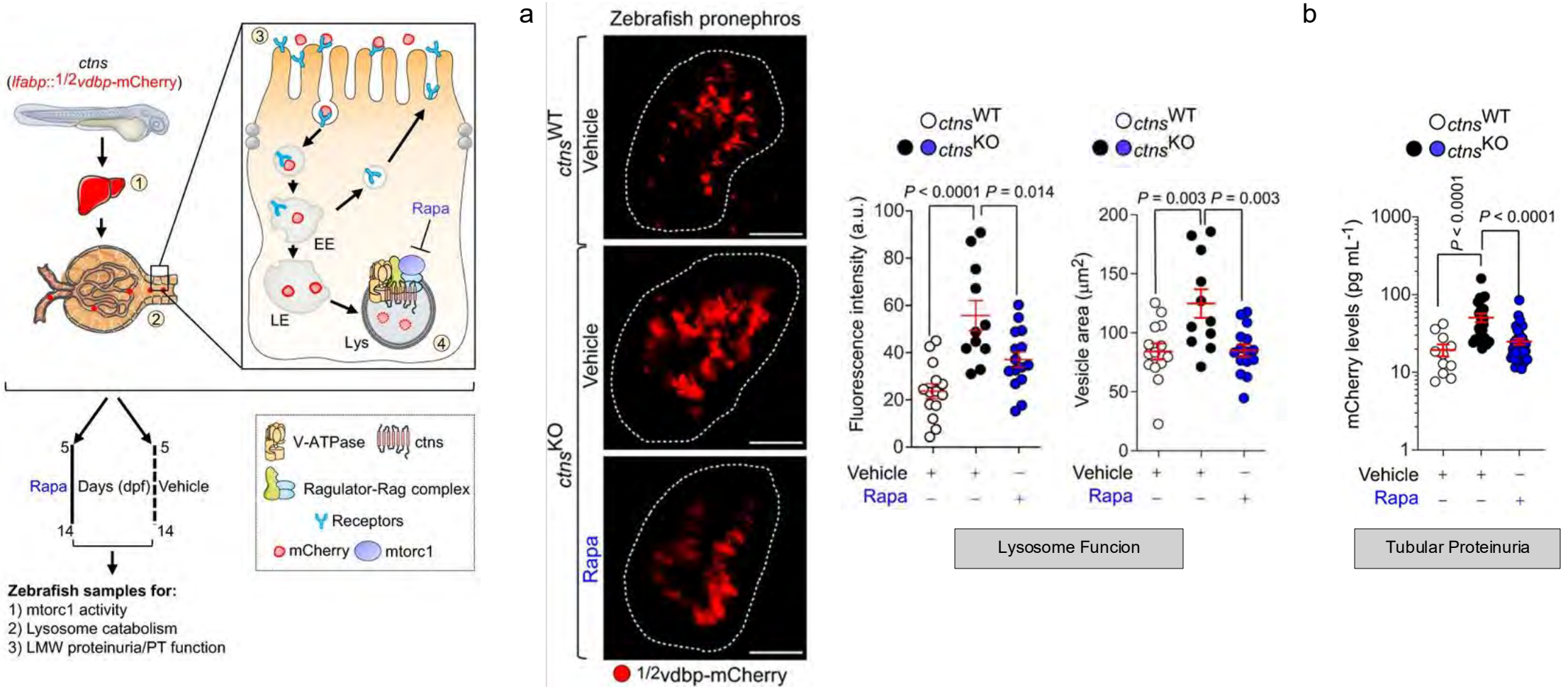

Modulation of lysosomal mTORC1 signalling as a new targetable pathway in cystinosis

Berquez et al. Nature Communications, 2023

Therapeutic Inhibition of mTORC1 Pathway in Preclinical Models of Cystinosis

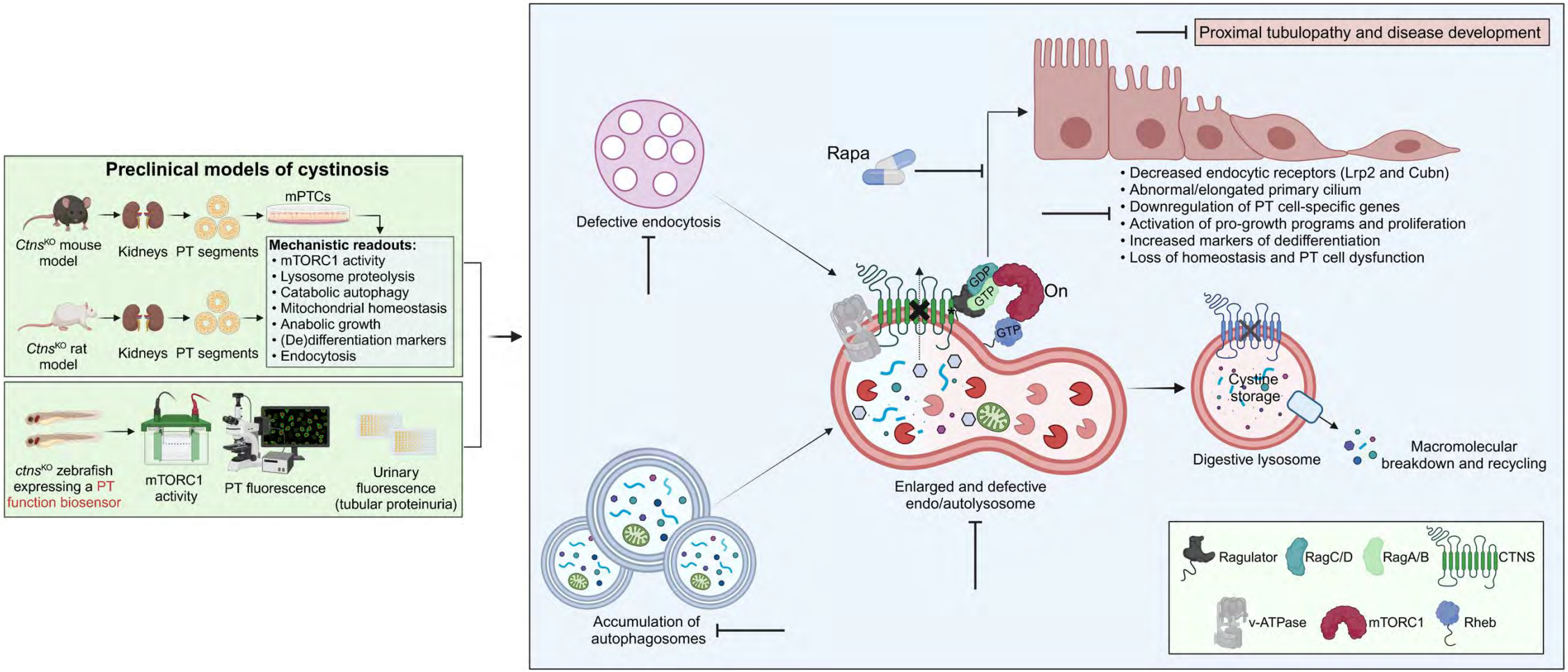

Rapamycin rescues lysosome, differentiation, and proximal tubulopathy downstream of cystine storage

Caution: Limited Translatability of Rapamycin to affected children due to its side effects

Berquez et al. Nature Communications, 2023

Concluding remarks:

- *Model systems lacking CTNS, which recapitulate early onset of disease phenotypes associated with cystinosis, represent powerful tools for drug testing and therapy discovery*
- *Leveraging artificial intelligence engines and multiomics integration identify disease pathway paradigms, prioritize therapeutic targets and accelerate drug discovery*
- *Role of CTNS-cystine-mTORC1 axis as a lysosomal signalling node in maintaining homeostasis in the kidney tubule epithelium*
- *Targeting nutrient sensing and mTORC1 signaling pathways (i.e., Rapamycin) prevents proximal tubulopathy in preclinical models of cystinosis*

These findings open new avenues for therapies targeting mTORC1 signaling (pharmacologic and nutritional strategies) to restore cellular homeostasis in cystinosis

Acknowledgements

Luciani Group, UZH
Alessandro Luciani
Federica Carloni
Louise Pierre

University of Zurich (UZH)
Olivier Devuyst
Zhiyong Chen
MIKD group members

TIGEM Institute, Naples
Carmine Settembre
Diego Medina
Antonella De Matteis

Bambino Gesu' Hospital, Rome
Francesco Emma
Francesca Diomedi Camassei
Francesco Bellomo

ETH Zurich and UZH
Alex Hainal
Simon Berger

San Raffaele Institute, Milan
Andrea Raimondi
Cesare Covino
Valeria Berno

Insilico Medicine, Hong Kong
Mike Korzinkin
Anna Gapanova
Alex Zhavoronkov

Genomics Center, UZH
Paolo Nanni
Alaa Othman

Louisiana University, USA
Alyssa Johnson

Nestlé Institute of Health Science, Lausanne
Philipp Gut
Jérôme Feige

National University of Singapore
Brian Kennedy
Vincenzo Sorrentino

KIT, Karlsruhe, Germany
Ravindra Parevali

Thank you for your attention

Program Evaluation and CE Credit

We need your assistance. Your opinion is important.

Please go to the link below and help us evaluate the program. You can also claim continuing education credit at this link.

ldrtc.cds.affinityced.com

Artificial Intelligence in Clinical Trials: Opportunities and Challenges in Lysosomal Diseases

Shoshana Revel-Vilk
Gaucher Unit & Pediatric Hematology/Oncology Unit
Shaare Zedek Medical Center
Jerusalem, Israel

2nd slide of your presentation

Disclosures

Shoshana Revel-Vilk

- Receives grant/research support from: Sanofi, Takeda
- Is a member of the Speakers Bureau for: Sanofi, Takeda
- Is a member of the Advisory Board for: Takeda

- Disclosure will be made when a product is discussed for an unapproved use.

•This continuing education activity is provided by AffinityCE, The Lysosomal and Rare Disorders Research and Treatment Center (LDRTC), and CheckRare CE. AffinityCE, CheckRare CE and LDRTC staff, planners, and reviewers, have no relevant financial relationships with ineligible companies to disclose. AffinityCE adheres to the ACCME's Standards for Integrity and Independence in Accredited Continuing Education. Any individuals in a position to control the content of a CME activity, including faculty, planners, reviewers, or others, are required to disclose all relevant financial relationships with ineligible companies. All relevant financial relationships when present, have been mitigated by the peer review of content by non-conflicted reviewers prior to the commencement of the activity.

•This activity has been supported by educational grants from commercial supporters. Please see
•the final program for a list of all supporters.

Learning outcomes

- Recognize that clinical trials are **more complex and expensive** than ever
- Describe the **application of artificial intelligence (AI)** in clinical trials
- **Discuss the benefits and challenges** with the use of AI in clinical trials in lysosomal disorders

Rising Costs and Timelines

- > 400,000 studies registered on ClinicalTrials.gov
  - representing a five-fold increase since 2005
- Industry invests approximately $200 billion annually in research and development, with 12% success rate and average costs reaching $2.6 billion per approved drug

- Contemporary Phase III trials require an average investment of **$19 million** and consume **6–7 years** from initiation to completion

Olawade DB et al., *Int J Med Inform* 2026; 206:106141.
https://doi.org/10.1016/j.ijmedinf.2025.106141.

Why Clinical Trials Fail ?

- **Poor Recruitment and Retention**
  - **Overly strict eligibility criteria**

  ~40% of trials amend protocols **before 1st patient visit**

  ~30% hit **initial recruitment targets**

  - **High participant burden** (travel, time, procedures)
  - **Limited engagement** of recruiters and trial teams

- **Design/Methodological flaws**
  - Inadequate endpoints, underpowered, poor measures

Desai, M. (2020). Perspectives in Clinical Research, 11, 51 - 53.

Why Clinical Trials Fail ?

- **Efficacy & Safety Challenges**
  ~ 50% of phase 3 studies fail due to **insufficient efficacy**
  ~ 20% fail due to **safety concerns**

- **Financial Barriers**
  ~ **$40K–$80K+**
  ~ 20–25% of studies fail due to **lack of funding**

Hwang TJ, et al. JAMA Intern. Med. 2016;176:1826–1833; Fogel DB, et al. Contemp Clin Trials Commun. 2018

Leading Causes of Failure in Rare Disease

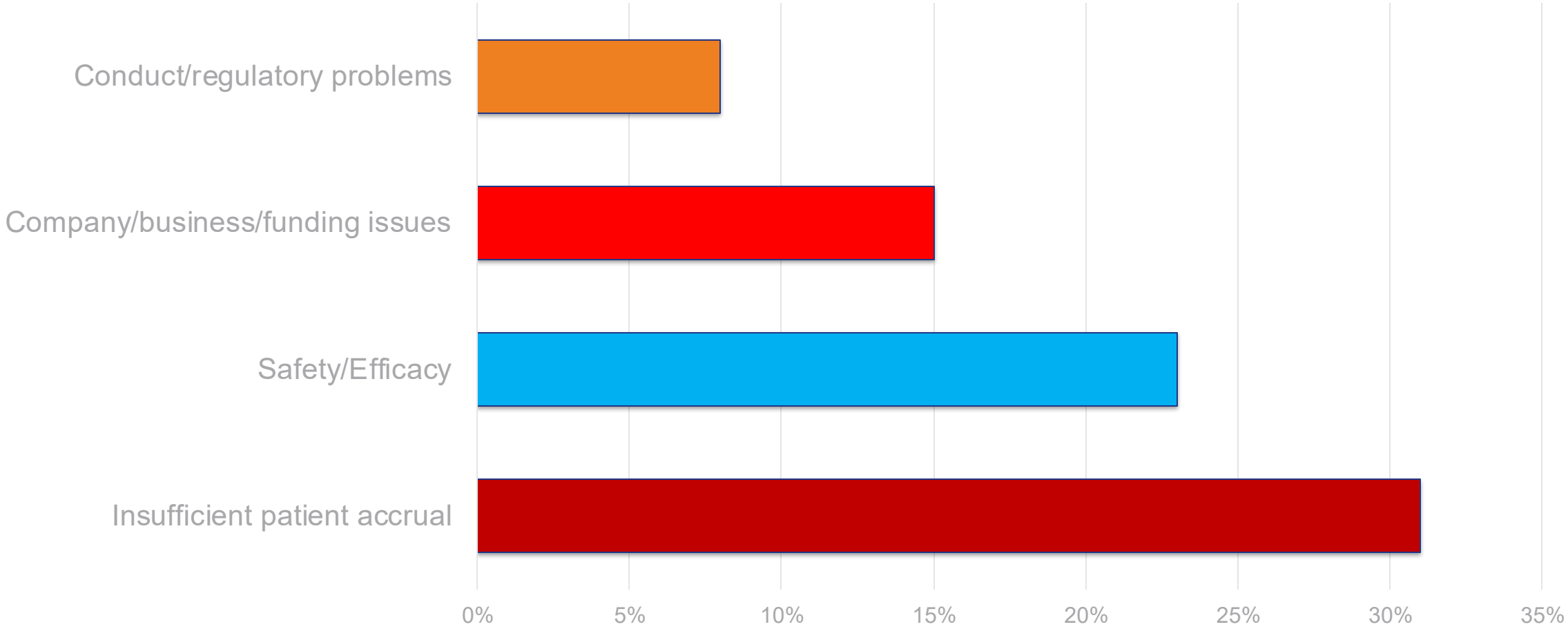

Rees C, et al. PLoS Medicine, 2019; Schoenen S, et al. Orphanet Journal of Rare Diseases, 2024

Integration of Artificial Intelligence

- Patient recruitment and screening
- Clinical trial design and feasibility
- Data capture, monitoring, and analysis

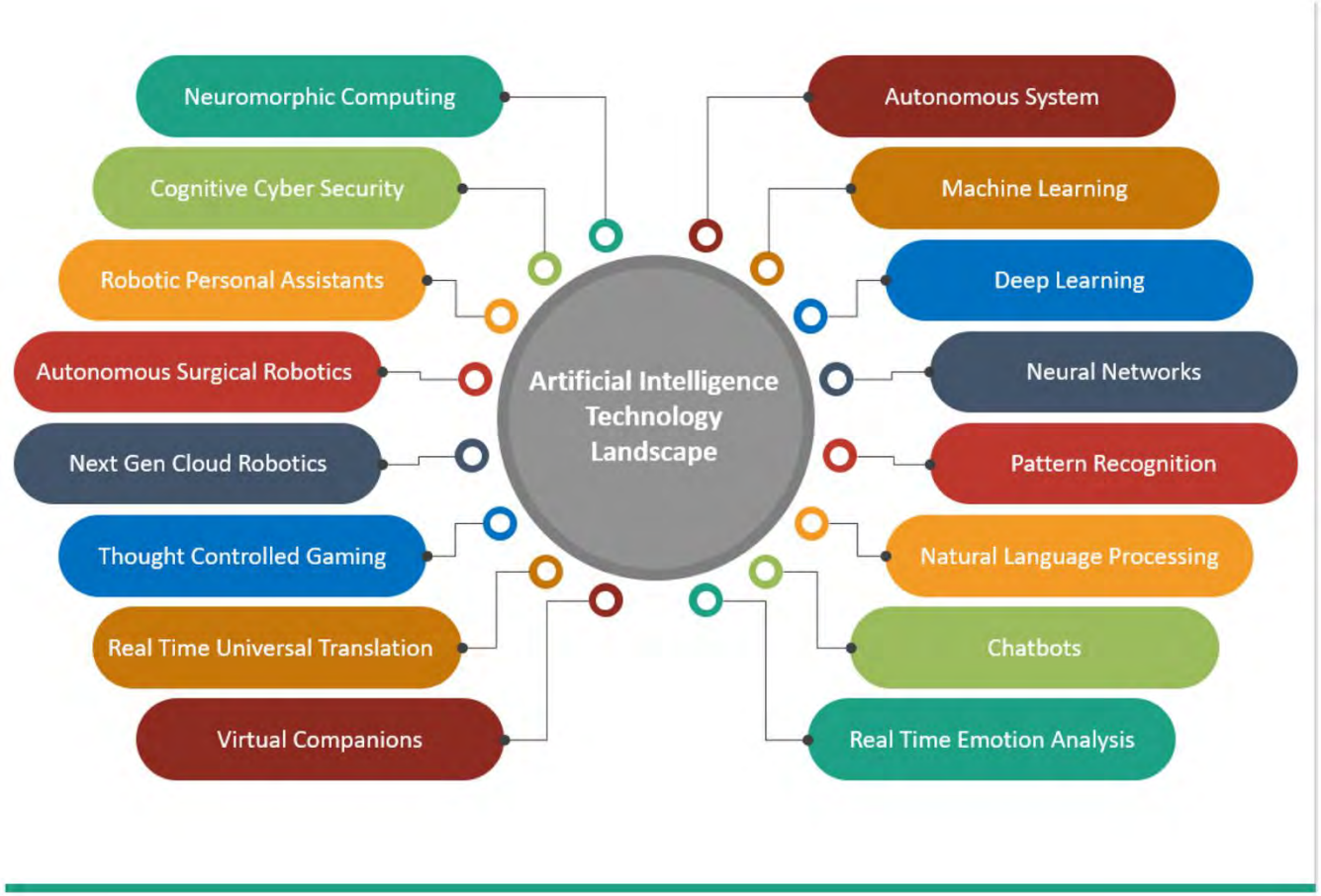

Aldoseri A, Al-Khalifa KN, & Hamouda AM (2023). *Applied Sciences*, *13*(12), 7082.

AI-Driven Recruitment: Evidence from Cancer Clinical Trials

- > 50 000 patients
- AI tools analyzing EHR + text data
- Finding patients missed by human review
- High confidence in excluding patients

- Significant time and cost reduction

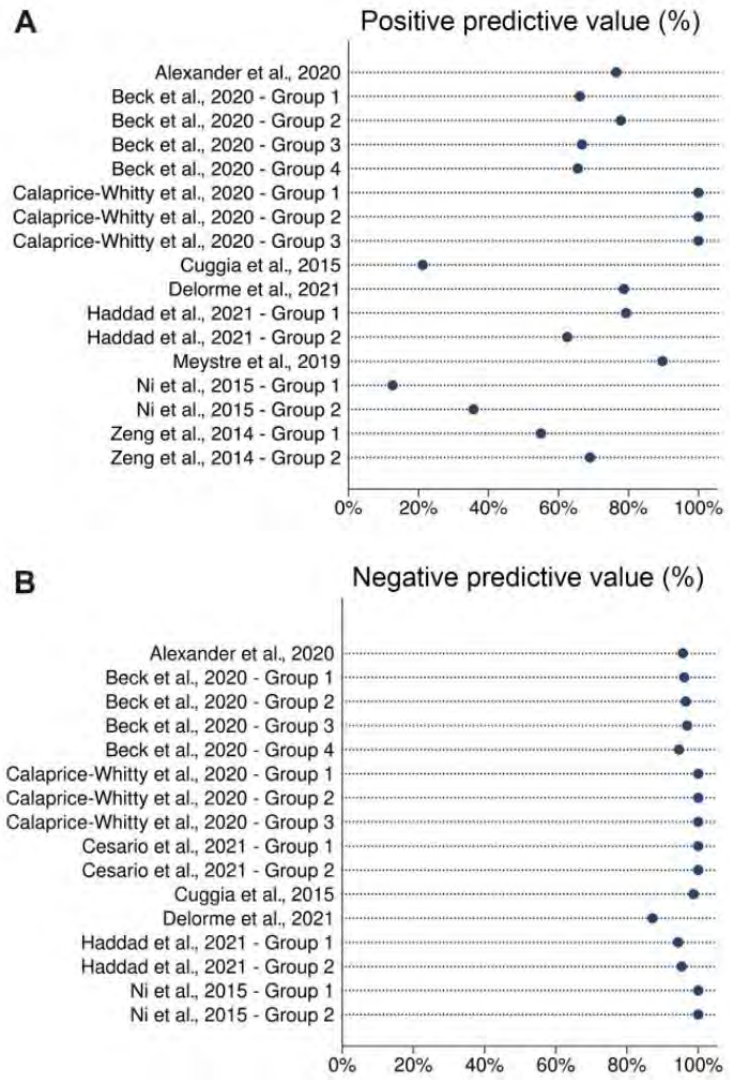

Chow R, et al. J Natl Cancer Inst. 2023 Apr 11;115(4):365-374

AI-Driven Recruitment: Evidence from a heart failure trial

- 4,476 patients
  - AI EMR screening: 458 eligible patients from ~2,242 screened
  - manual: 284 eligible from ~2,234 screened.
- Enrolments: 35 in AI arm vs 19 in manual arm (P = .04)

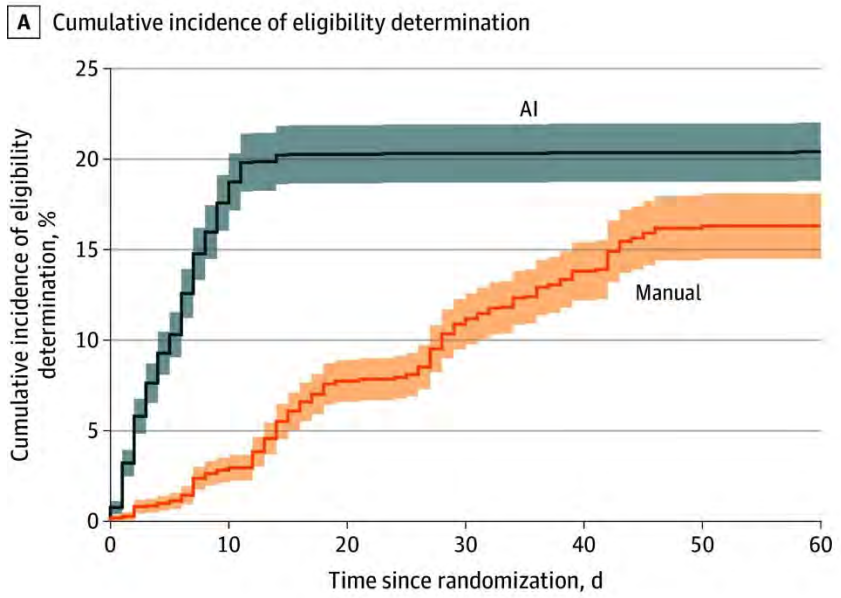

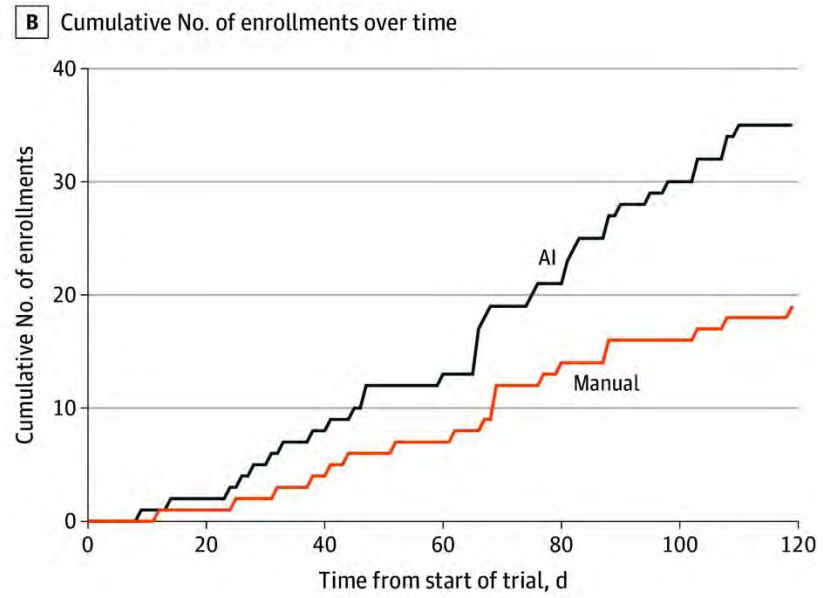

Unlu O, et. A. JAMA. 2025 Mar 25;333(12):1084-1087.

Patient Recruitment and Trial Matching

- 52 patients with solid tumors
- > 60,000 interventional, cancer-related clinical trials covering a wide range of malignancies mapped through the OncoTree ontology and the phenOncoX vocabulary
- In real-world validation, 92% of oncology patients had at least one relevant trial retrieved within the top 20 recommendations.

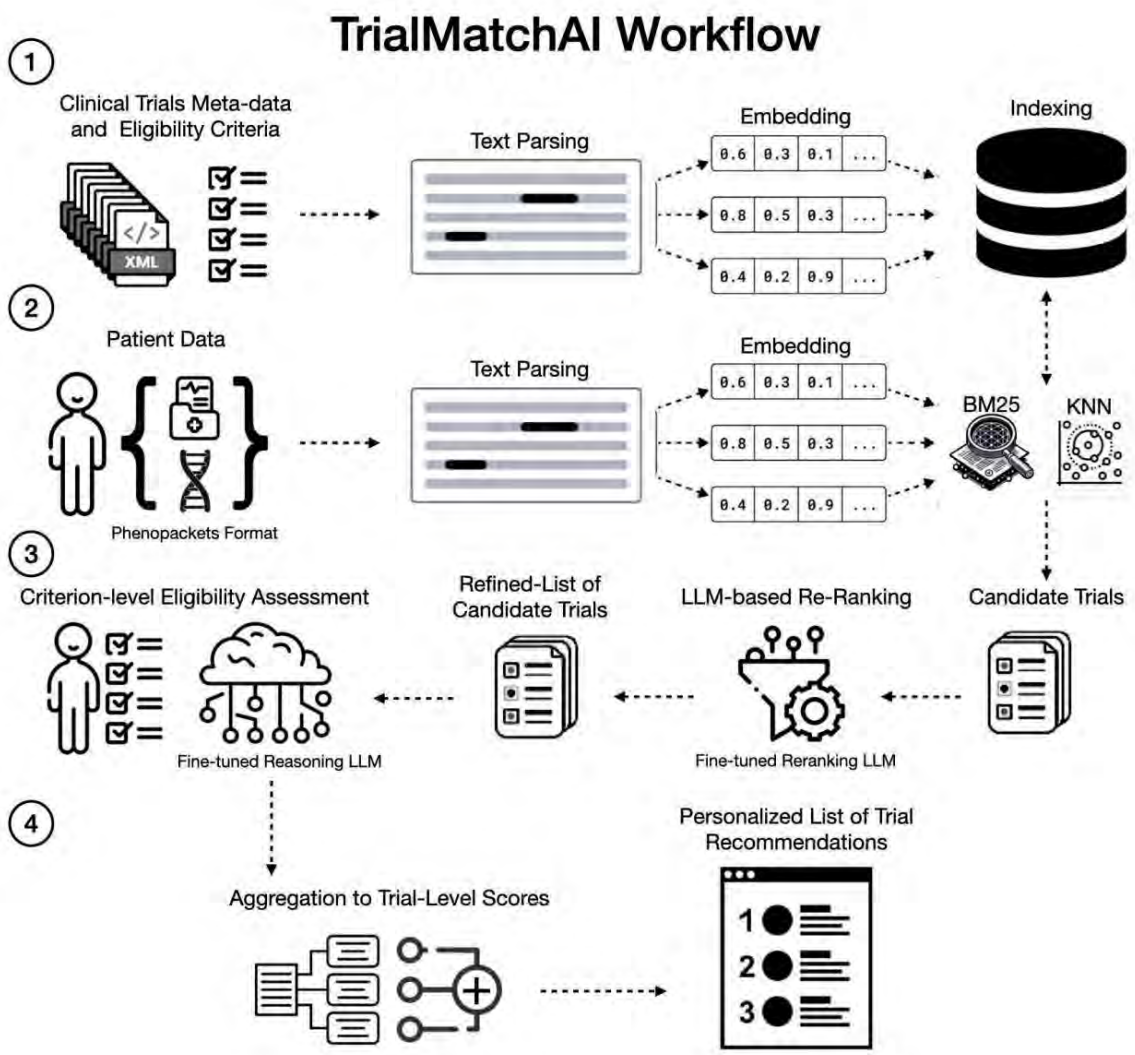

Abdallah M, et al. (2025). ***TrialMatchAI: An end-to-end AI-powered clinical trial recommendation system to streamline patient-to-trial matching*** **(Preprint). arXiv.** https://arxiv.org/abs/2505.08508

TrialGPT

- TrialGPT-Retrieval
- TrialGPT-Matching
- TrialGPT-Ranking

- TrialGPT-Retrieval can recall over 90% of relevant trials using less than 6% of the initial collection.
- Accuracy of 87.3%
- Reducing screening time by 42.6%

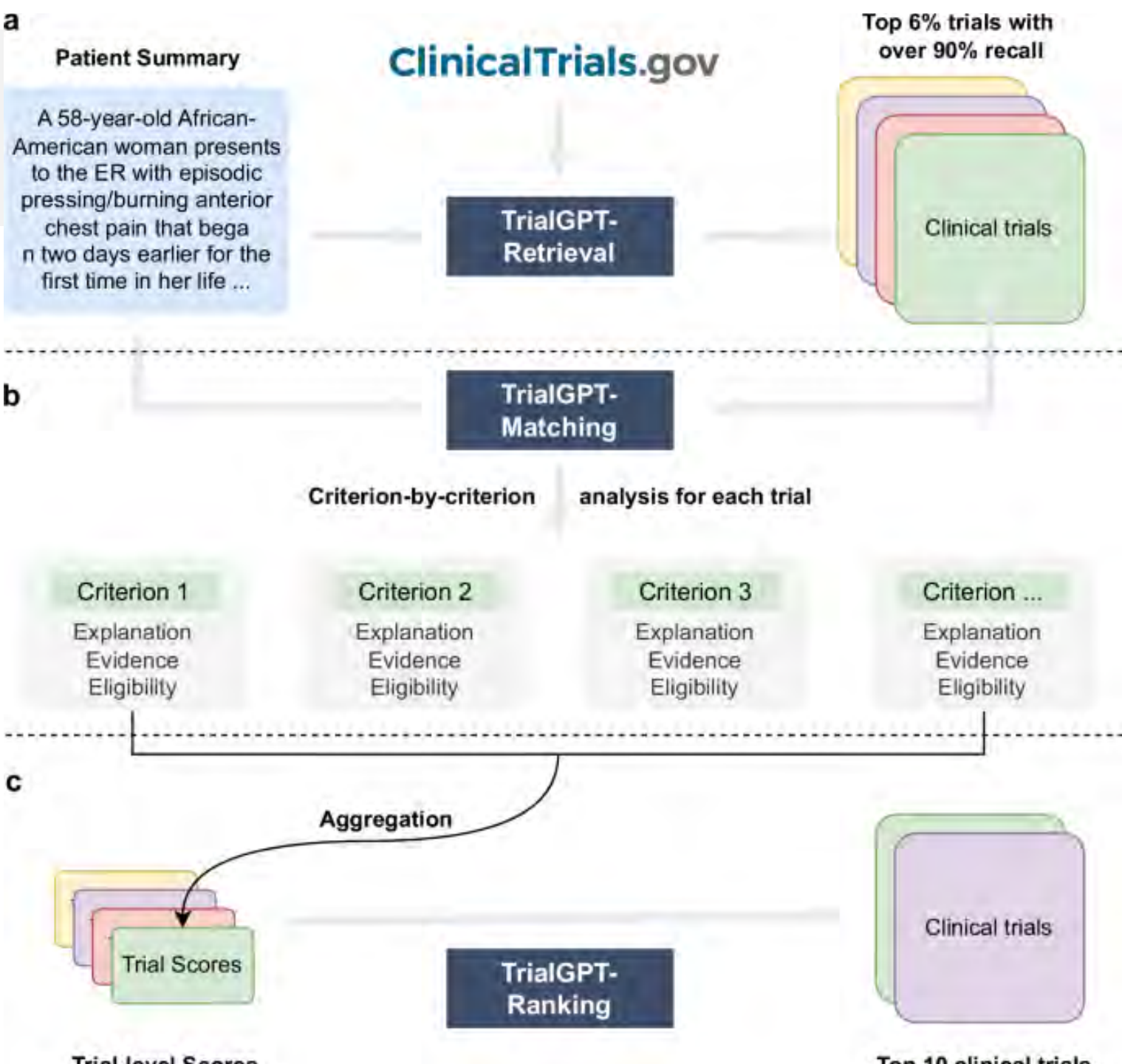

Jin Q, *et al.* *Nat Commun* 15, 9074 (2024)

AI-Driven Site Selection

- Demographic data
- Disease prevalence
- Healthcare infrastructure
- Investigator experience
- Historical site performance
- Geographical Factors

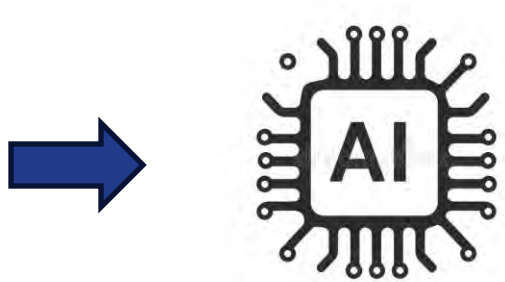

Improve timeline forecasting and resource planning —

reducing delays, inefficiencies, and cost overruns

S. Singh, A.I. Leveraging. World J Adv Res Rev., 26 (1) (2025). Kumar, M. et al. J. Clin. Trials, 11 (4) (2021), pp. 234-242

AI-Driven Protocol Optimization

- **Propose the development of application-specific language models (ASLMs) for clinical trial design across three phases**
- Step 1 → Development by regulatory bodies
- Step 2 → Customization by Health Technology Assessment bodies
- Step 3 → Deployment to stakeholders

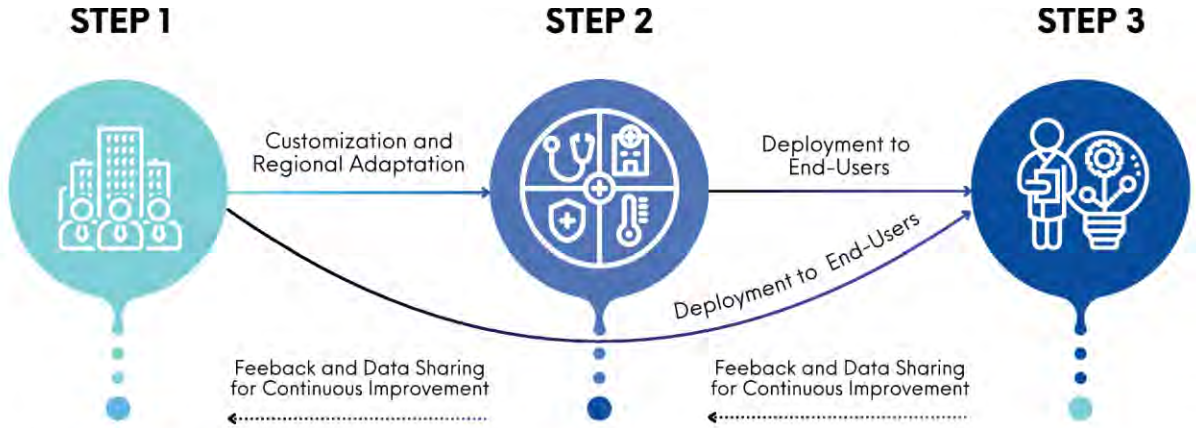

Development of Functional ASLMs by Regulatory Bodies

Utilizing unique datasets:
Trial protocols
Regulatory documents
Records of successful and unsuccessful trial applications

Objectives:
Enhance trial design quality
Address common pitfalls in protocols
Improve safety and efficacy assessments

Customization by HTA Bodies

Incorporating regional data:
Local healthcare costs
Real-world evidence
Data from previous assessments

Objectives:
Evaluate clinical significance and benefit after trial results are available
Evaluate design and results of clinical trials against relevant comparators
Enhance cost-effectiveness analysis based on clinical trial outcomes

Deployment to Researchers and Protocol Developers

Access to ASLMs:
Through secure APIs or web-based interfaces
Potential for open-source availability

Usage:
Proactively improve trial designs before submission
Optimize inclusion/exclusion criteria
Select appropriate endpoints and methodologies
Prepare submission packages for HTA assessments

Objectives:
Increase initial submission quality
Reduce revision cycles
Accelerate drug development processes

Liddicoat JE, *et al.* A policy framework for leveraging generative AI to addres enduring challenges in clinical trials. *npj Digit. Med.* 8, 33 (2025).

AI-Driven Protocol Optomization

- 24 virtual pediatric subjects
- 49 time-point concentration profiles (from 0 h to 96 h) by randomly sampling each parameter based on its variability distribution
- Across 10 runs, the model consistently converged on 7 optimal timepoints

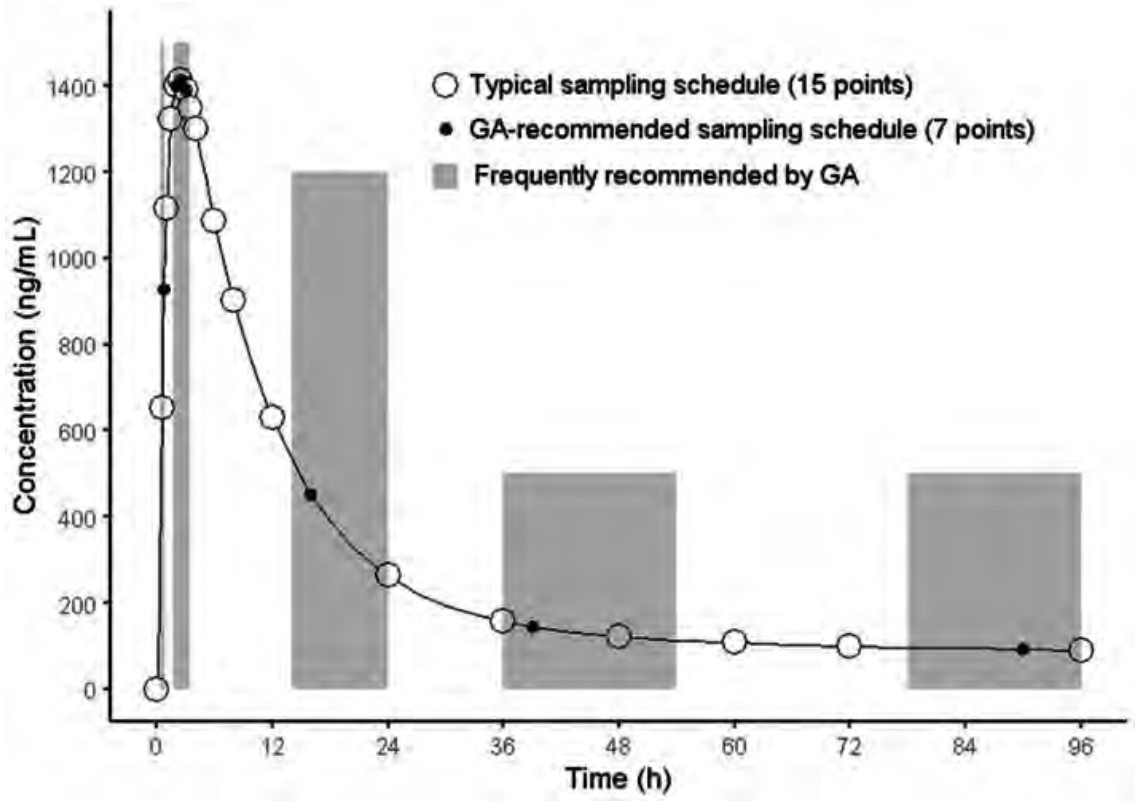

Tsuchiwata S, Tsuji Y. *CPT Pharmacometrics Syst Pharmacol.* 2023;12:522–531.

AI-Driven Virtual Screening and Remote Consent Processes

- Virtual screening
  - analyze medical images
  - process patient-reported outcomes and digital health data

- Intelligent chatbots and conversational AI systems for remote consent processes
  - providing personalized information delivery
  - addressing participant questions in real-time
  - adapt communication style and content based on participant literacy levels, cultural backgrounds, and individual preferences

Tashman K, *et al. Digit. Biomark.* 2021;5(3):119–130; 72. Goodwin TR, *et al. J. Biomed. Inform.* 2023;143:104386. Patel N, *et al. Clin. Trials J.* 2019;16(5):467–475.; Mamae A, *et al. PLoS One*. 2025;20:e0329896; Luo Y, *et al. J. Am. Med. Inform. Assoc.* 2022;29(1):31–38; Alsumidaie M, *et al. Clin. Trials Arena.* 2021; Mishra V, *et al. Digit. Biomark.* 2021;5(3):119–130.

Decentralized clinical trials

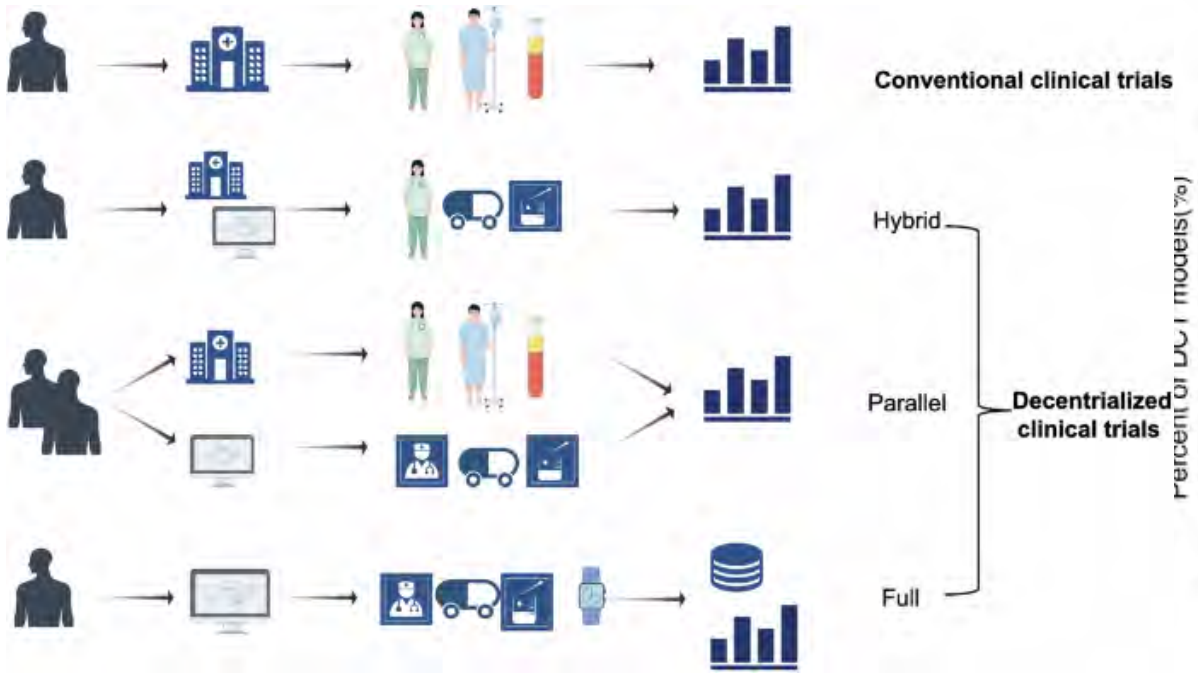

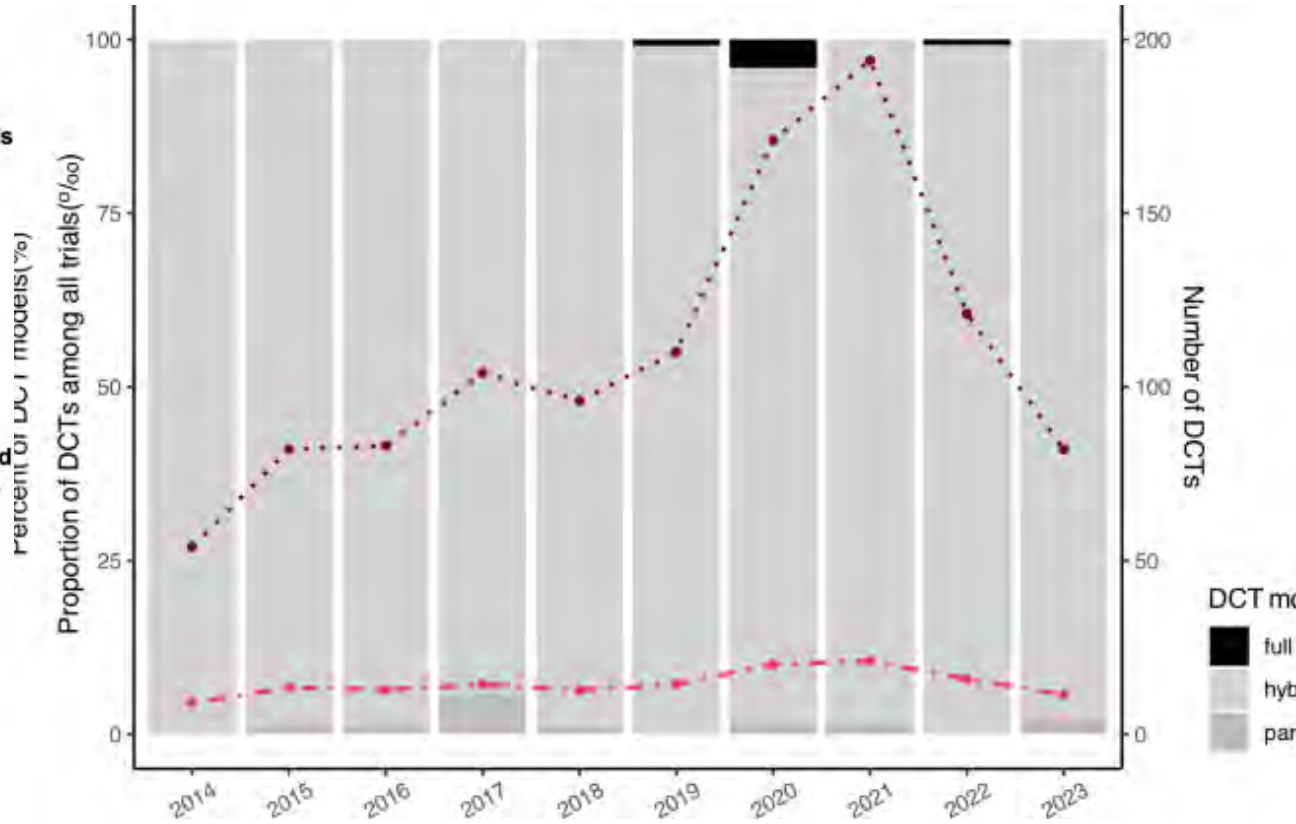

Jiang Y, *et al.* Understanding the gap between expectations and reality in decentralized clinical trials. *npj Digit. Med.* 8, 408 (2025).

AI-Driven Data capture and Monitoring

- Continuous monitoring with deep learning analytics
- Enhance sensitivity for adverse event detection
  - Traditional monitoring: 70–75 % sensitivity
  - AI-powered systems: ≈ 90 % sensitivity, real-time alerts
- Enable continuous monitoring and earlier detection of clinical changes.

PD-related digital biomarkers

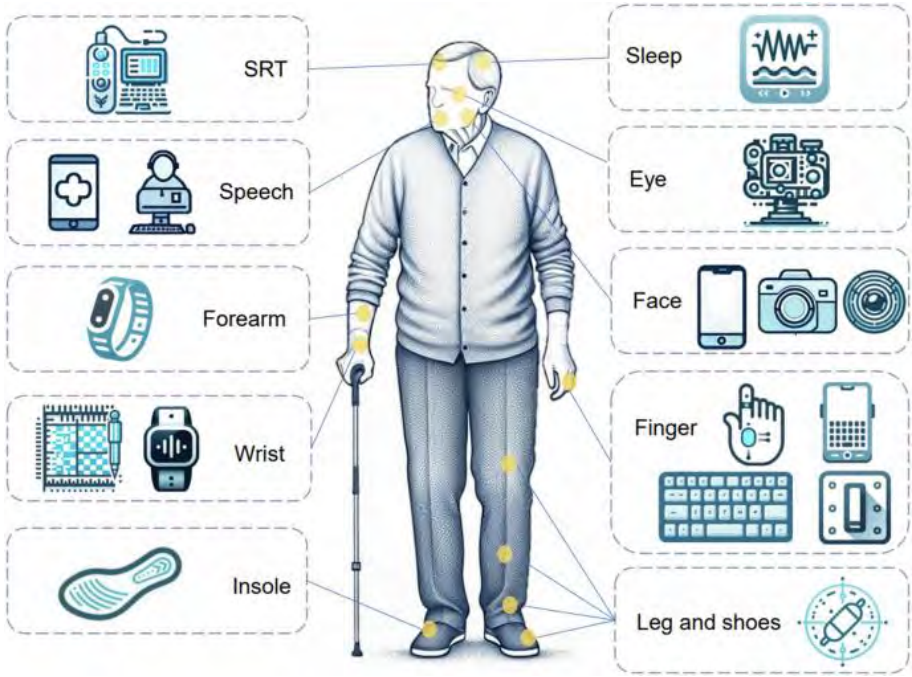

Sun, YM, *et al. npj Digit. Med.* 7, 218 (2024). Esteva A, et al. *Nature Medicine.* 2021; 25(1):24–29. Rajpurkar P, et al. *Nature Medicine.* 2022; 28(1):31–38. Tashman K, et al. *Digital Biomarkers.* 2021; 5(3):119–130. Dorsey ER, et al. *The Lancet.* 2020; 395(10227):859–865.

AI-Driven Risk-Based Monitoring and Quality Assurance

- Transforms trial oversight from reactive to proactive
  - detect and prevent issues in real time, improving data integrity and efficiency
- Real-time insight
  - Identify anomalies and protocol deviations within 24–48 h of data entry
- Predictive monitoring
  - Flag sites at risk for non-compliance and target interventions
- Efficiency
  - Focus human review on high-risk areas → ↑ trial quality, ↓ monitoring costs by 30–40 %

Liu Y, et al. J Am Med Inform Assoc 29 (5) (2022) 901–910; Khosravi P, et al. Nat Commun 12 (2021) 5648; [93] Xu J, et al. J Clin Transl Sci 6 (1) (2022) e100; Li X, et al. J Biomed Inform 129 (2022) 104069; Vashisht R, et al. Drug Discov Today 27 (10) (2022) 103330.

AI-Driven Automated Data Cleaning and Standardization

- Automates data integrity checks
  - reducing manual effort and errors
- Detects and corrects inconsistencies, missing values, and entry errors
- Accelerates workflows:
  - reduces cleaning time by 60–80 %
    → from 4–6 weeks of manual review to 24–48 hours of automated processing
- Enhances quality
  - ensures consistent, reliable data across study sites

[Rajasekaran M, et al. *Journal of Clinical Trials.* 2021; **11**(4):234–242.
Lamberti MJ, et al. *Clinical Trials*. 2018; **15**(3):232–242.
Müller M, et al. *Computers in Biology and Medicine.* 2020; **124**:103926.
Ruchlin I, et al. *Journal of Clinical Oncology.* 2024; **42**(16_suppl):1558.

Experience in lysosomal disease

AI-Driven Recruitment

Journal of *Clinical Medicine*

MDPI

Article

Supporting the Diagnosis of Fabry Disease Using a Natural Language Processing-Based Approach

Adrian A. Michalski [1,2,†], Karol Lis [1,3,*,†], Joanna Stankiewicz [1,4], Sylwester M. Kloska [1,5], Arkadiusz Sycz [1,6], Marek Dudziński [1,7], Katarzyna Muras-Szwedziak [8,9], Michał Nowicki [8,9], Stanisława Bazan-Socha [8,10], Michal J. Dabrowski [1,11,‡] and Grzegorz W. Basak [1,3,‡]

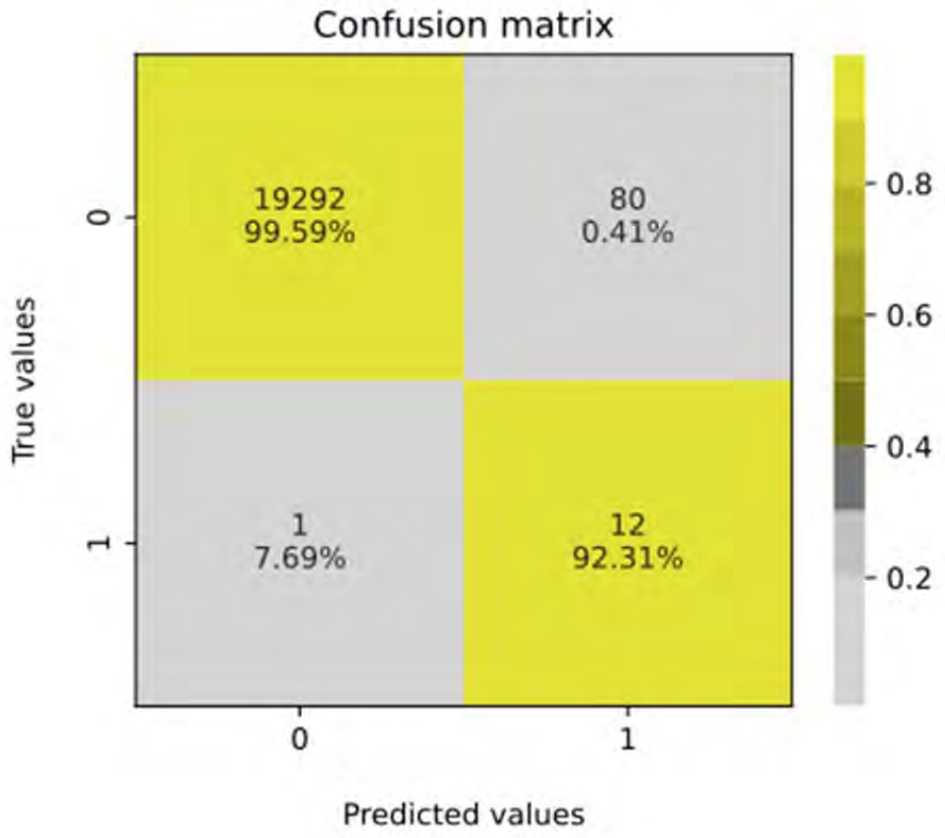

One patient who obtained a high-risk score was referred for DBS assay and confirmed to have Fabry disease

AI-Driven Recruitment

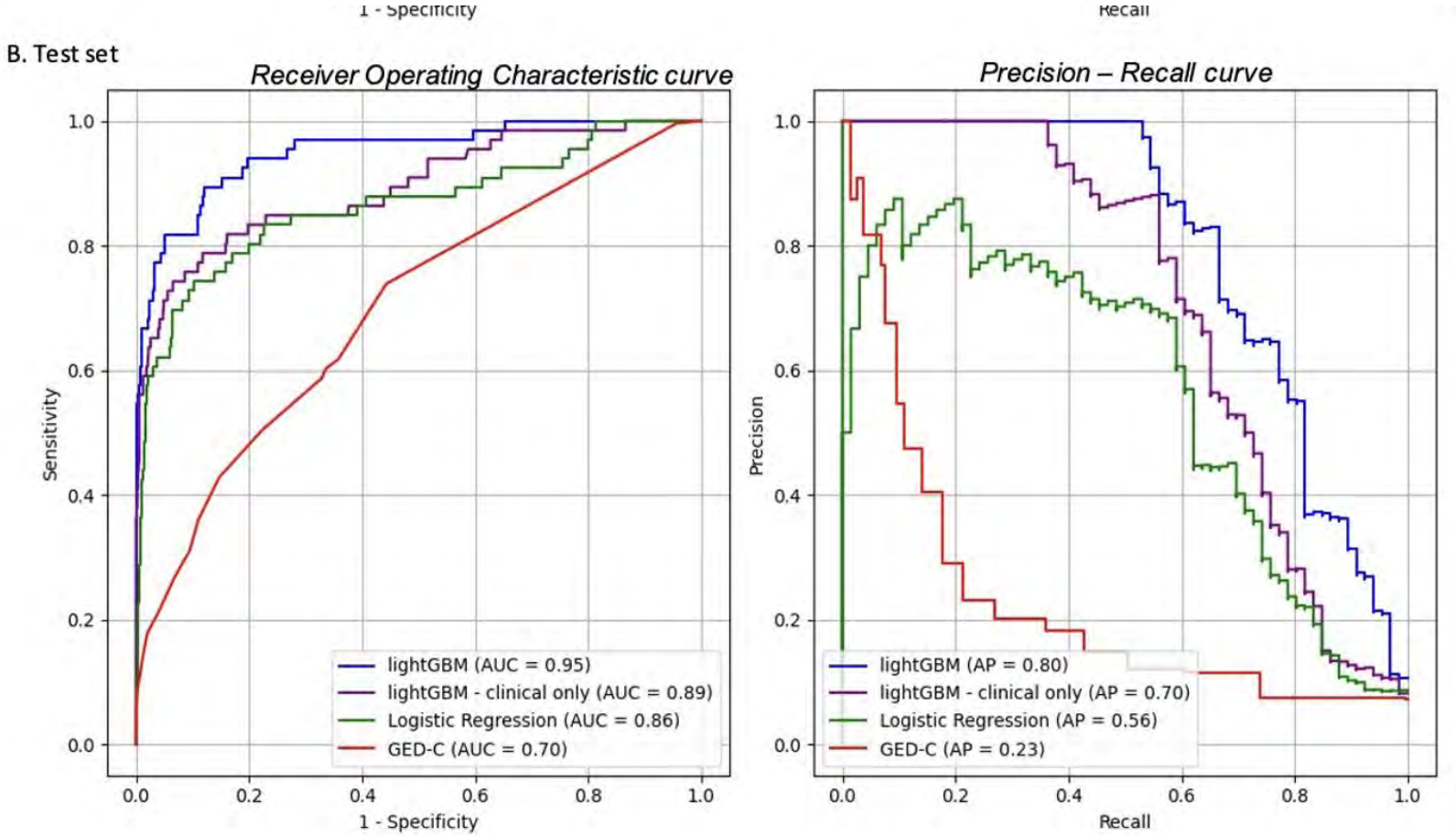

GED-C- Gaucher early diagnosis- consensus [see Mehta, et al. Intern Med J 2019, 49, (5), 578-591.] LightGBM- light gradient-boosting machine, AUC- area under the curve c

Tenenbaum A, Revel-Vilk S, et al. *J Clin Epidemiol* 2024; 175: 111517

Germain *et al.*
Orphanet Journal of Rare Diseases (2025) 20:186
https://doi.org/10.1186/s13023-025-03655-x

Orphanet Journal of
Rare Diseases

REVIEW Open Access

Applying artificial intelligence to rare diseases: a literature review highlighting lessons from Fabry disease

Dominique P. Germain[1,2*], David Gruson[3], Marie Malcles[4] and Nicolas Garcelon[5]

- AI electrocardiography for the evaluation of cardiac involvement in Fabry disease
- Selection of Fabry disease patients for clinical trials

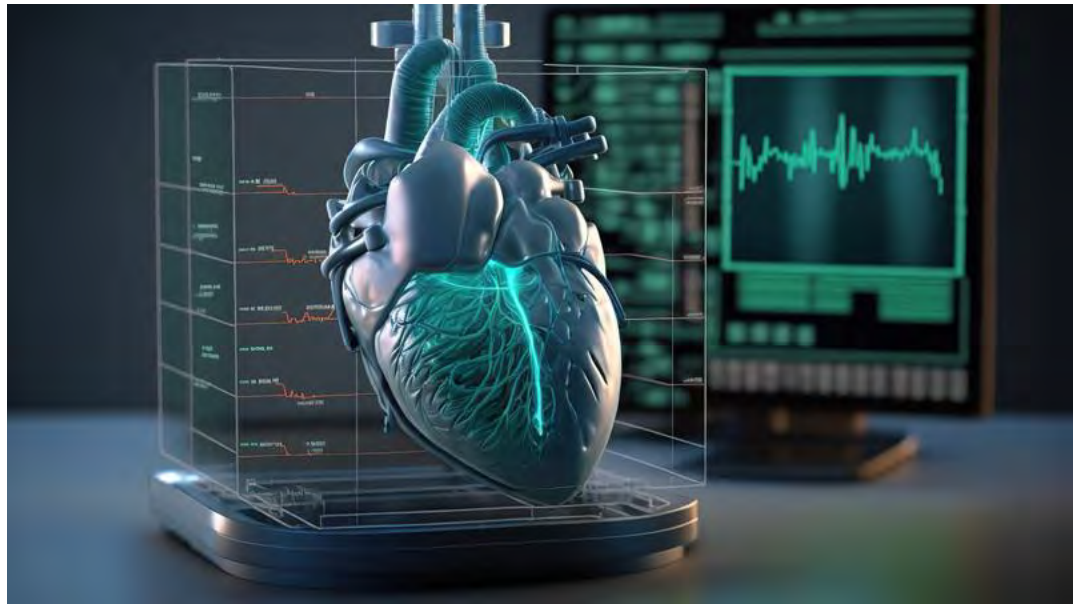

Wearable experience in Gaucher disease

- 21 patients (16 nGD, 5 GD1)
- Wearable accelerometer + Aparito mobile app
- Collected: step counts, events (e.g., bone pain, sleep), PROs (CHU9D, PedsQL Fatigue, Sleep & Stress Scales)
- Patients with GD1 showed ~2.5× higher daily step counts vs nGD

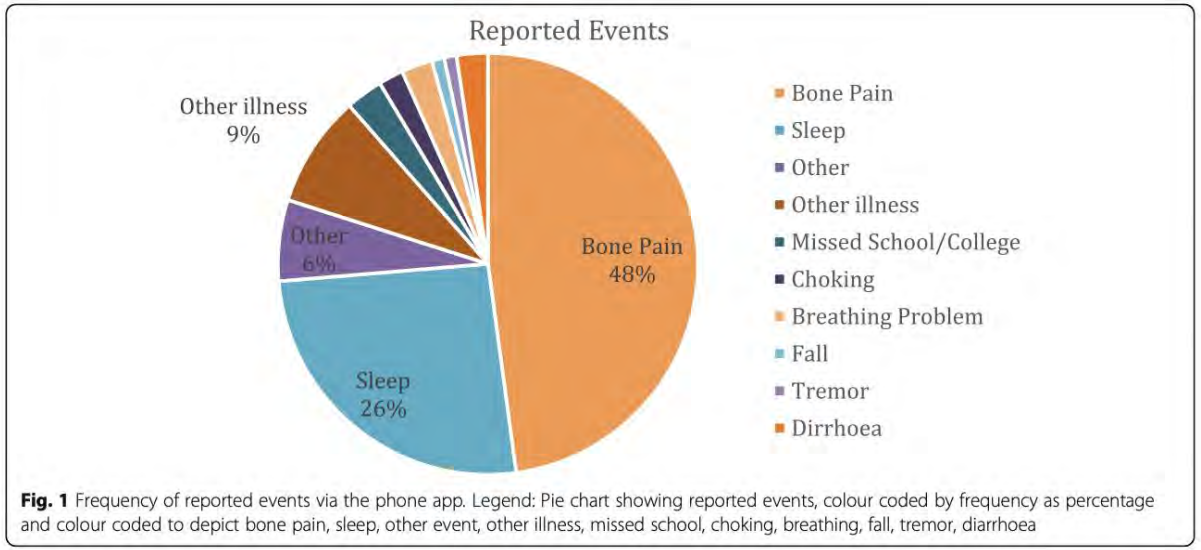

Fig. 1 Frequency of reported events via the phone app. Legend: Pie chart showing reported events, colour coded by frequency as percentage and colour coded to depict bone pain, sleep, other event, other illness, missed school, choking, breathing, fall, tremor, diarrhoea

Donald A. et al., Orphanet J Rare Dis, 2019;14:212

AI-Driven personalized treatment strategies

Journal of *Clinical Medicine*

MDPI

Article

A Feasibility Open-Labeled Clinical Trial Using a Second-Generation Artificial-Intelligence-Based Therapeutic Regimen in Patients with Gaucher Disease Treated with Enzyme Replacement Therapy

Noa Hurvitz [1], Tama Dinur [2], Shoshana Revel-Vilk [2,3], Samuel Agus [4], Marc Berg [4,5], Ari Zimran [2,3,†] and Yaron Ilan [1,3,*,†]

1 Departments of Medicine and Neurology, Hadassah Medical Center, Jerusalem 9112001, Israel; noa.hurvitz@mail.huji.ac.il
2 Gaucher Unit, The Eisenberg R&D Authority, Shaare Zedek Medical Center, Jerusalem 9103102, Israel; dinurtama@gmail.com (T.D.); srevelvilk@gmail.com (S.R.-V.); azimran@gmail.com (A.Z.)
3 Faculty of Medicine, Hebrew University, Jerusalem 9112001, Israel
4 Oberon Sciences and Area 9 Innovation, Chestnut Hill, MA 02467, USA; sam.agus@samagus.com (S.A.); marc@area9.dk (M.B.)
5 Stanford University, Palo Alto, CA 94305, USA
* Correspondence: ilan@hadassah.org.il; Tel.: +972-2-6778511
† These authors contributed equally to this work.

Background

- **>10% of patients** show incomplete or diminishing response to current Gaucher disease therapies
- **Circadian and biological rhythms** regulate immune, endocrine, and metabolic pathways; their disruption may affect disease activity and treatment response
- **Physiologic variability** across genetic, autonomic, and metabolic systems is essential for health—its loss is linked to poorer outcomes and reduced treatment efficacy
- Applying **AI-driven adaptive dosing can** tailor treatment patterns and potentially improve I GD-related therapy effectiveness

Methods

- **Design:** 6-month, open-label, single-center, proof-of-concept study
- **Participants:** 5 adults with GD1 on stable ERT (30–60 U/kg/month)
- **Platform:** *Altus Care*™ mobile app
- Randomized ERT **dosage** and **administration intervals**
  - Dosing interval: **10–18 days** (vs. standard 14).
  - Randomized infusion time: **7 a.m.–2 p.m.**

Table 2. An example of drug administration based on the randomization algorithm for one of the subjects in the study.

Administration time: Days since recruitment	1	14	31	45	62	74	91	104	121	135	149	165
Dosage	3200	2000	4400	800	1200	4000	800	4400	3600	1600	2000	3200
Administration time—hour	8:30	9:45	8:45	9:00	9:30	8:15	7:15	7:00	9:00	7:45	9:00	8:45

Hurvitz, N., et al. J. Clin. Med. 2024, 13, 3325.

Results

- **Completion:** 5/5 patients completed 6 months; n
- **Adherence:** 100% engagement through the Altus

- **Quality of Life (SF-36):** ↑ in 1, stable in 3, slight ↓
- **Hemoglobin:** Stable in 4, ↑ in 1 (Δ +0.7 g/dL)
- **Platelets:** ↑ in 2, ↓ in 2, stable in 1.
- **Lyso-Gb1:** ↓ in 2 patients (mean –25 ng/mL)

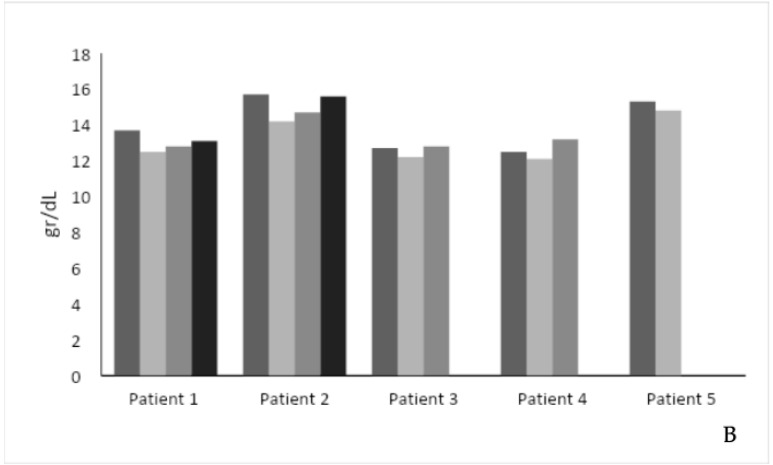

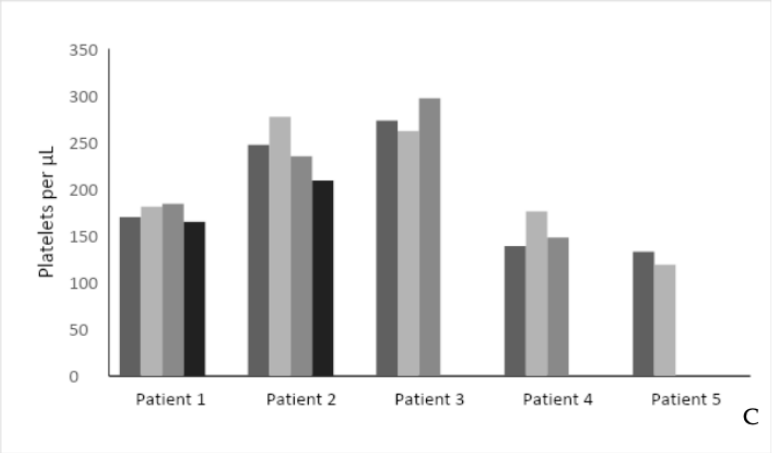

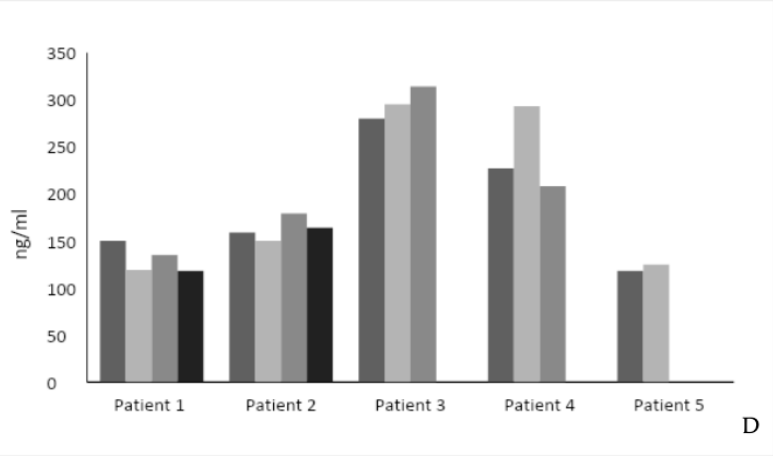

Hurvitz, N., et al. J. Clin. Med. 2024, 13, 3325.

Summary

Benefits of AI Tools in Clinical Research

- **Increased efficiency and cost savings**
  - Streamlines workflows, reduces human error, and accelerates patient recruitment.
- **Improved accuracy and predictive power**
  - Enhances diagnostic precision and early detection of disease patterns.
- **User-friendly interfaces**
  - Promote clinical adoption and improve patient satisfaction through intuitive design.
- **Remote access and monitoring**
  - Supports telemedicine and decentralized trial participation

Lu A, et al., *Journal of the American Medical Informatics Association*, Volume 31, Issue 11, November 2024, Pages 2749–2759,

Drawbacks of AI Tools in Clinical Research

- **Unreliable under data constraints**
  - Limited, heterogeneous datasets reduce robustness and reproducibility
- **Limited generalizability**
  - Models trained on specific datasets may not apply across populations or settings.
- **Algorithmic complexity and “black box” issues**
  - Hinders transparency and clinician trust.
- **Lack of external validation and standardized guidelines**
  - Limits clinical translation and regulatory approval.
- **Added implementation costs**
  - Requires investment in infrastructure, data management, and personnel training.

Lu A, et al., *Journal of the American Medical Informatics Association*, Volume 31, Issue 11, November 2024, Pages 2749–2759,

Challenges in Lysosomal diseases

- **Data limitations:** Rare diseases like lysosomal disorders often have small patient populations, leading to data scarcity and limiting the training and generalizability of AI models
- **Model generalizability:** A model trained on data from one healthcare system may not perform well on data from another due to differences in patient populations and data collection methods, a problem known as "dataset shift"
- **Complexity of models:** Complex models, particularly deep learning, require large datasets to function effectively, which is often not feasible for rare diseases

Germain D P et al. Orphanet J Rare Dis 2025; 20:186.; Olawade D B et al. Int J Med Inform 2026; 206:106141.

Digital Twins for Predictive Modeling in Rare Disease Trials

- Digital twins are virtual models of individual patients that mirror their biological and clinical characteristics over time.
  They allow us to simulate and predict how a patient—or even a population—might respond under different scenarios.
- **Predict future states**
  - interim trial assessment, treatment forecasting
- **Predict intermediate states**
  - adverse or progression events
- **Predict population effects**
  - trial design, inclusion criteria, subgroup simulation

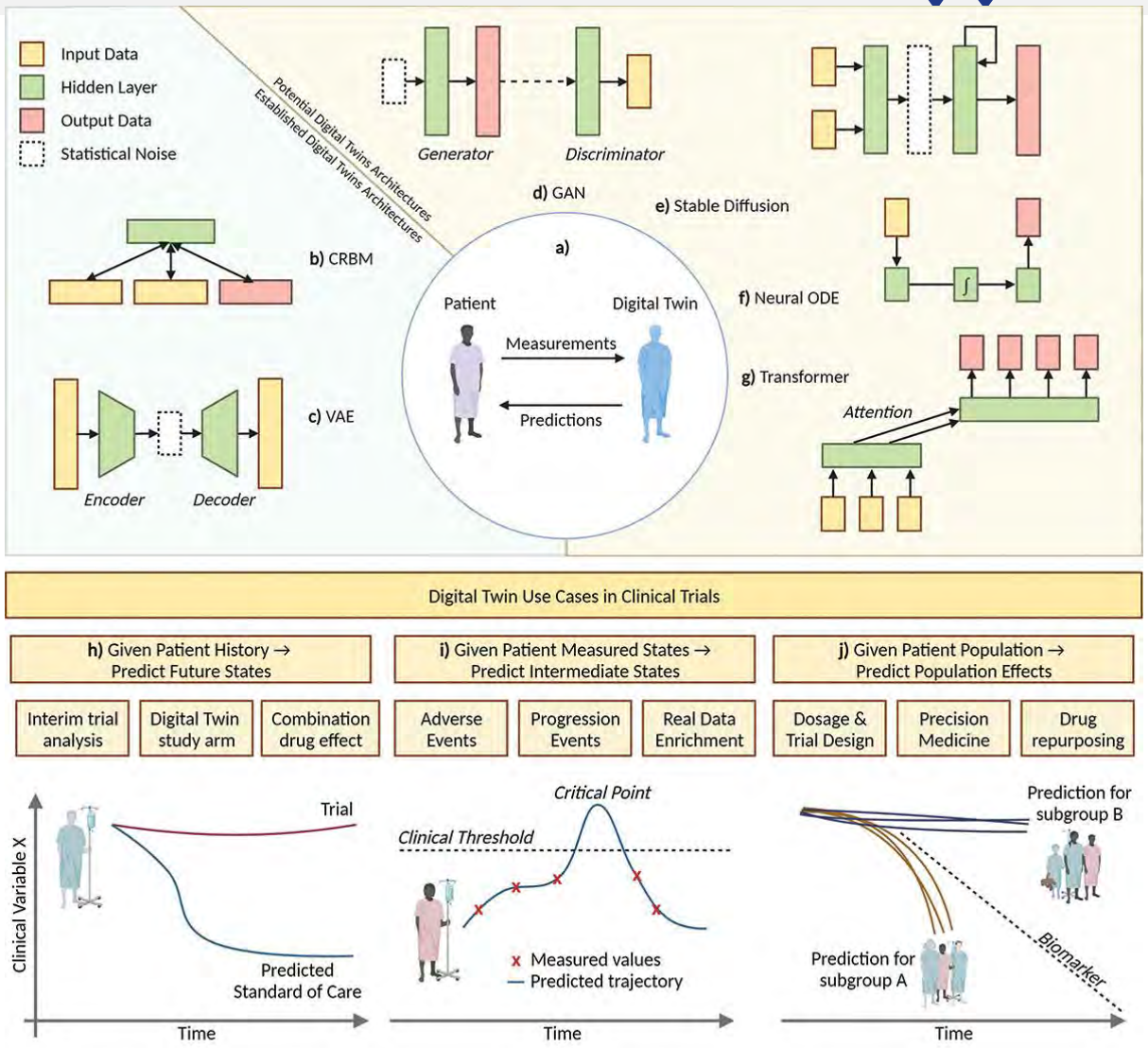

Bordukova, M., et al. 2023;*19*(1), 33–42

Challenges in Lysosomal diseases

- **Need for clinical acceptance and trust:** Patients and clinicians may be hesitant to fully trust AI-based diagnoses or treatment recommendations, particularly when they conflict with a doctor's opinion.

- **Regulatory and ethical hurdles:** Developing and implementing AI in clinical trials requires robust governance structures and clear policies to ensure accountability and mitigate risks

Germain D P et al. *Orphanet J Rare Dis* 2025; 20:186.; Olawade D B et al. *Int J Med Inform* 2026; 206:106141.

Thanks for your attention !

SZMC Gaucher Unit

IWGGD The International Working Group on Gaucher Disease

Supportive care working group

New subgroup working on Digital Health

Please contact me if interested in joining

Srevelvilk@gmail.com

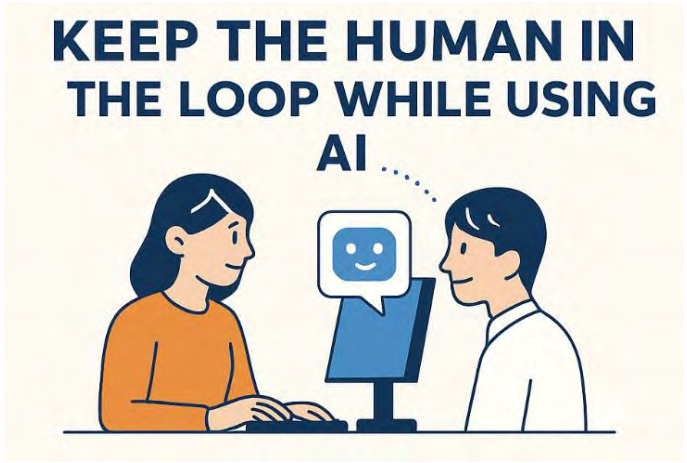

Last slide of your presentation

Program Evaluation and CE Credit

- We need your assistance. Your opinion is important.
- Please go to the link below and help us evaluate the program. You can
- also claim continuing education credit at this link.

- ldrtc.cds.affinityced.com

UNIVERSITY OF CAMBRIDGE

Evaluating osteonecrosis using AI-based technology.

Boliang Yu, Tristan Whitmarsh, Philipp Riede, Scott McDonald, Joshua Kaggie, Timothy M. Cox, Kenneth Poole, Patrick Deegan

and the MRC Gaucherite consortium

B. Yu, T. Whitmarsh, P. Riede, et al., Deep learning-based quantification of osteonecrosis using magnetic resonance images in Gaucher disease, *Bone* (2023), https://doi.org/10.1016/j.bone.2024.117142

Disclosures

- Dr. Deegan is a consultant and advisory board member with Sanofi, Takeda, and Amicis. He also receives research support from Sanofi and Amicus.
- Disclosure will be made when a product is discussed for an unapproved use.
- This continuing education activity is provided by AffinityCE, The Lysosomal and Rare Disorders Research and Treatment Center (LDRTC), and CheckRare CE. AffinityCE adheres to the ACCME's Standards for Integrity and Independence in Accredited Continuing Education. All individuals in a position to control the content of a CME activity are required to disclose all relevant financial relationships with ineligible companies. All relevant financial relationships for anyone in control of content for this activity have been mitigated.
- Monetary commercial supported was received in the form of educational grants from ineligible companies. Please see the final program for a list of all supporters.

Osteonecrosis

- Osteonecrosis is the death of bone tissue. About 43% of adult Gaucher disease patients have a history of ON in the UK. *[Deegan, Medicine, 2011]*
- Osteonecrosis is the most important contributor to loss of quality of life.
- Estimation of prevalence of osteonecrosis is complicated by terminology and definition.
- Here we focus on a radiological definition based on Magnetic Resonance Imaging of the vertebral column and femora.
- It is important to measure osteonecrosis to establish baseline bone disease severity and to optimize treatment.
- Such work may contribute to the debate about standardisation of terminology and measurement.

Magnetic Resonance Imaging of Gaucher Bone

- MR Imaging modality
  - T1w-most sensitive for bone marrow infiltration
    - Water is dark, fat is bright on T1
  - T2w, short tau inversion recovery (STIR)
  - Osteonecrosis has characteristic features on MRI that evolve over time
    - A region of low signal on T1 with a “geographic” outline
    - Often a double-line on T2
    - Areas of low signal on T1 and T2 indicate late sclerosis

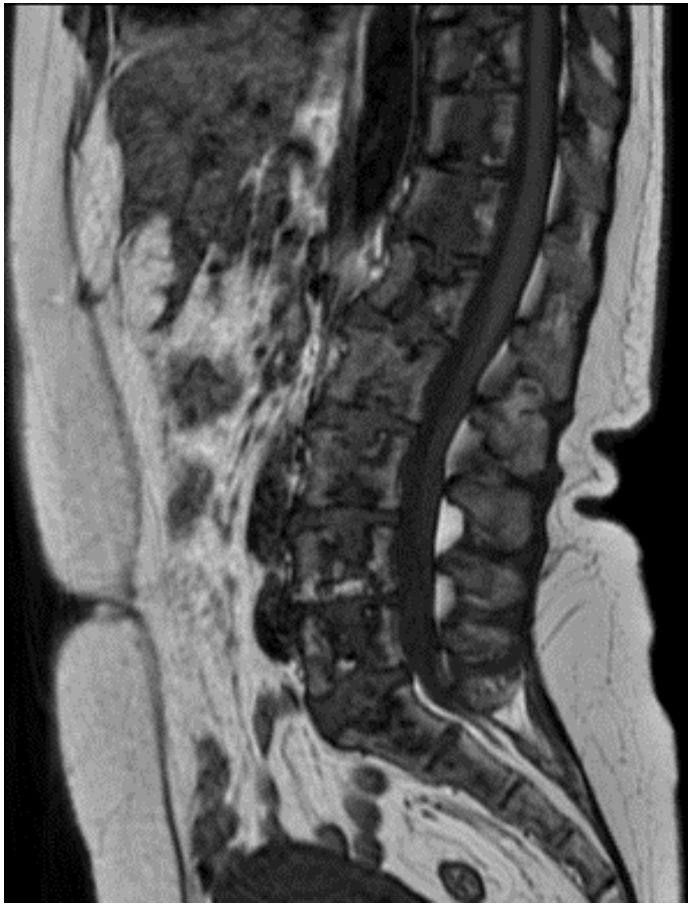

Objectives

- Segmentation of marrow space within spine and femoral T1W images
- Segmentation of osteonecrosis within the marrow space and by subtraction the bone marrow unaffected by osteonecrosis (UBM).
- 3D volumetric recreation from individual image slices
- Volumetric quantification of osteonecrosis
- Correlation with clinical risk factors for osteonecrosis

Segmentation of osteonecrosis and UBM

- Gaucherite study image database
  - 250 patients from 8 UK centres gave consent to Gaucherite study

	Patients	T1w images	Manual Seg
Total	217	917	344
Spine	212	520	176
Femur	145	397	168

- Datasets split

	Total	Train	Validation	Test
Spine	176	111	32	33
Femur	168	121	25	22

Manual segmentation

- Carried out on 344 MR studies, each with multiple slices
- 18 months work for an experienced image analyst
- Based on rules agreed with radiologists and clinicians, in turn based on recognized MR appearances of osteonecrosis.
- Focus on defining the border between affected and unaffected marrow
- Iterative process based on any emergent questions / concerns
  - Agreed to limit analysis of full width of sacrum
  - Set minimum volume of region of osteonecrosis
  - Weighting given to confluency and to appearance of adjacent slices
  - Heterogenous Marrow

Training of Automatic Segmentation

- U-Net model with EfficientNet encoder

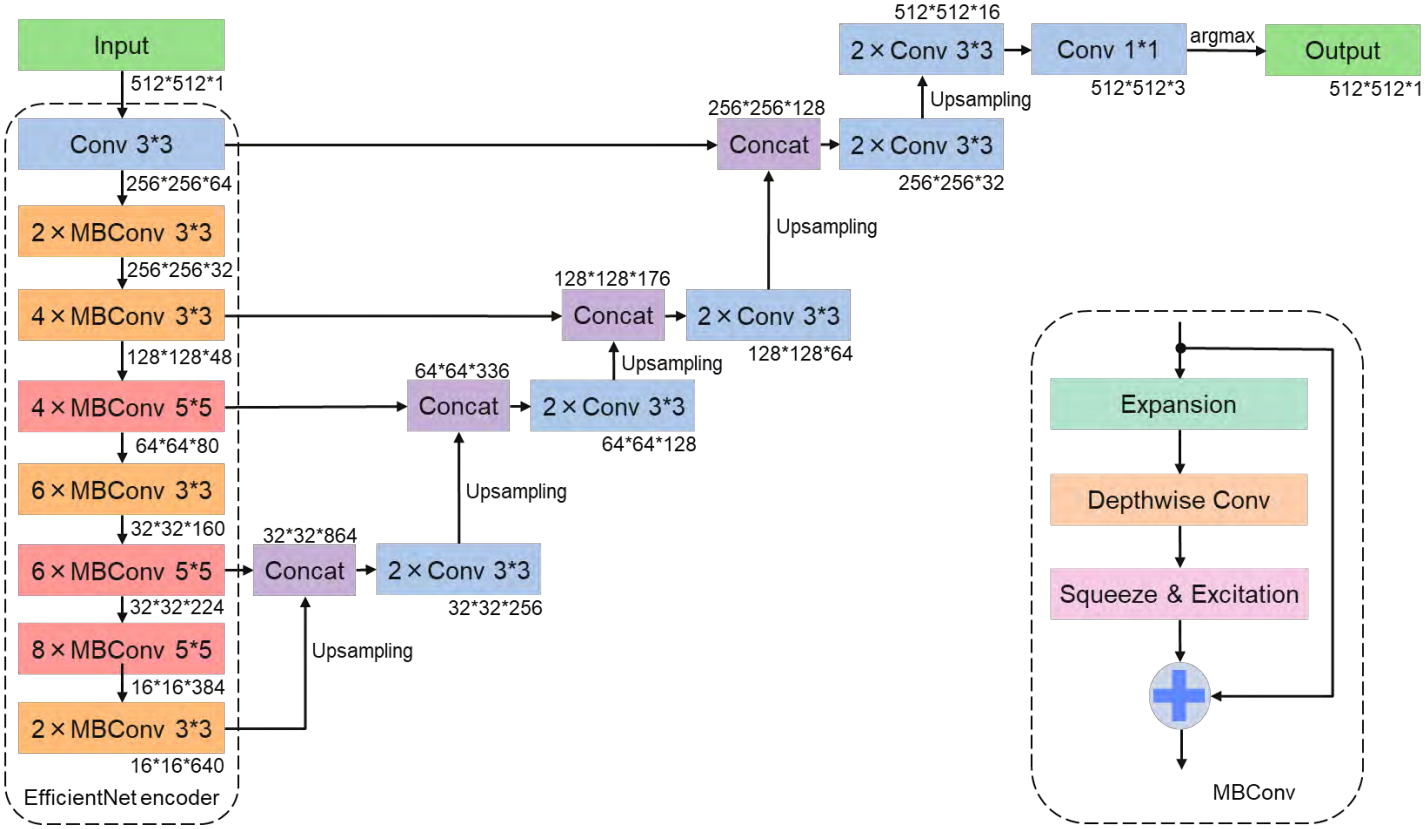

Segmentation of spine in test datasets

GAU007_20170815132011_3

GAU250_20160225182335_10

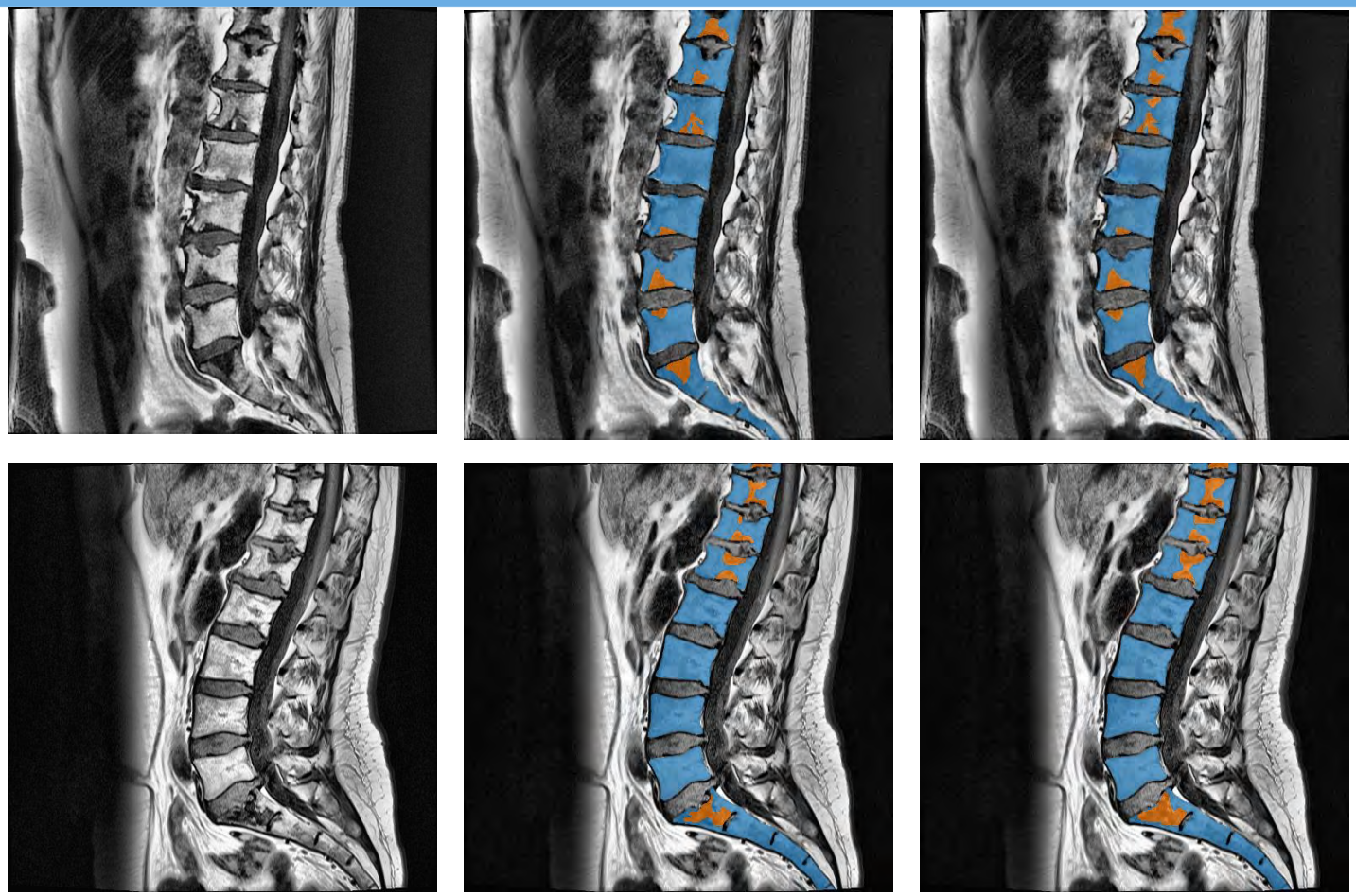

Original slice

Ground truth (Manual Segmentation)

Automatic segmentation

Segmentation of femur in test datasets

GAU050_20190312113219_7

GAU193_20130325160241_301

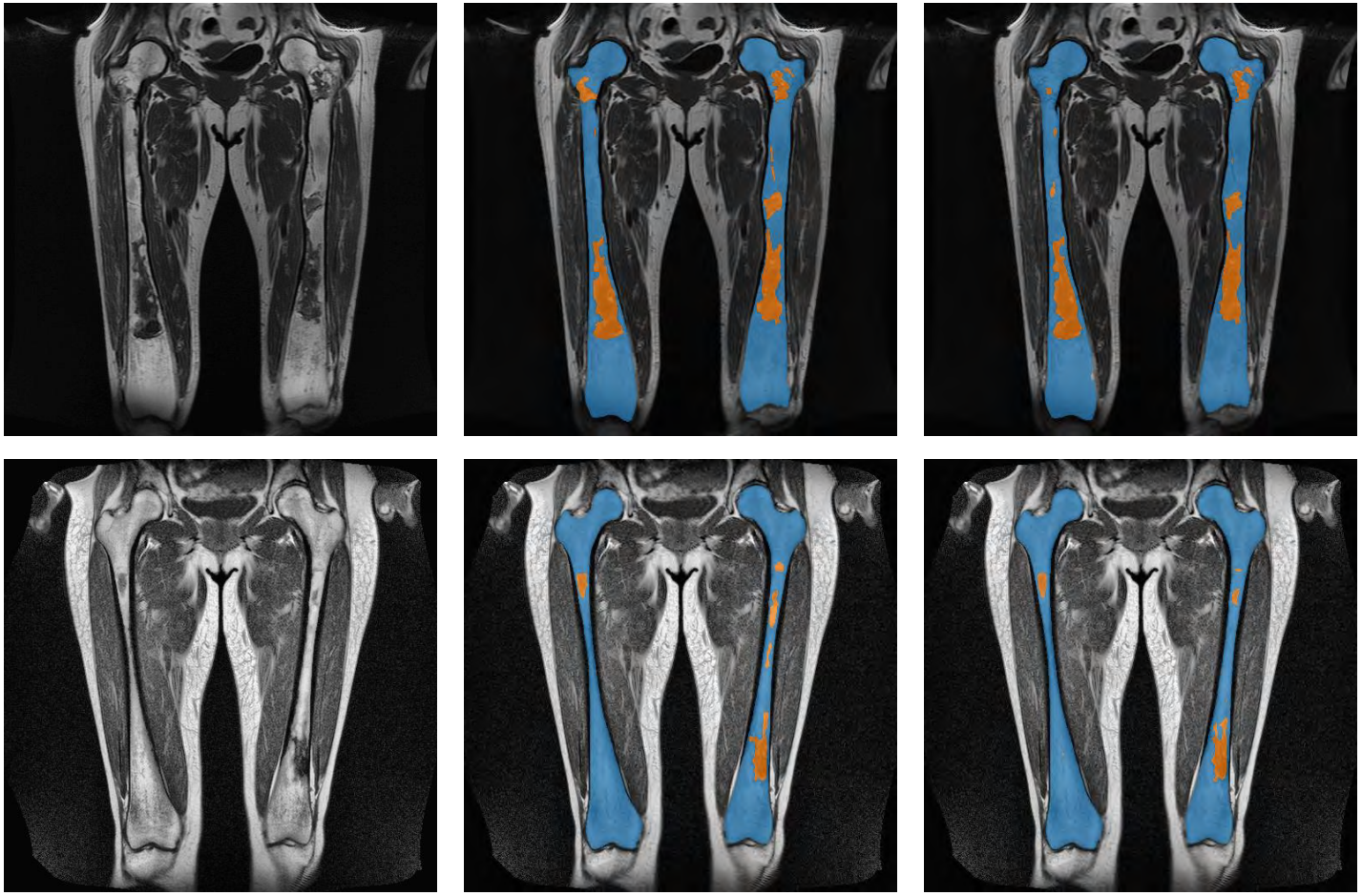

Original slice | Ground truth (Manual Segmentation) | Automatic segmentation

Segmentation of spine images

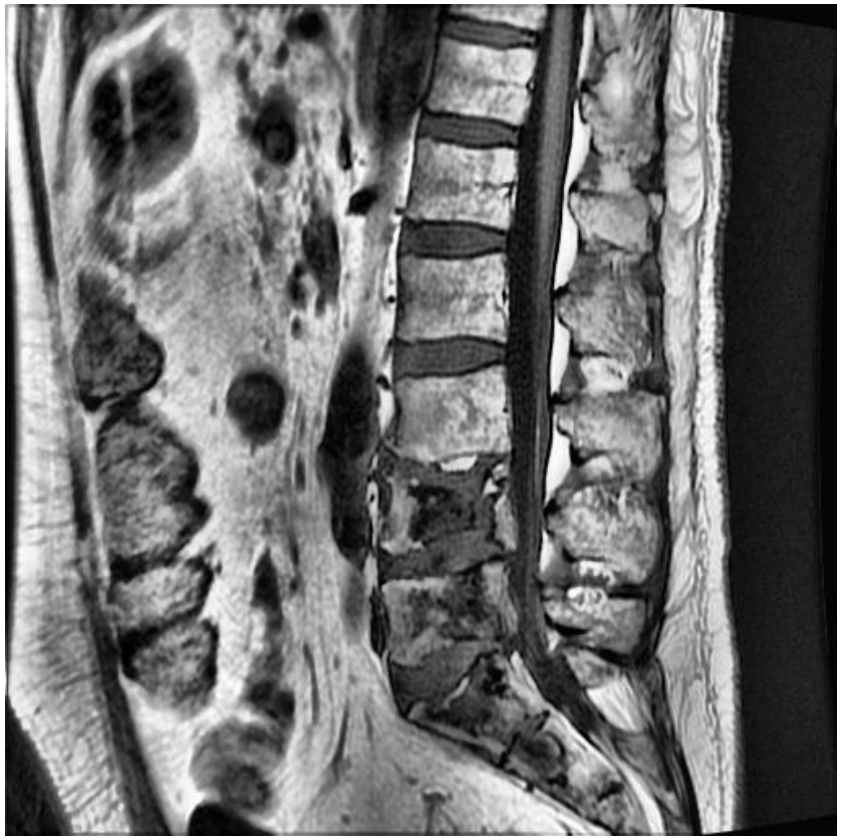

Original slice

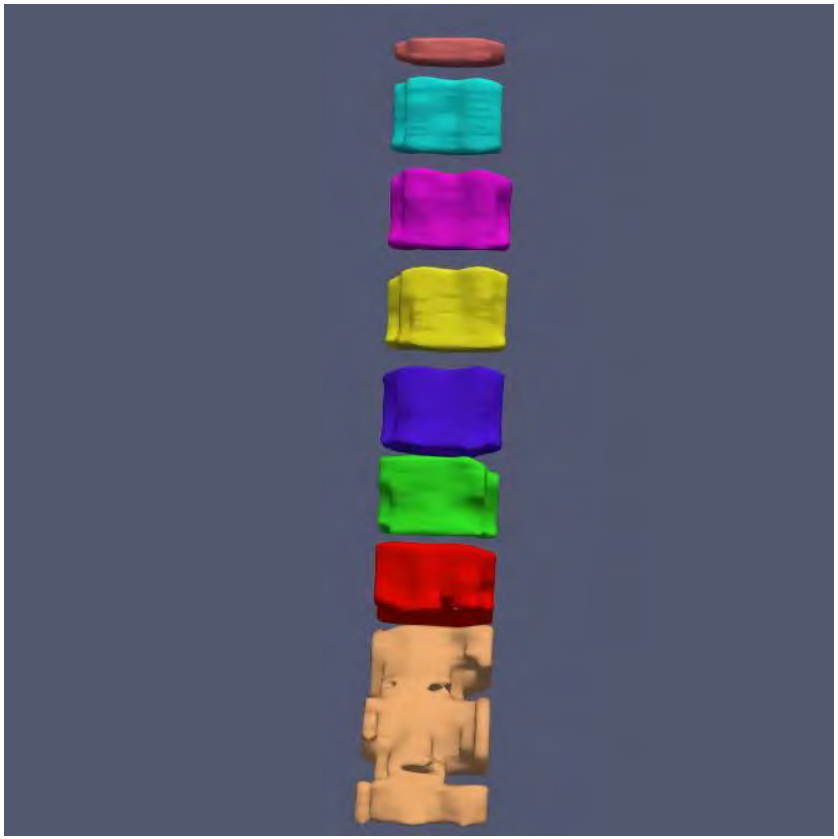

3D rendering

Segmentation of femur images

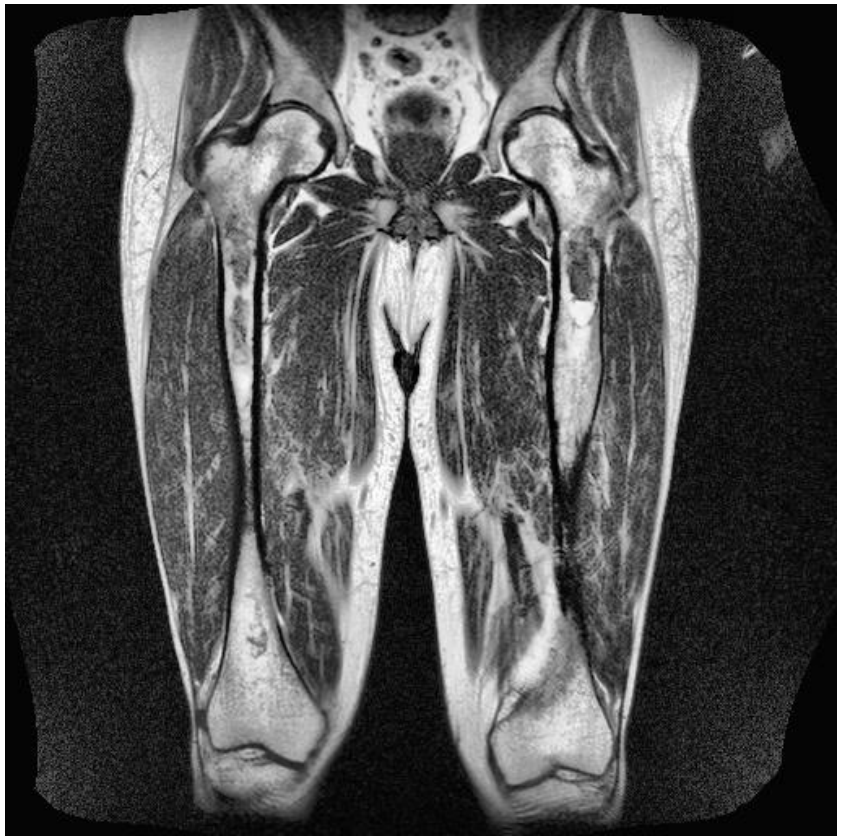

Original slice

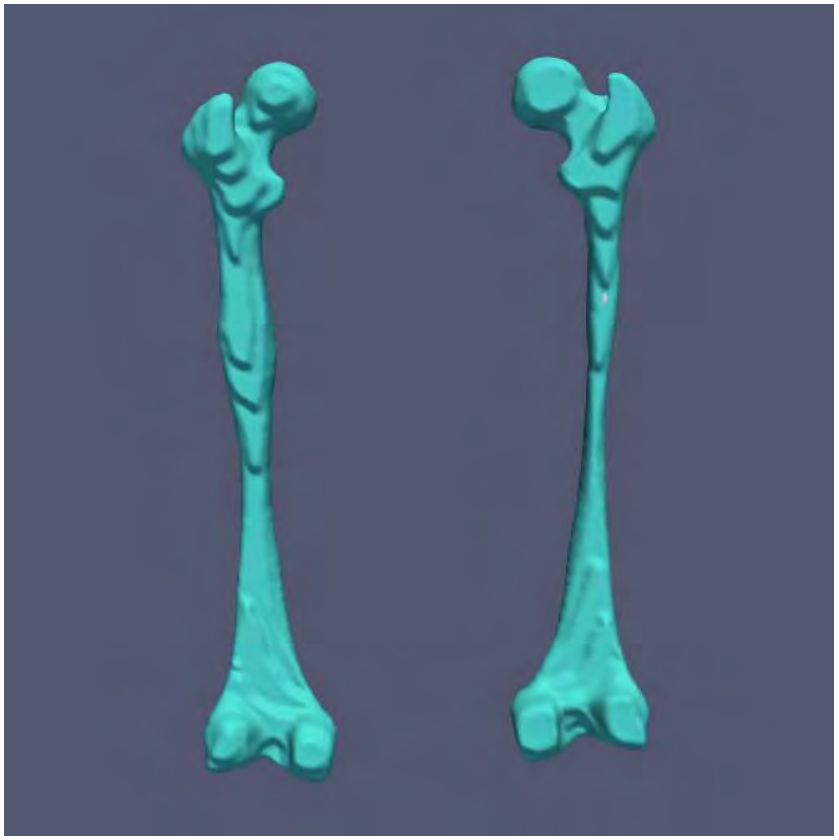

3D rendering

Potential Confounder: Heterogeneous Marrow

2012
Before ERT

2019
ON ERT

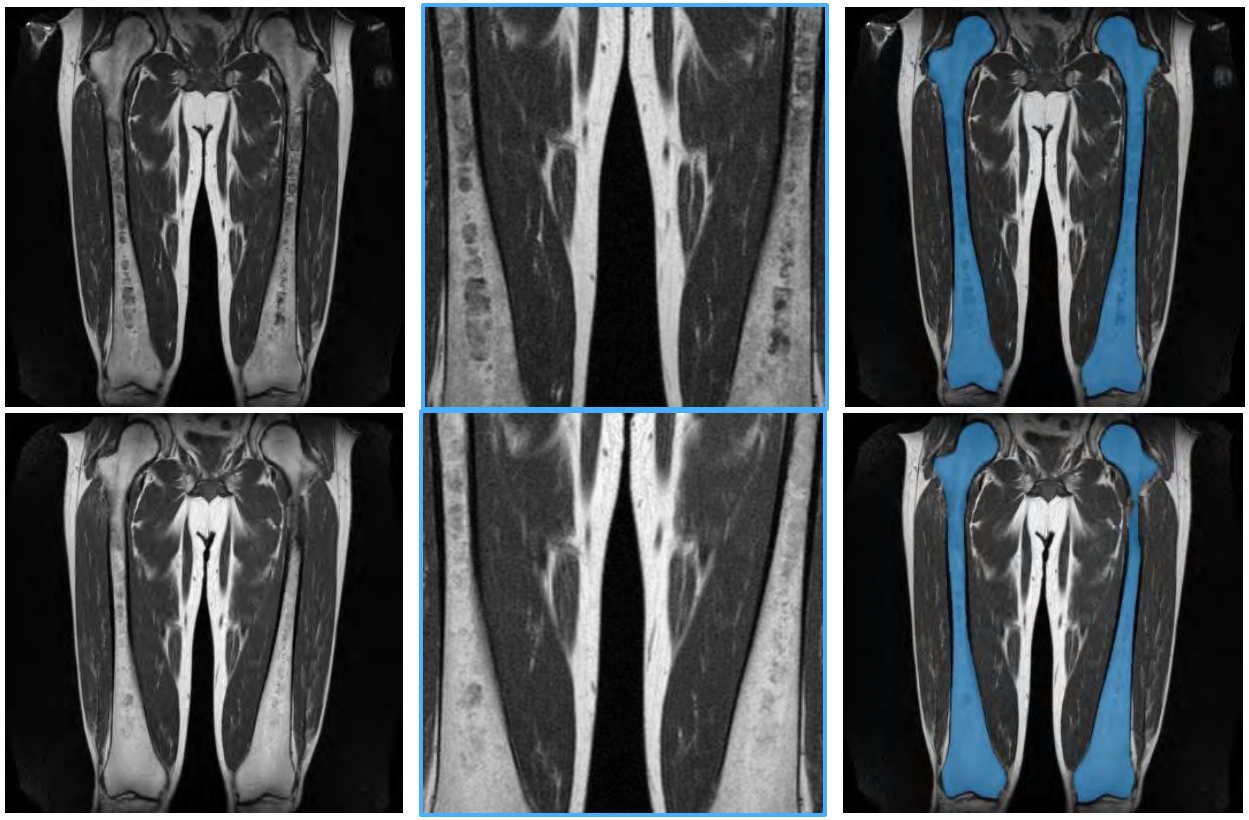

Evaluation of segmentation accuracy

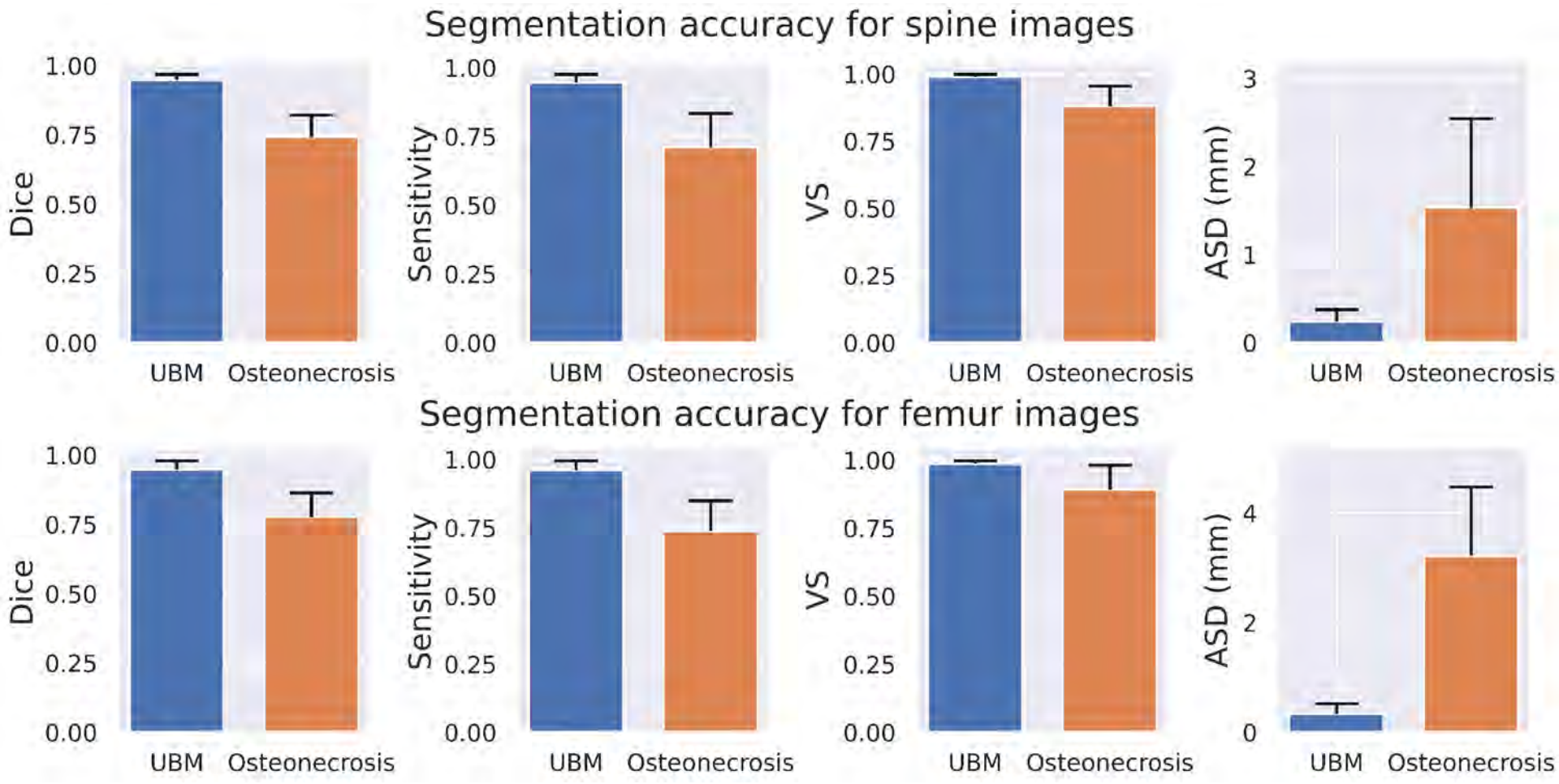

Quantitative analysis

- Quantification of osteonecrosis and UBM
  - ON.V, UBM.V, ON.F (ON.V/(ON.V+UBM.V))

MR studies were divided according to the presence or absence of ON, based on a threshold ON fraction of 0.001

	Total (n)	ON (n)	ON.V	UBM.V	ON.F
Spine	520	97	19.620±16.029	222.856±52.356	0.080±0.063
Femur	397	99	78.138±58.722	662.792±139.232	0.105±0.074

Relationship between osteonecrosis and splenectomy – strong effect in spine

P<0.001

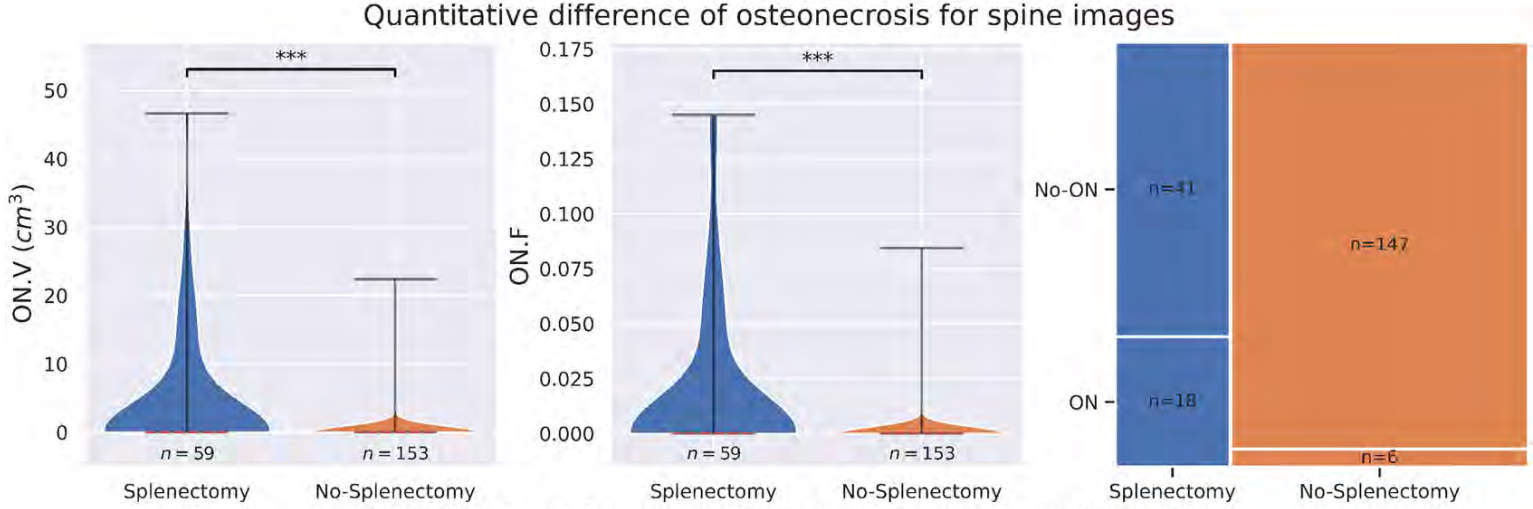

P<0.000001

P<0.05

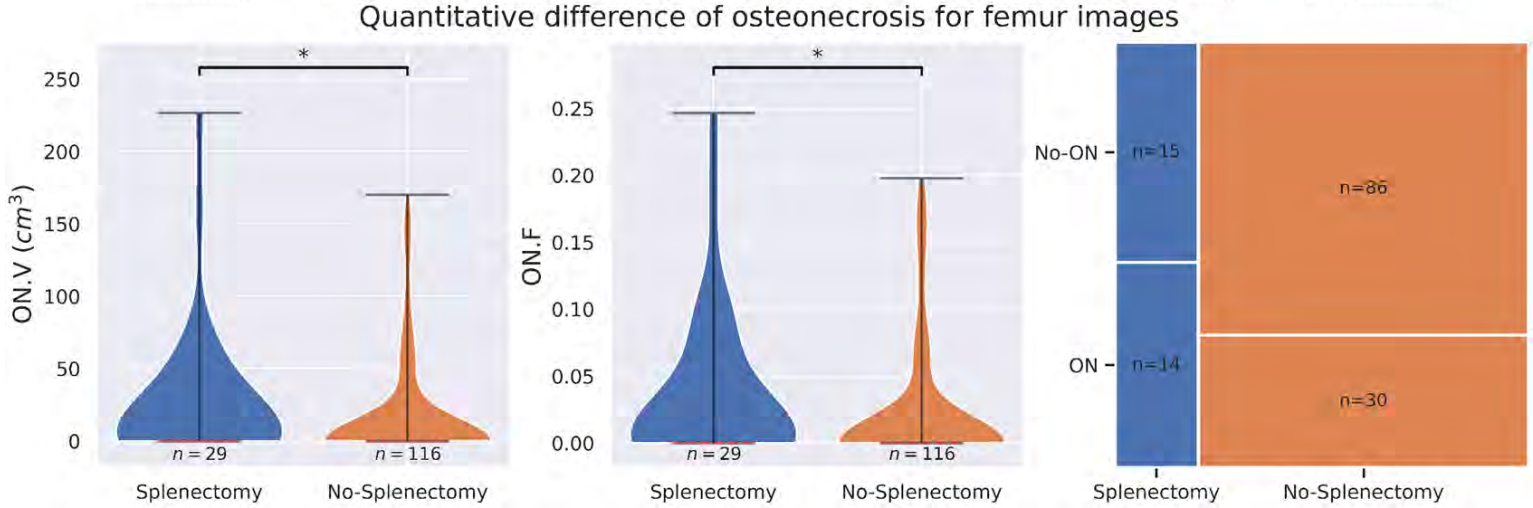

P<0.05

Relationship between osteonecrosis and untreated disease duration

P<0.001

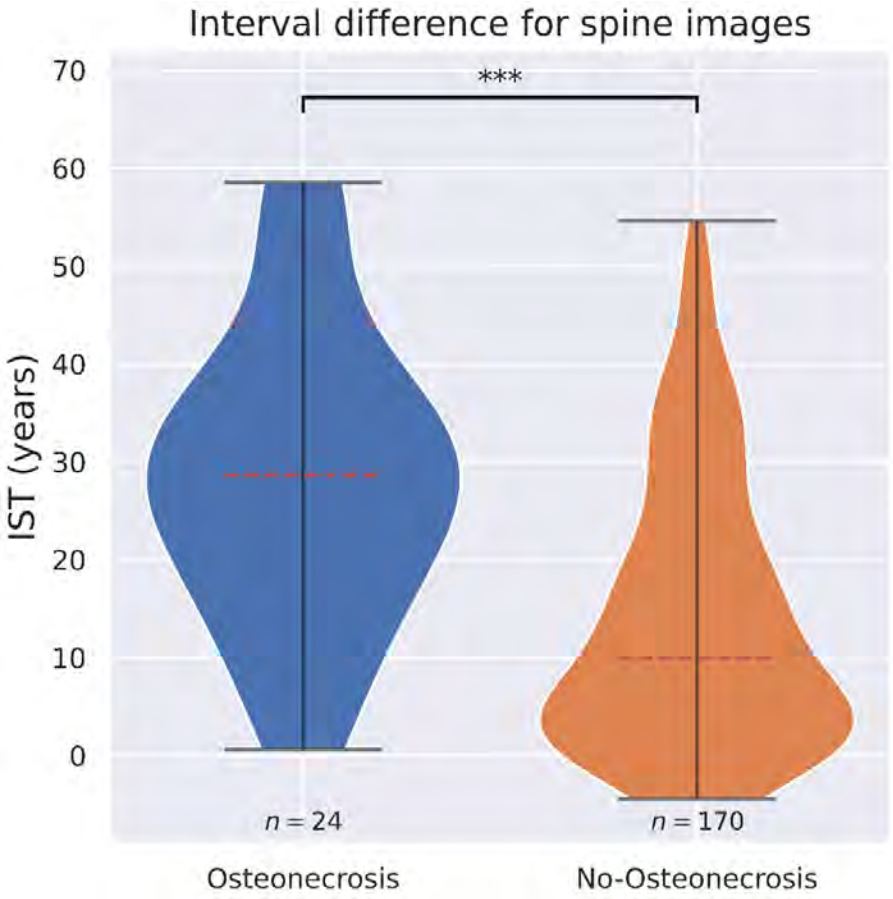

P<0.001

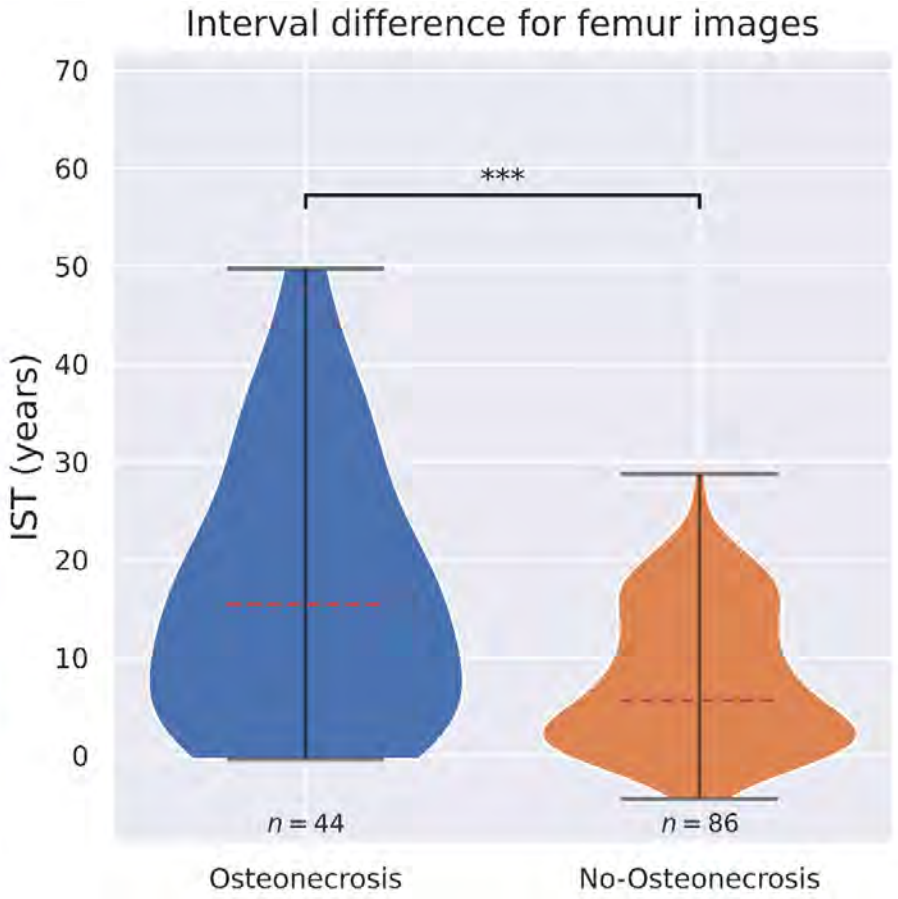

Correlation with BMB score in femur only

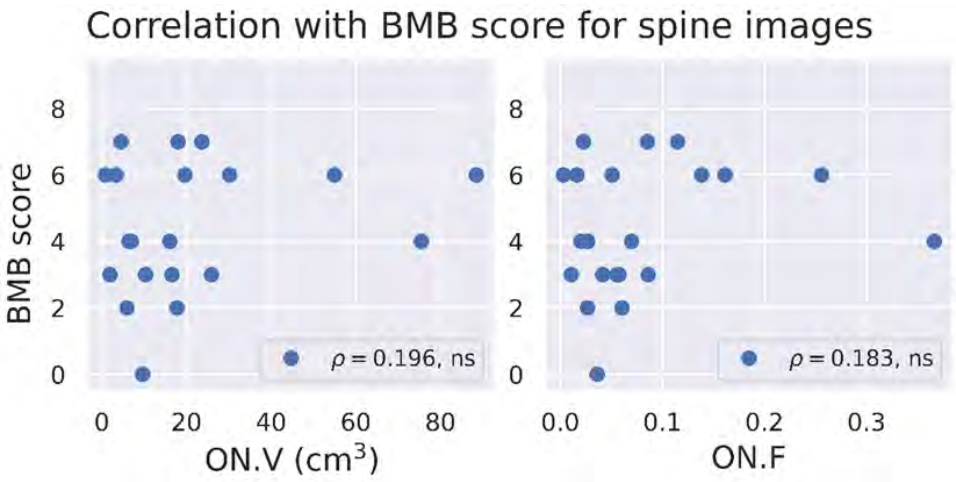

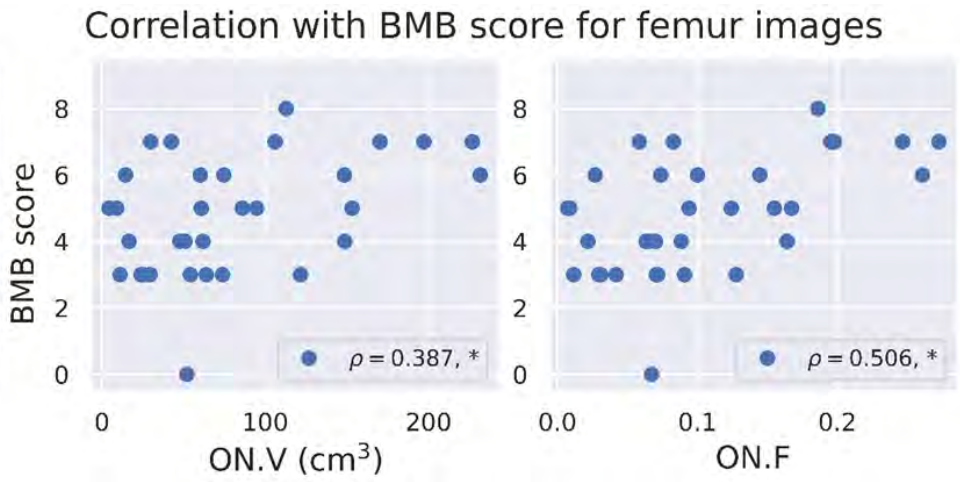

P<0.05

Caveats

- Validity for longitudinal analysis needs more work – effect of evolving MR technology and changes in scanning protocol
- Dependent on original definition of osteonecrosis and the resulting “rules” to guide manual segmentation
- Segmentation of anatomical boundaries more precise than boundaries between diseased and non-diseased tissues

Summary

- Here we demonstrate a new method to quantify osteonecrosis using machine learning
- The method shows good agreement with manual segmentation
- Replication of established risk factors serves as initial clinical validation
- Risk factors for ON at spine and hip are subtly different

Acknowledgements

- This research was supported by an independent Investigator Sponsored Study Award from Aventis Sanofi (TMC and PD). Deeply phenotyped clinical data and images were obtained through the clinical consortium. The UK Medical Research Council funded the cohort development and initial analytical studies (2013-9) under the Stratified Medicine Programme scheme, (Gaucherite, MR/K015338/1) later partially co-funded by the National Institute for Health Research (NIHR) Cambridge Biomedical Research Centre (Grant Number IS-BRC-1215-20014). An add-on contribution to independent statistical support (KT) was kindly donated by Shire International GmbH (2018-9).
- The Gaucherite Consortium: T M Cox (Chief Investigator, Dept Medicine University of Cambridge) & F M Platt (Co-Principal Investigator, Dept of Pharmacology, University of Oxford); A Chakrapani, P B Deegan, T Geberhiwot, D A Hughes, S Jones, R H Lachmann, S Santra, R Sharma, A Vellodi (Great Ormond Street Hospital, London).

Assessment of Bone Involvement in Gaucher Disease Using Advanced Imaging & AI

Ravi S. Kamath, MD, PhD
Fairfax Radiological Consultants & Inova Health System
University of Virginia School of Medicine
Fairfax, Virginia, USA

FAIRFAX RADIOLOGY CENTERS

INOVA®

UNIVERSITY of VIRGINIA

Disclosures

- Dr. Kamath is on an advisory board for Intrinsic Therapeutics. He is also a consultant for Sanofi, Takeda, and Spur Therapeutics.

- Disclosure will be made when a product is discussed for an unapproved use.

- This continuing education activity is provided by AffinityCE and The Lysosomal and Rare Disorders Research and Treatment Center (LDRTC) and CheckRare CE. AffinityCE, CheckRare CE, and LDRTC staff, planners, and reviewers, have no relevant financial relationships with ineligible companies to disclose. AffinityCE adheres to the ACCME's Standards for Integrity and Independence in Accredited Continuing Education. Any individuals in a position to control the content of a CME activity, including faculty, planners, reviewers, or others, are required to disclose all relevant financial relationships with ineligible companies. All relevant financial relationships, when present, have been mitigated by the peer review of content by non-conflicted reviewers prior to the commencement of the activity.

- This activity has been supported by educational grants from commercial supporters. Please see the final program for a list of all supporters.

Learning Objectives

- At the conclusion of this activity, participants should be able to

1. Recognize the imaging features of Gaucher disease on x-ray and MRI
2. Discuss the potential benefits of artificial intelligence and machine learning applied to imaging of Gaucher patients
3. Explain the term radiomics and the advantages this offers over conventional imaging techniques
4. Describe new and advanced imaging techniques for the assessment of bone density and risk of fragility fracture

Outline

- Imaging of Gaucher bone disease
  - MRI, comparison of X-ray and MRI
- AI & machine learning in radiology
  - Definitions, radiomics
- Applications of AI & advanced imaging
  - Fracture
  - Osteonecrosis
  - Bone lesions
  - Dark marrow

Gaucher Disease

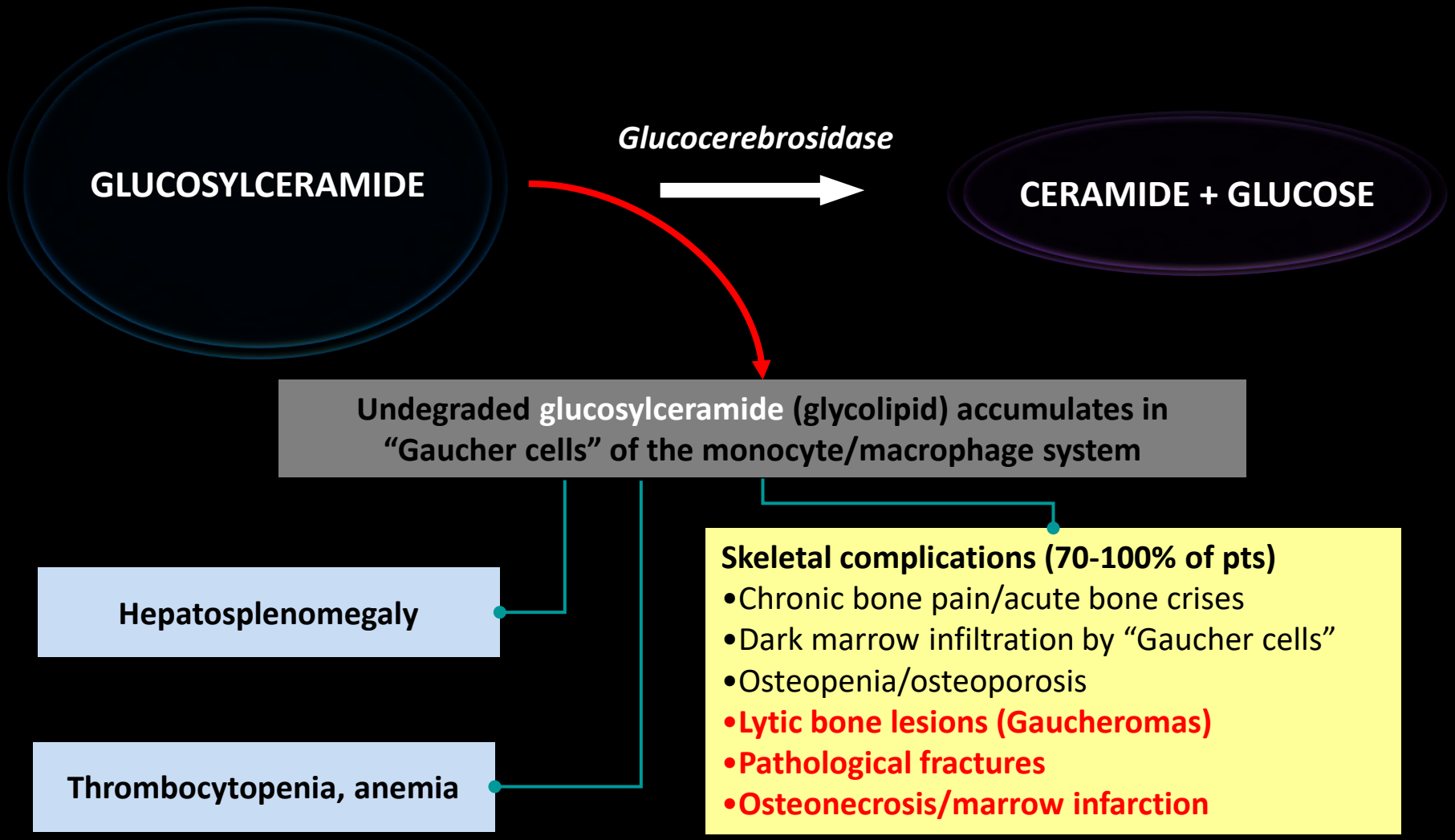

Imaging of Gaucher Bone Disease

Radiographs (X-rays)	MRI	DEXA
Fracture	Fracture	
Osteonecrosis/marrow infarction	Osteonecrosis/marrow infarction	
Bone lesions	Bone lesions	
Bone remodeling (e.g. Erlenmeyer flask deformity)	Bone remodeling (e.g. Erlenmeyer flask deformity)	
Hardware/prosthesis imaging	Hardware/prosthesis imaging	
Cortical thinning/tunneling (osteopenia/osteoporosis)	**Dark marrow** (and quantitative imaging)	**Bone mineral density** (osteopenia/osteoporosis)

MRI of Gaucher Disease

- On MRI, marrow infiltrated with Gaucher cells typically appears hypointense (dark) on both T1- and T2-weighted images (‘dark marrow’)
- Very sensitive for detecting major bone complications: fracture, osteonecrosis/marrow infarction, lytic bone lesions

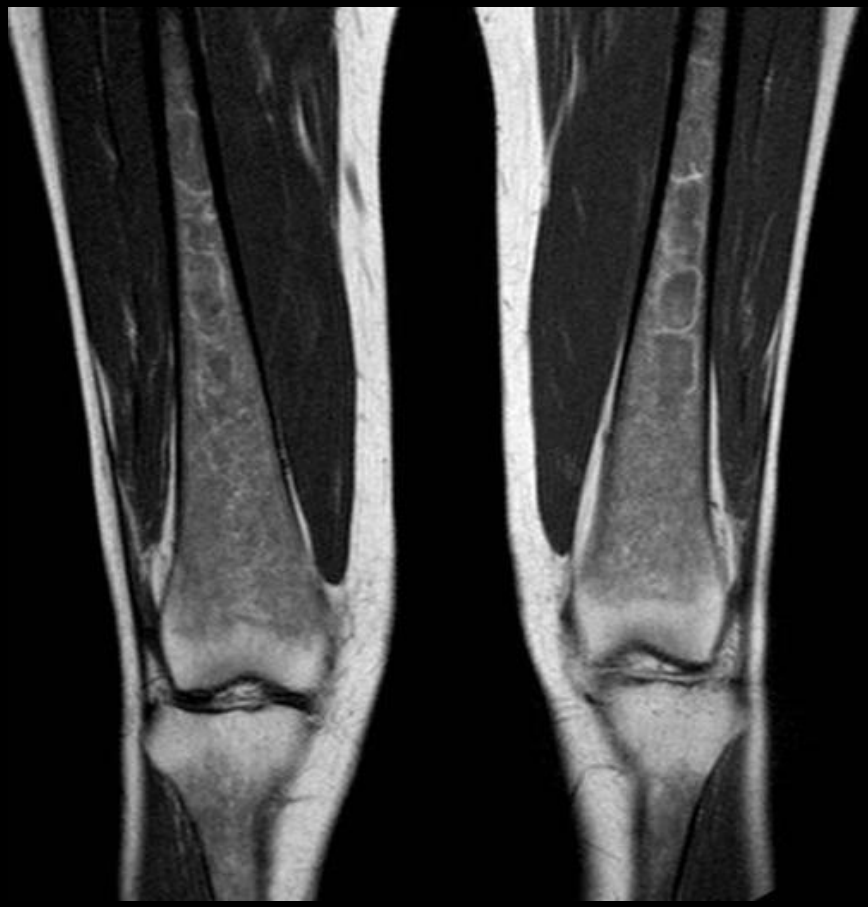

MRI: Femurs

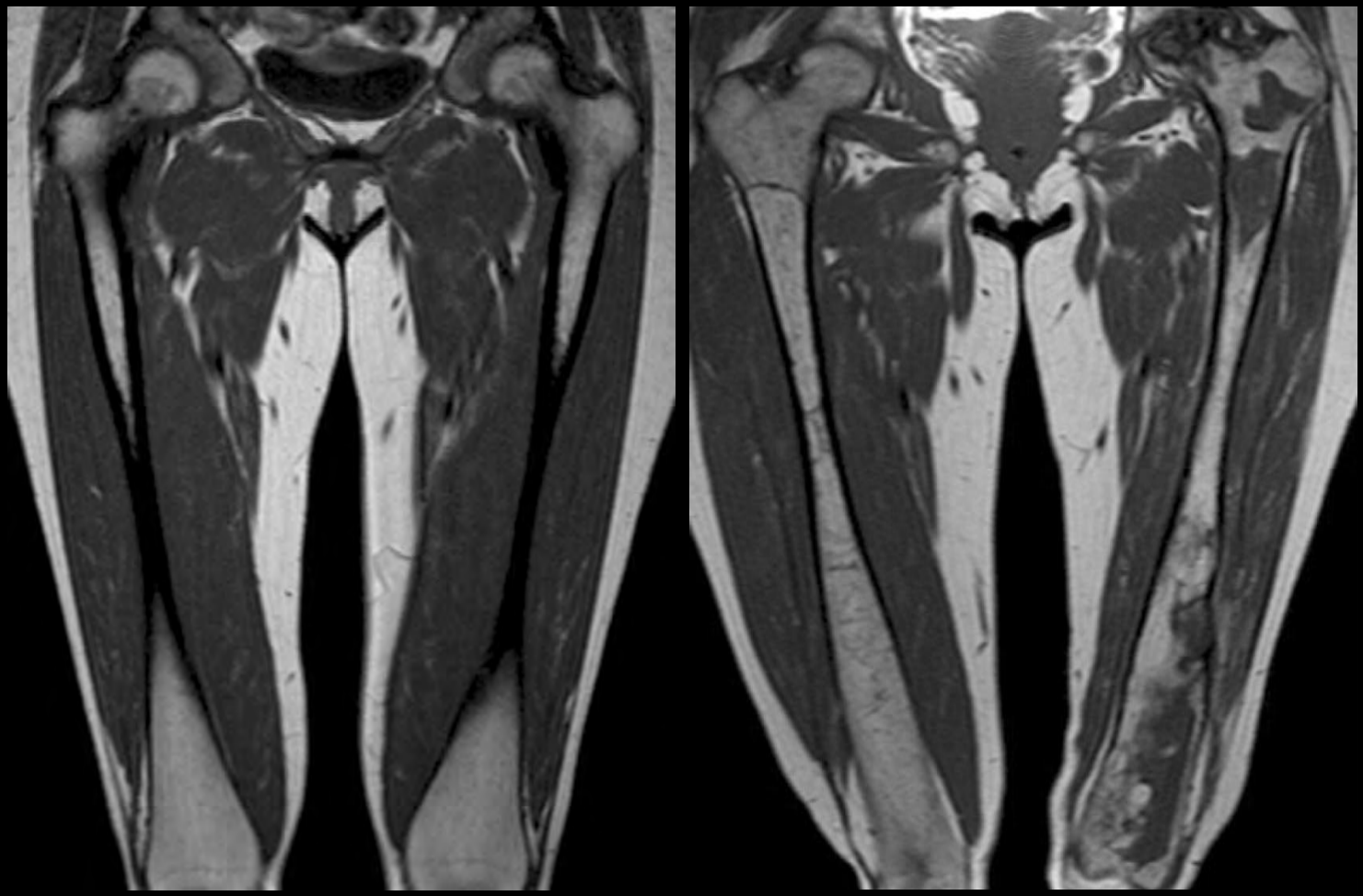

MRI: Lumbar Spine

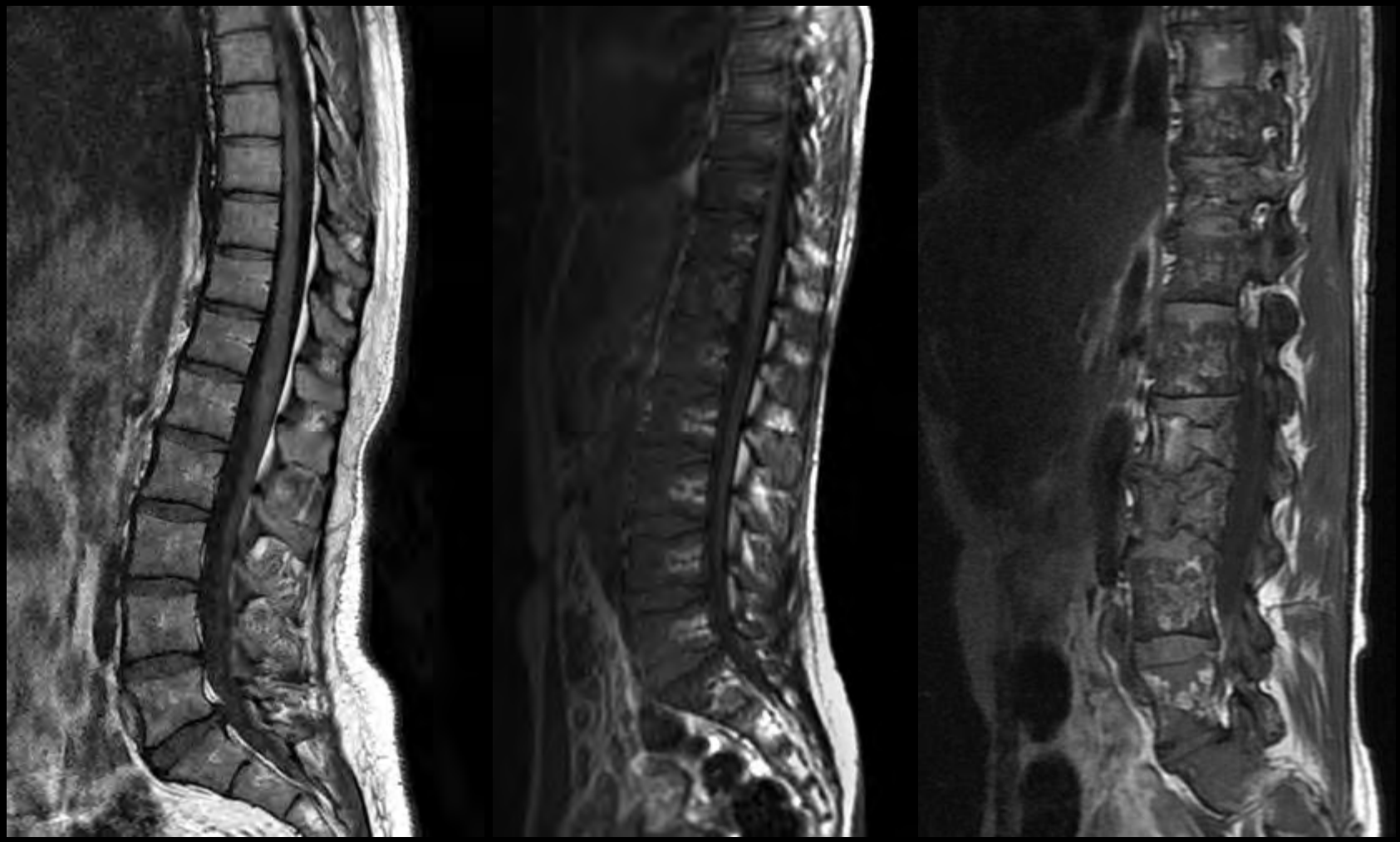

MRI Marrow Change with Therapy

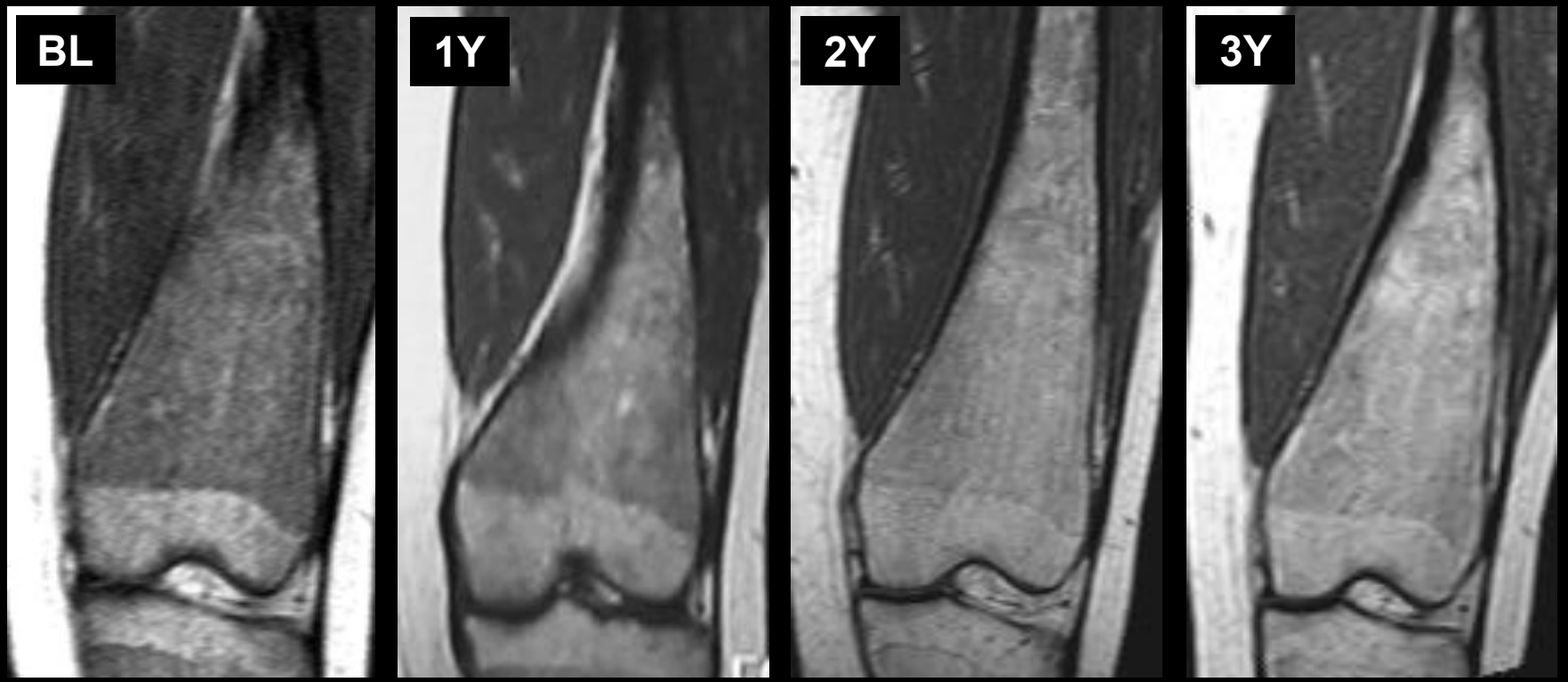

Roughly 60-70% of patients demonstrate bone marrow improvement with medical treatment

From Kamath *et al.*, *Skel Radiol* 2014; 43: 1353-1360.

X-Ray vs MRI: Dark Marrow

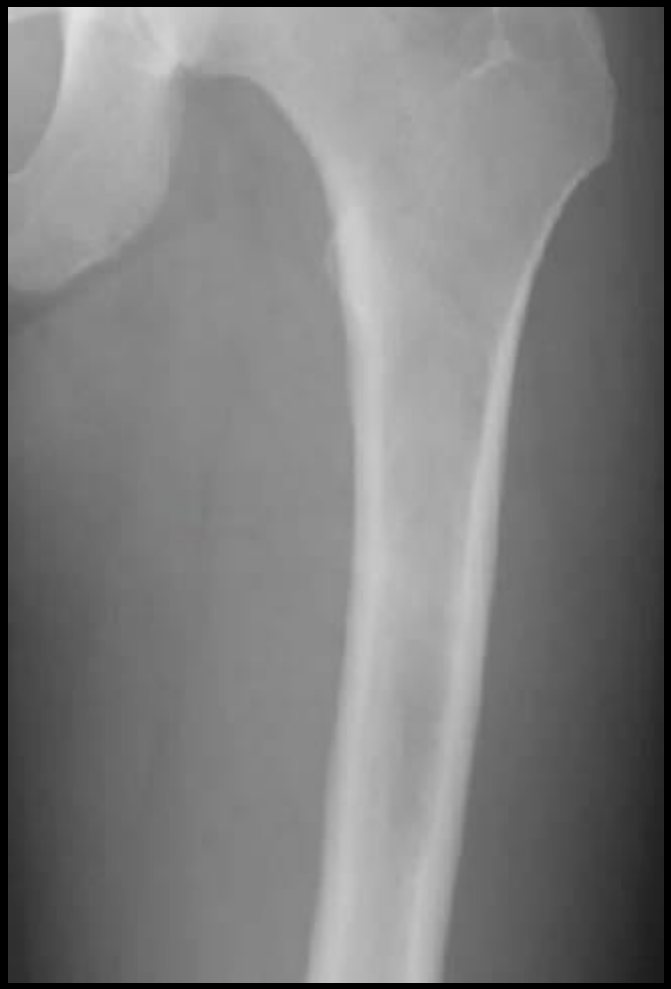

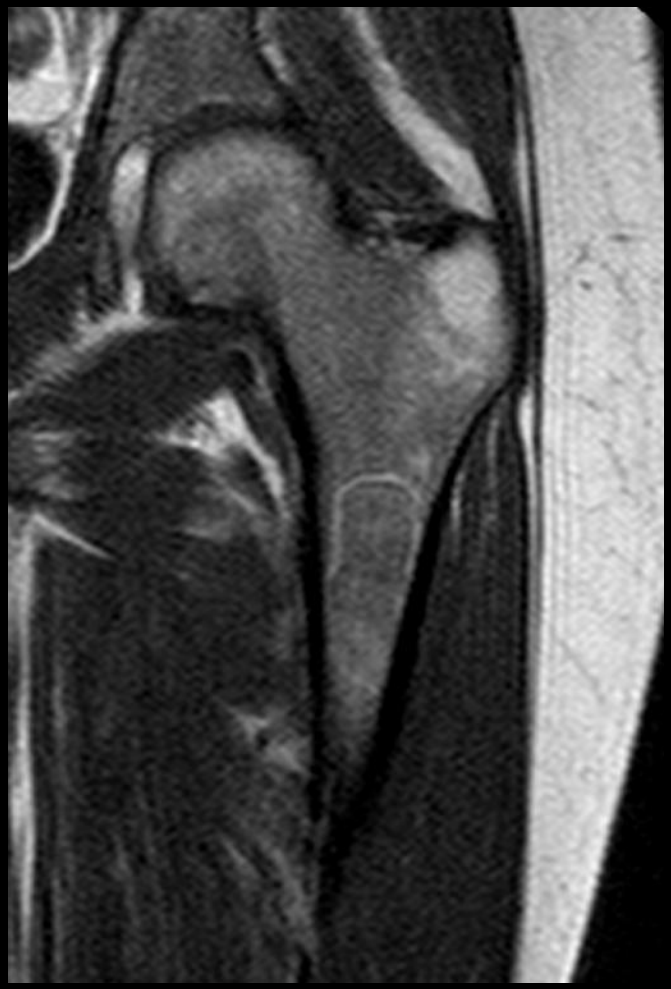

X-Ray vs MRI: Fracture

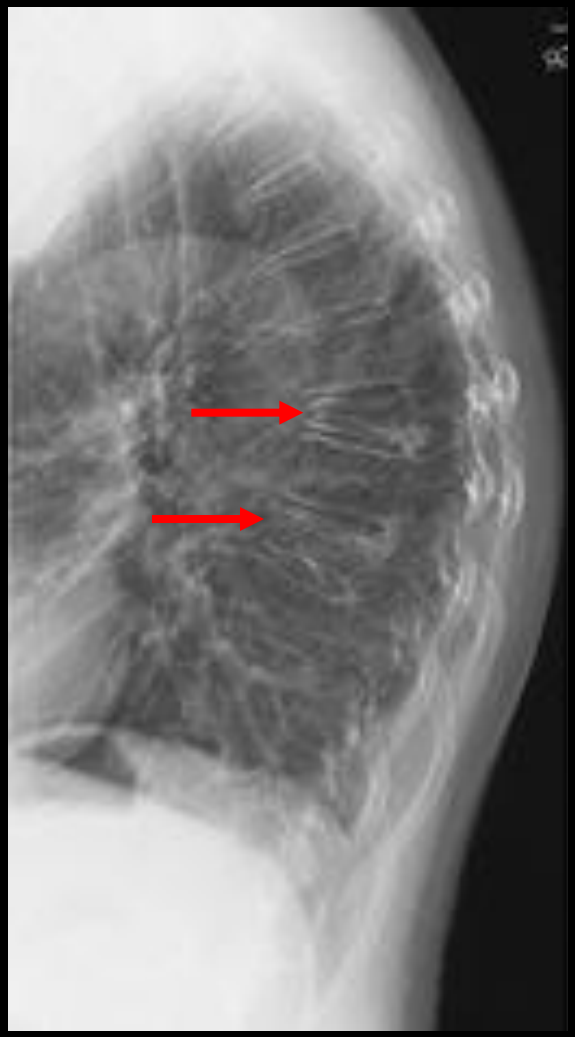

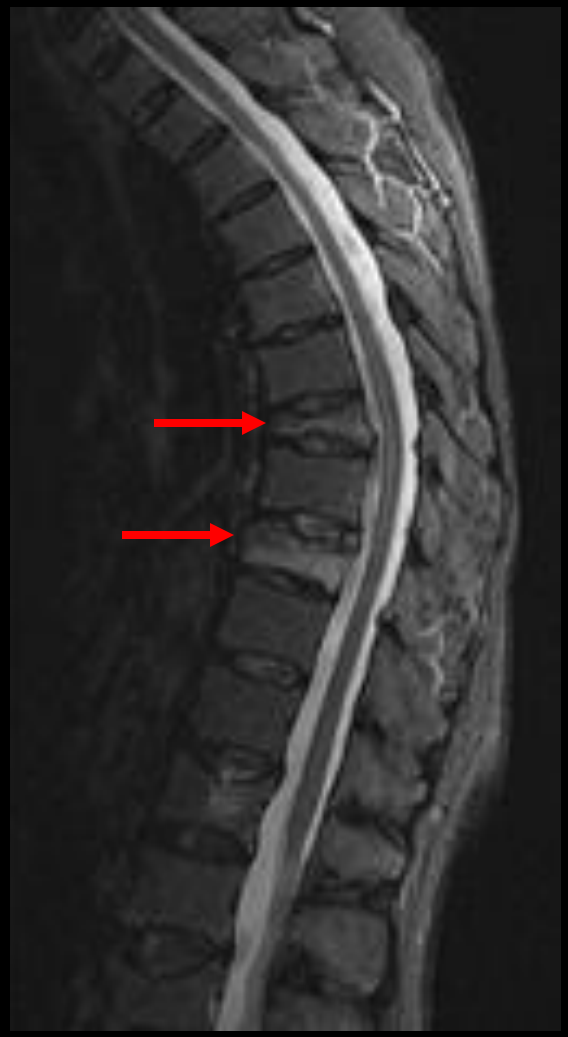

X-Ray vs MRI: Osteonecrosis

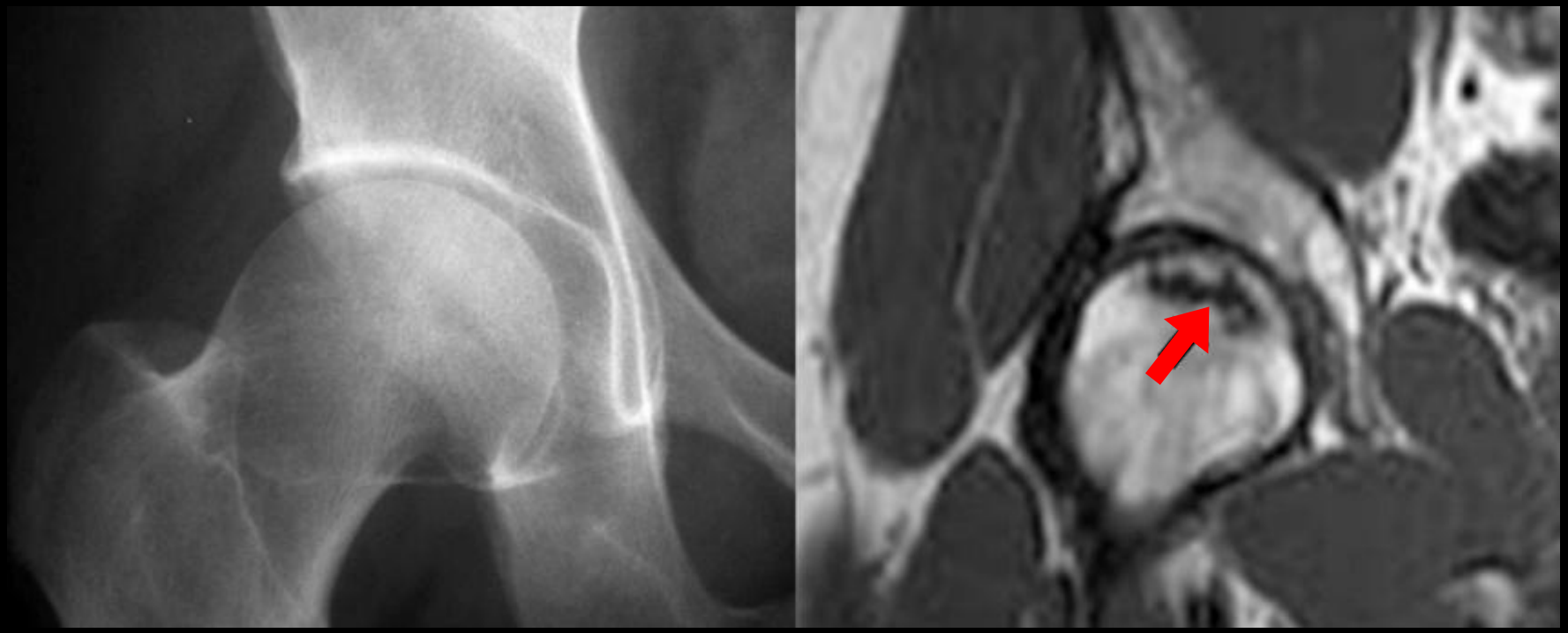

X-Ray vs MRI: Osteonecrosis

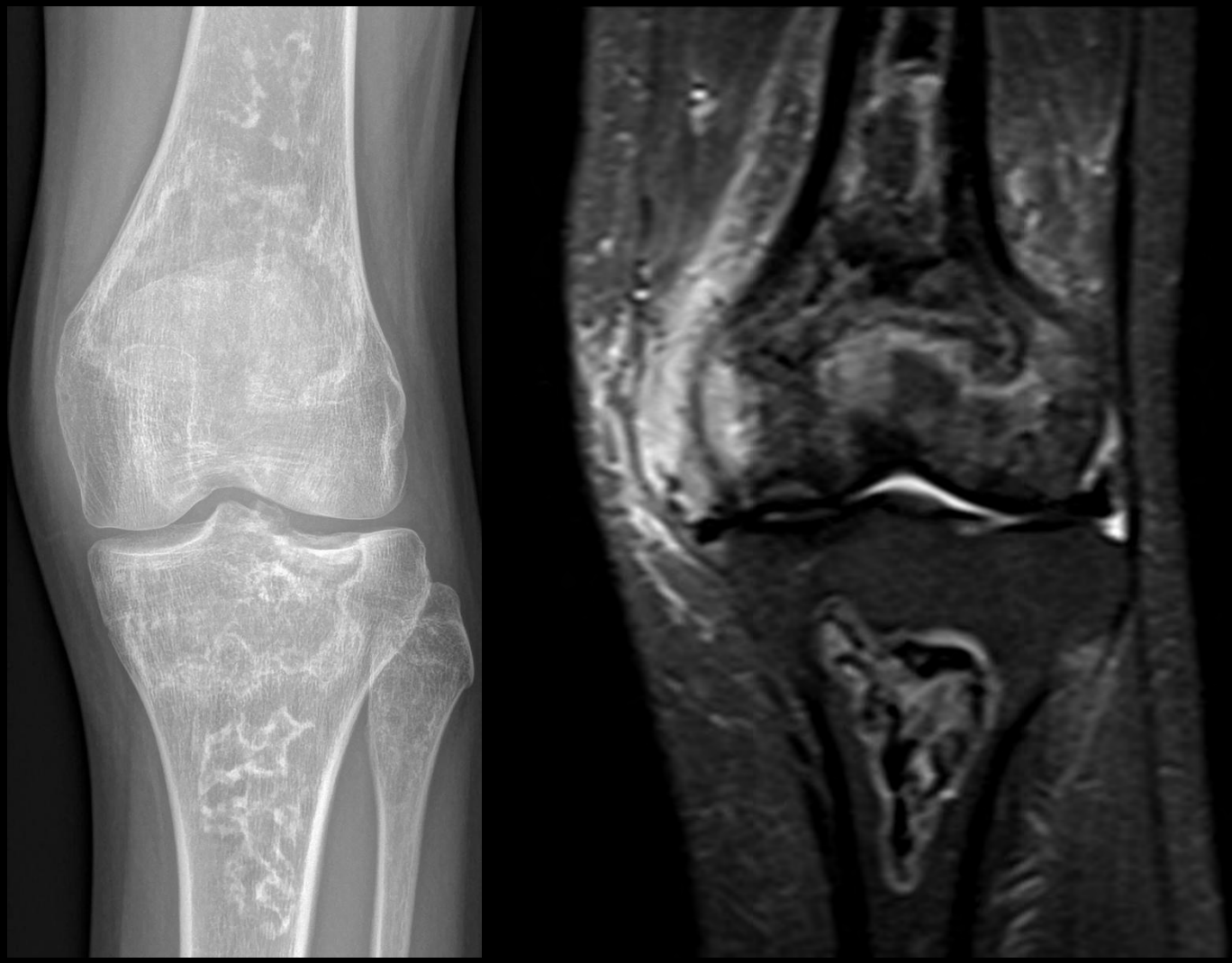

X-Ray vs MRI: Bone Lesion

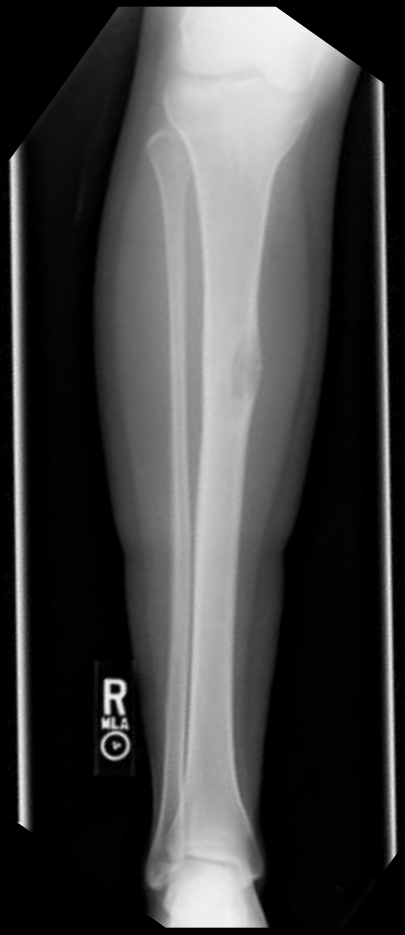

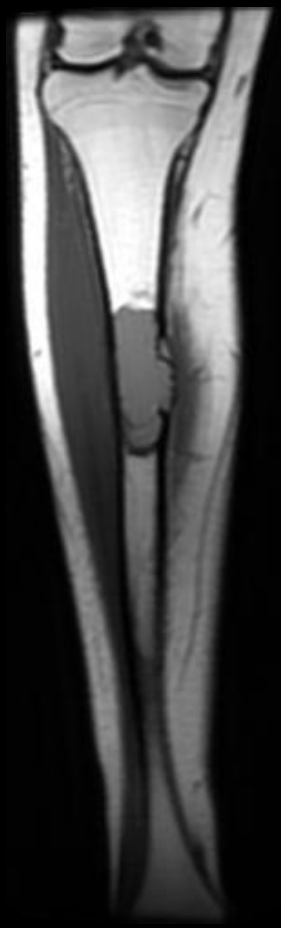

AI & Machine Learning in Imaging

Definitions

- Artificial intelligence (AI): broad term for computer-based systems that mimic human intelligence when performing human tasks

- Machine learning (ML): sub-field of AI that allows computers to learn and adapt by drawing inferences from patterns in data without following explicit instructions, uses observations from data to create algorithms and then employs these to determine future output with the goal of designing a system that can learn automatically without human intervention

- Deep learning (DL) is a specialized sub-field of ML that uses multiple processing layers to progressively extract higher-level features from raw input presented in the form of large datasets

Definitions

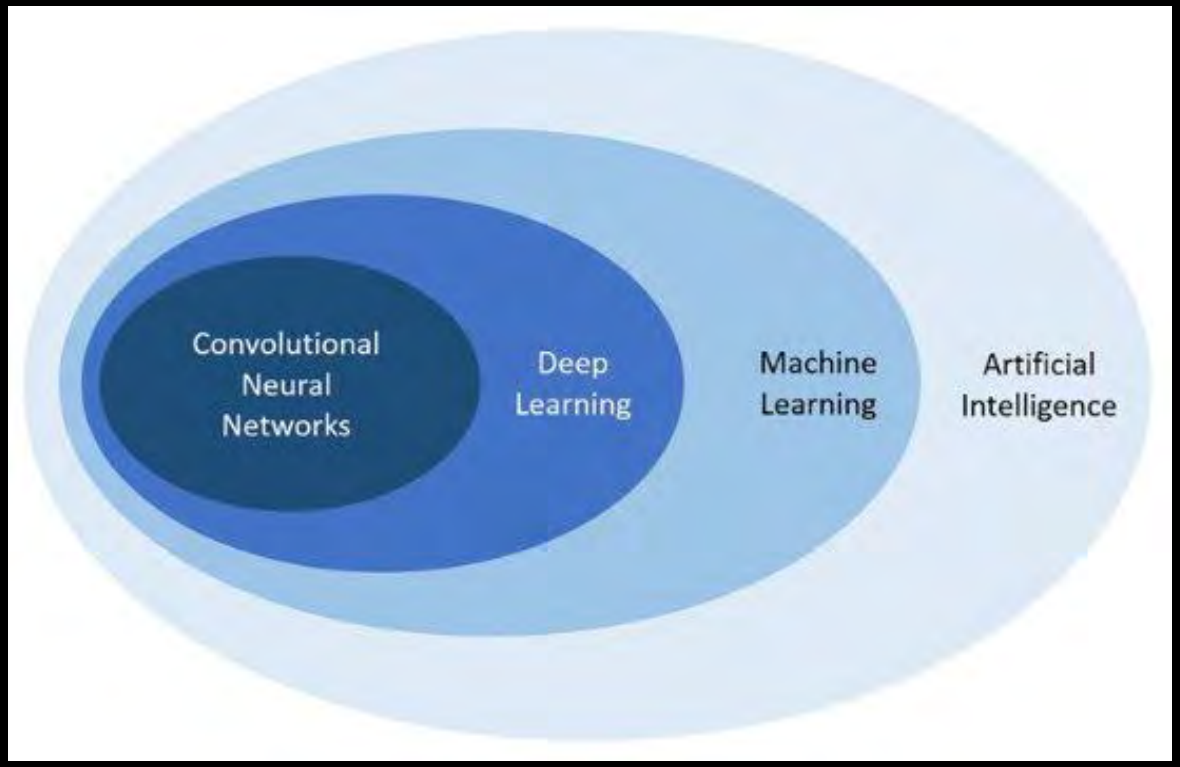

From Debs and Fayad. *Frontiers in Radiology* 2023.

AI & ML in Radiology

- Development of AI models requires training on large datasets with high-quality images and annotations

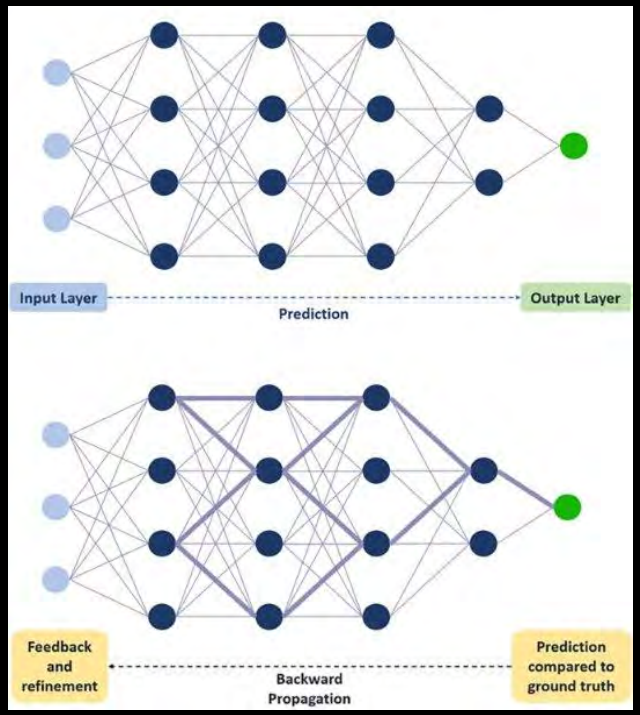

From Debs and Fayad. *Frontiers in Radiology* 2023.

Radiomics

- Radiomics: “Use of advanced mathematical analysis and AI to perform high-throughput extraction of quantitative features from images, creating a large dataset that is subjected to data mining for potentially improved decision support” --> can discern features that are not visible to the human eye

- Examples:
  - Identify tumor characteristics that correlate with how the tumor will respond to treatment and the patient’s likelihood of survival
  - Create computational models to help with personalized diagnosis and treatment
  - Detect subtle signs of drug efficacy and safety
  - Identify patients likely to respond to a particular treatment

Radiomics

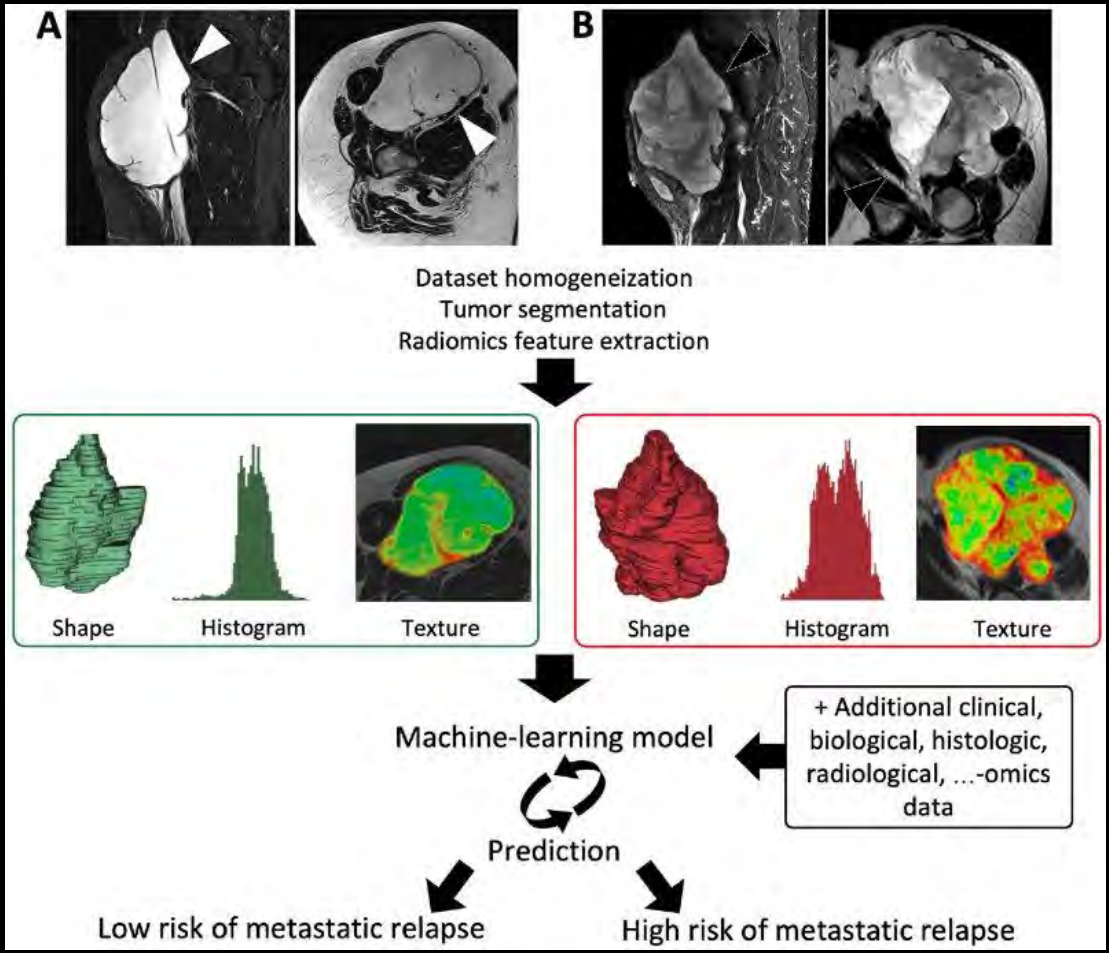

From Crombe *et al. Acad Radiol* 2023; 30(2): P322-340. (skewness and kurtosis)

AI/ML in Gaucher Disease

1. Identify fracture and osteonecrosis on XR/MR
   - Determine acuity on XR

2. Segment bone from soft tissue on MRI

3. Within bone, segment and quantify bone lesions and osteonecrosis from background bone marrow on MRI
   - Determine risk of collapse

4. Analyze dark marrow content in background bone marrow

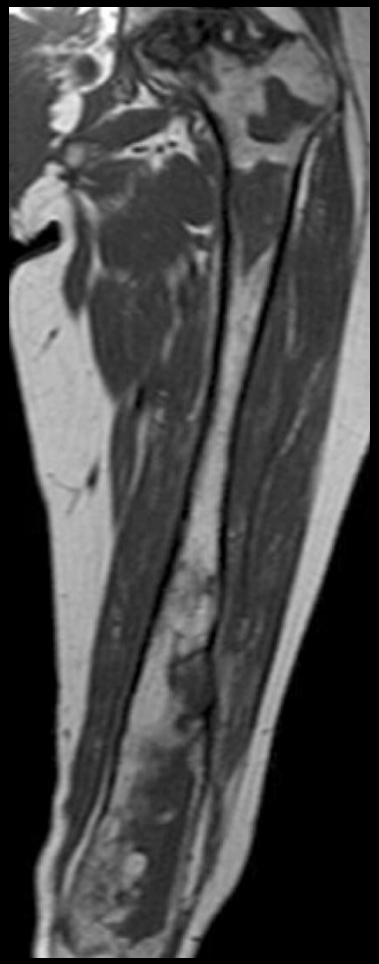

Detection by AI: Fracture (XR)

Many AI algorithms are available for fracture detection, including some in routine clinical use

X-Ray vs MRI: Fracture

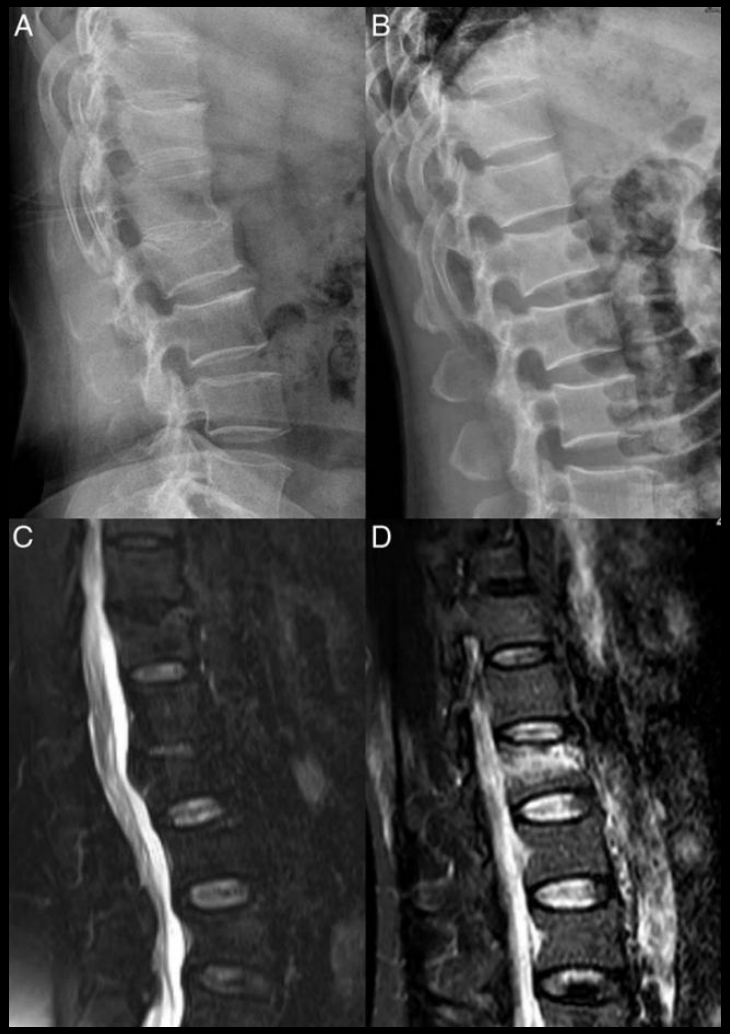

From Li *et al.*, *Spine* 2024; 50(16): E330-E335.

XR DL Prediction Fracture Acuity

(Radiomics)

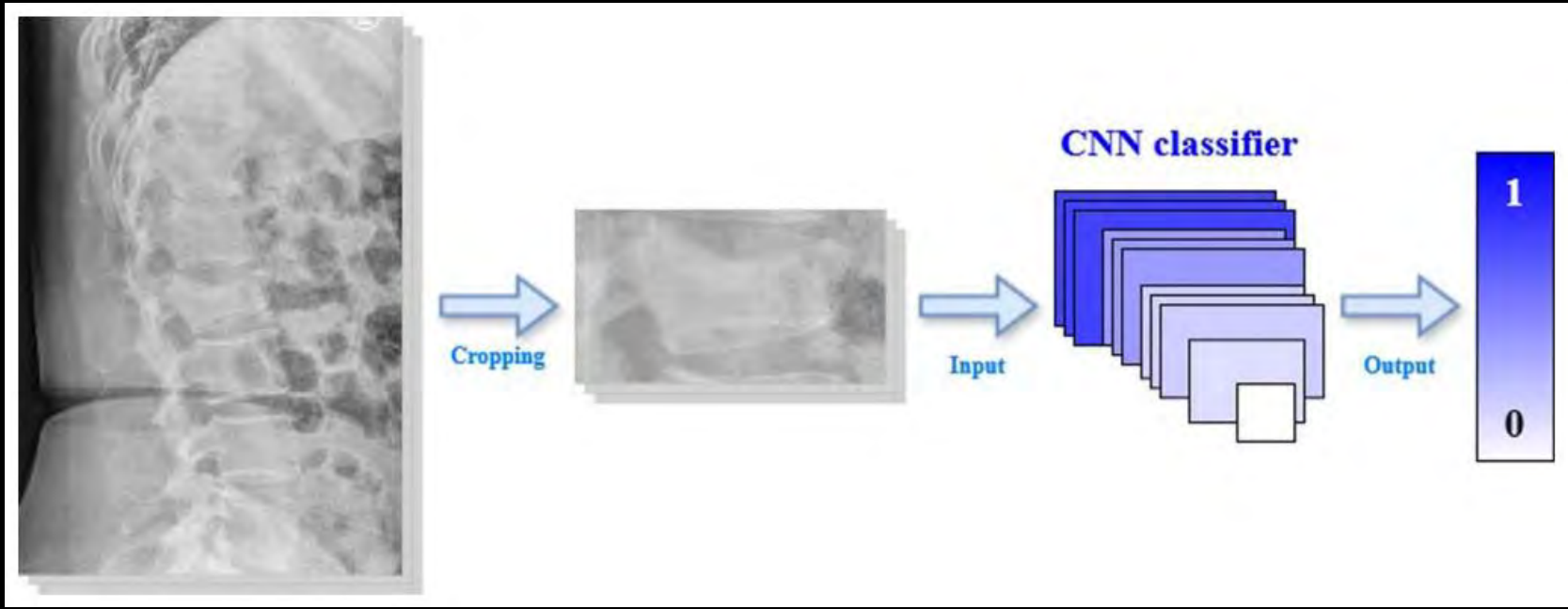

From Li *et al.*, *Spine* 2024; 50(16): E330-E335.

XR DL Prediction Fracture Acuity

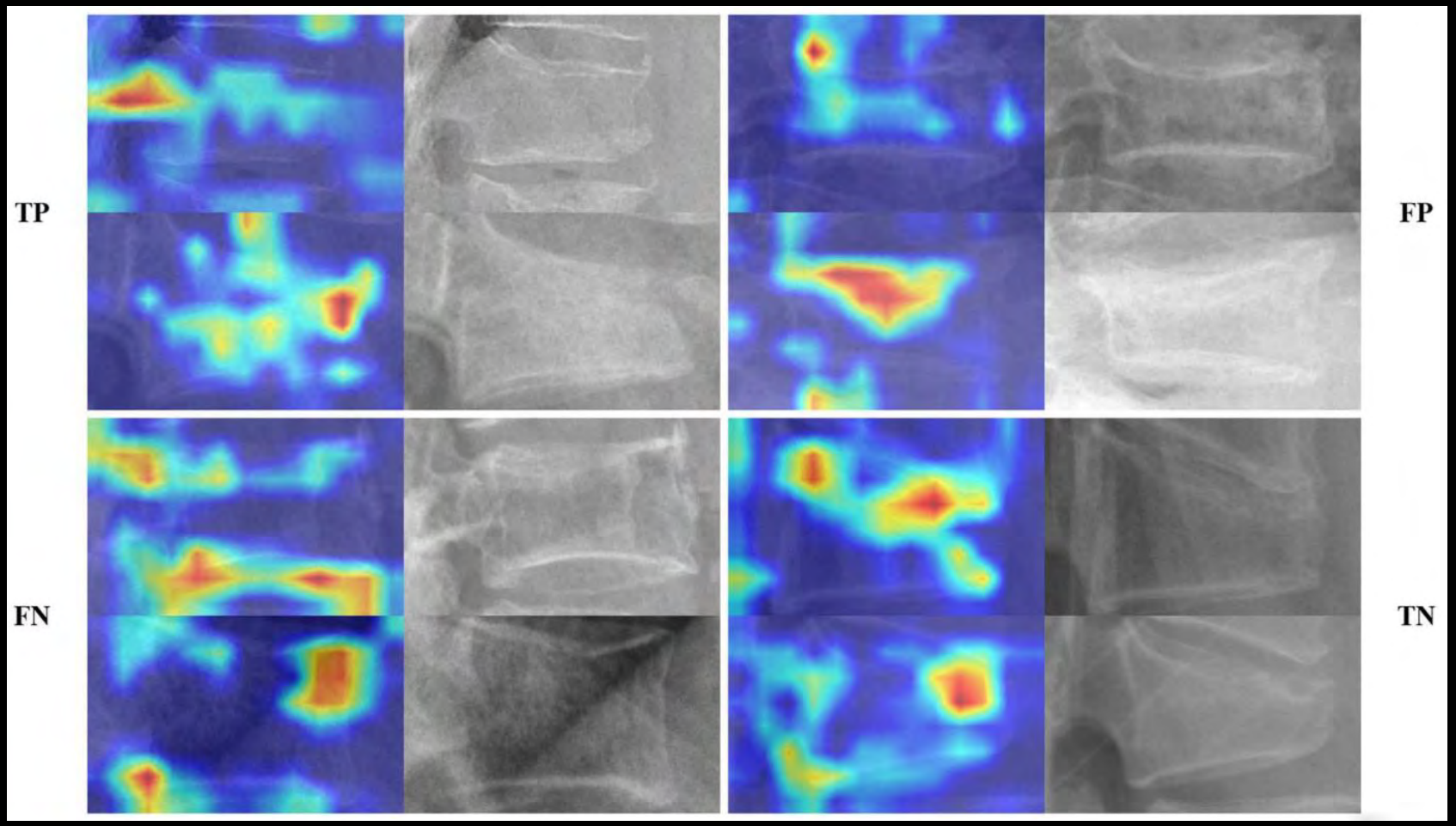

From Li *et al.*, *Spine* 2024; 50(16): E330-E335.

XR DL Prediction Fracture Acuity

TABLE 1. The Performance of Testers in the Validation and Control Set

Data Set	Testers	Accuracy (%)	Sensitivity (%)	Specificity (%)	F1 Score (%)	Precision (%)
Validation set	DL Version 1	83.0	87.3	64.9	88.5	87.3
	DL Version 2	82.4	91.7	57.3	88.3	85.2
	DL Version 3	82.2	93.2	52.7	88.4	84.1
Control Set	DL Version 1	78.1	85.2	64.8	83.5	81.9
	DL Version 2	78.1	91.1	53.7	84.4	78.6
	DL Version 3	80.7	91.1	61.1	86.0	81.4
	Junior spine surgeon	68.4	64.8	68.3	70.9	78.4
	Senior spine surgeon	74.2	83.3	69.3	80.8	88.6

- Machine learning model has performance similar to or exceeding that of an experienced specialist surgeon
- Even better performance may be possible when used as an auxiliary tool by radiologists (Chen *et al.*, *Eur Radiol* 2022; 32(3): 1496-1505)
- Limited by image quality and artifacts
- Provides results without demonstration of specific prognostic features identified by the model

From Li *et al.*, *Spine* 2024; 50(16): E330-E335.

Detection by AI:
Osteonecrosis (XR & MR)

Osteonecrosis Classification (FICAT)

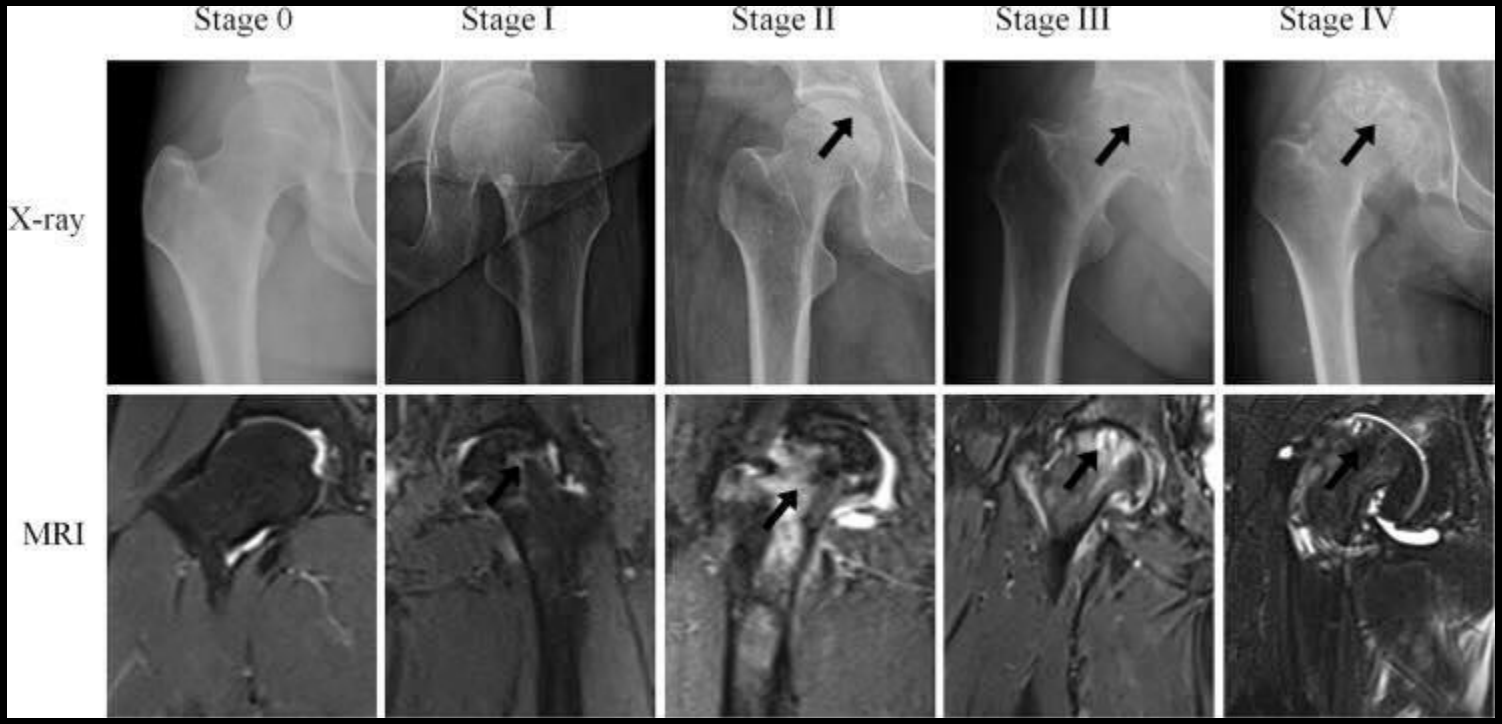

From *Radiology Archive*, 21 June 2020.

XR DL Detection of Osteonecrosis

Table 2 Diagnostic performance of Deep Learning (DL) algorithms for avascular necrosis of femoral head (AVNFH) in digital radiography

Performance Measure	SVM[1] (Comparison of stage 0 with stage 2)	SVM[1] (Comparison of stage 0 with other stages)	ANFIS[2] (Comparison of stage 0 with other stages)
AUC* (95% CI)	73.58% (62.30–83.19%)	82.88% (74.21–88.13%)	86.60% (77.80–93%)
Sensitivity	50.00% (32.43–67.57%)	67.65% (55.21–78.49%)	77.05% (64.50–86.85%)
Specificity	97.17% (91.95–99.41%)	98.11% (93.35–99.77%)	96.46% (91.18–99.03%)
PPV**	85.00% (63.87–94.78%)	95.83% (85.23–98.92%)	92.16% (81.63–96.88%)
NPV***	85.83% (81.21–89.47%)	82.54% (77.01–86.97%)	88.62% (83.08–92.51%)
Accuracy	85.71% (78.80–91.05%)	86.21% (80.18–90.96%)	89.66% (84.14–93.75%)

Note—Data in parentheses are 95% Confidence intervals

1: Support vector machine, 2: Adaptive Neuro-Fuzzy Inference System

* : Area under the curve, **: Positive Predictive Value, ***: Negative Predictive Value

From Rakhshankhah *et al.*, *BMC Musculoskel Disorders* 2024; 25: 547.

XR DL Detection of Osteonecrosis

Table 4 Comparison of SVM algorithm to radiologists

	SVM[1] algorithm	Less Experienced [A]	Experienced [B]
AVNFH detection (stage 0 from other stages) AUC * (%95 CI)	82.88%	79.68%	88.4%
p-value **		0.53	0.10
PRE-COLLAPSE AVNFH detection (stage 0 from stage 2) AUC * (%95 CI)	73.58%	60.70%	73.33%
p-value		< 0.001***	0.30

A: second-year radiology resident, B: 10-year experienced radiologist

1: Support vector machine

DeLong's test p-values on AUC between SVM and radiologists

*: Area under the curve, **: p-value of the comparison of each reader to SVM; ***: statistically significant value

Table 5 Comparison of ANFIS algorithm to radiologists

	ANFIS1 algorithm	Less Experienced A	Experienced B
AVNFH detection (stage 0 from other stages) AUC* (%95 CI)	86.60%	79.68%	88.40%
p-value**		0.04***	0.2

A: second-year radiology resident, B: 10-year experienced radiologist

1: Adaptive Neuro-Fuzzy Inference System

DeLong's test p-values on AUC between ANFIS and radiologists

*: Area under the curve, **: p-value of the comparison of each reader to ANFIS; ***: statistically significant value

From Rakhshankhah *et al.*, *BMC Musculoskel Disorders* 2024; 25: 547.

MR DL Detection of Osteonecrosis

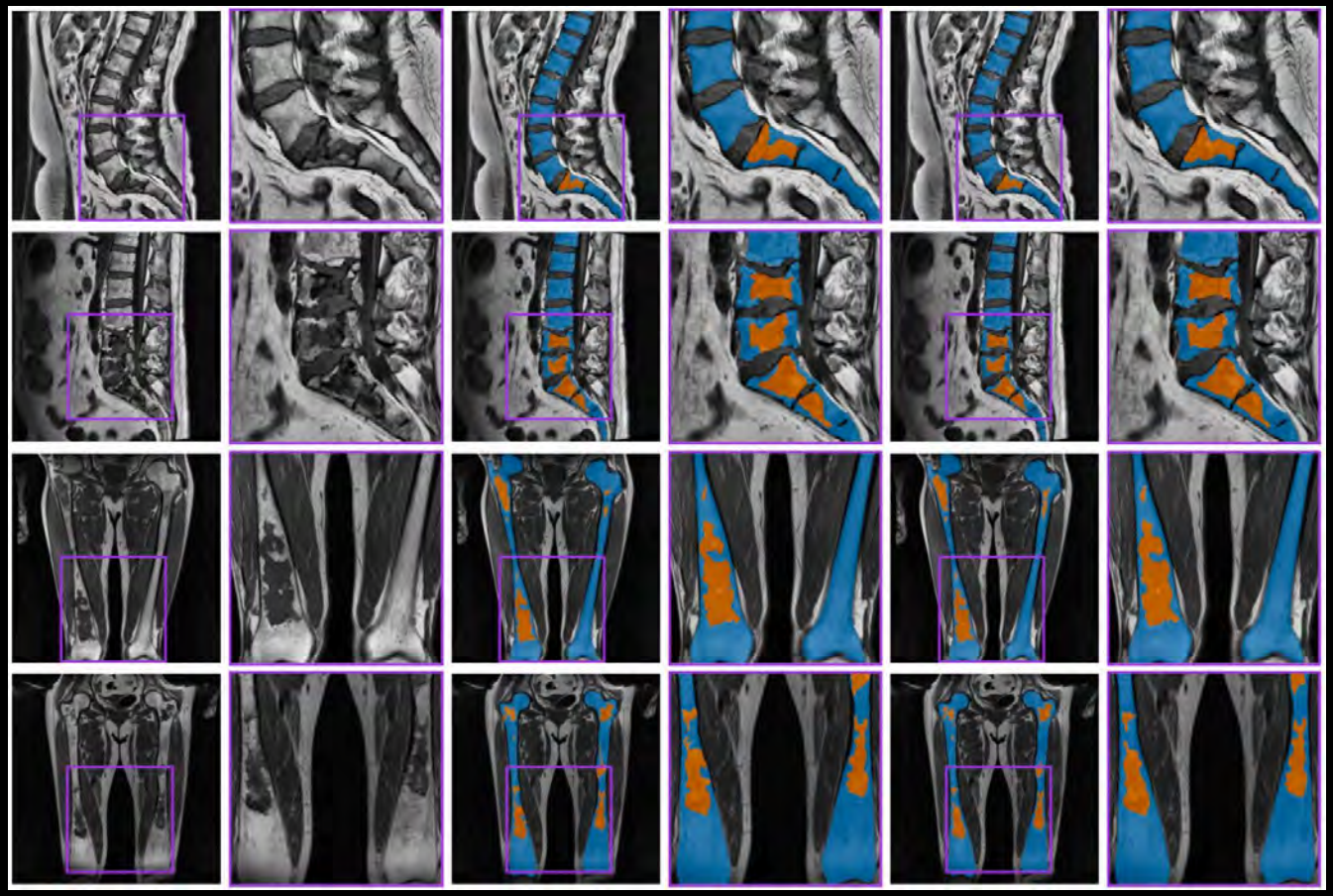

orange = osteonecrosis, blue = bone marrow unaffected by osteonecrosis

From Yu *et al*. *Bone* 2024; 186: 1-11.

MR DL Detection of Osteonecrosis

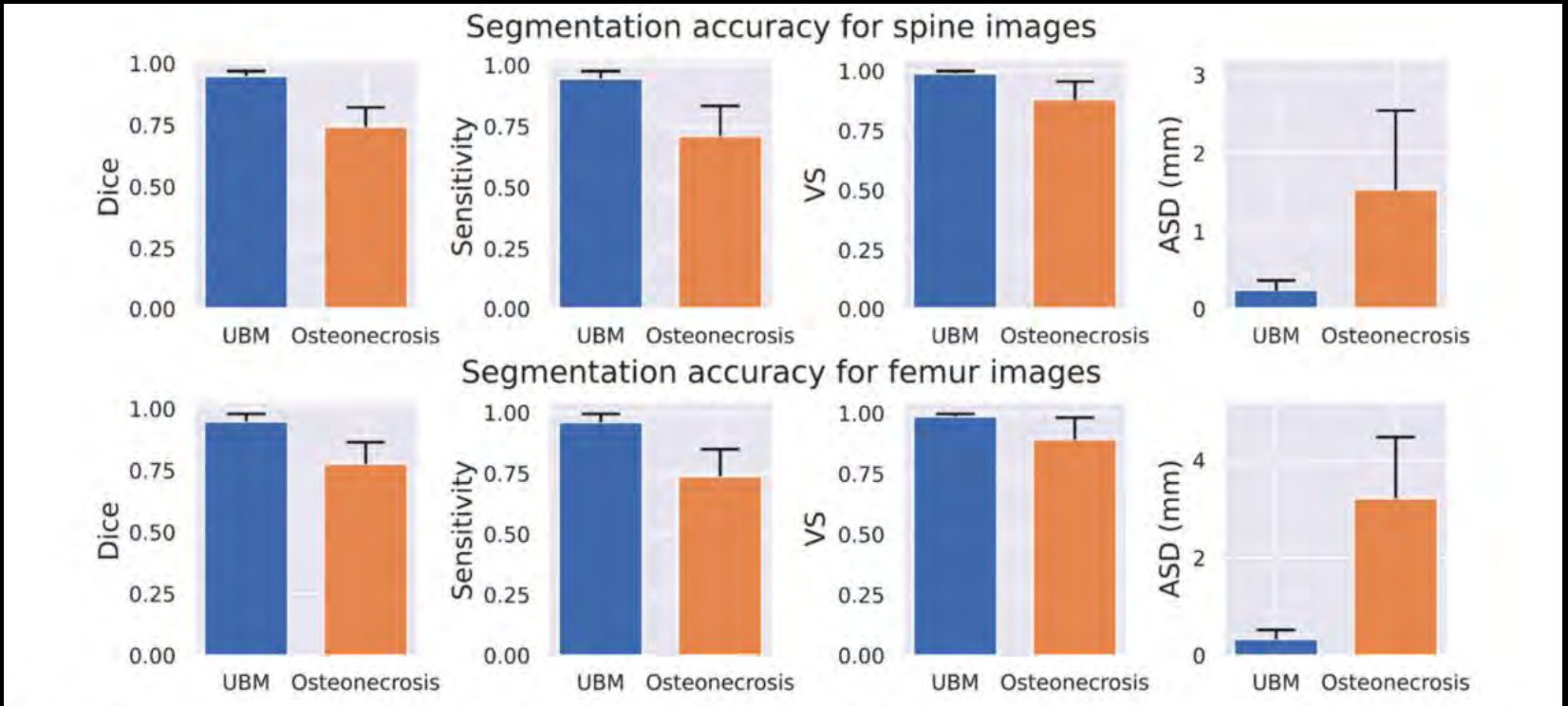

Fig. 5. Evaluation parameters showing the segmentation accuracy for spine and femur T1w images in the test datasets. The bar charts show the mean and the error bars represent the standard deviation. From left to right: Dice coefficient; Sensitivity; Volume similarity; Average surface distance.

Model accurately segments osteonecrosis from background bone marrow in spine and femur

From Yu *et al*. *Bone* 2024; 186: 1-11.

MR DL Risk of Femoral Collapse

(Radiomics)

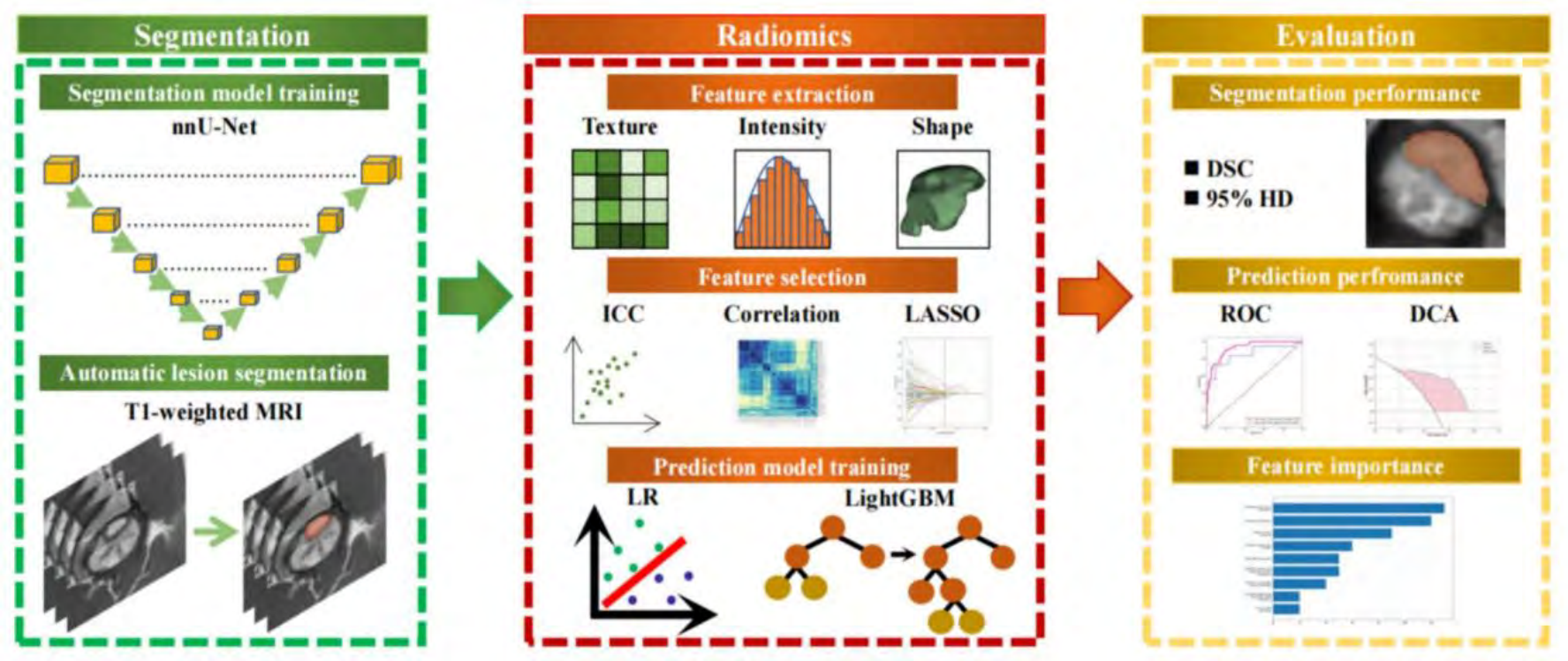

From Gao *et al.*, *BMC Med Inform Dec Making* 2024; 24: 430.

MR DL Risk of Femoral Collapse

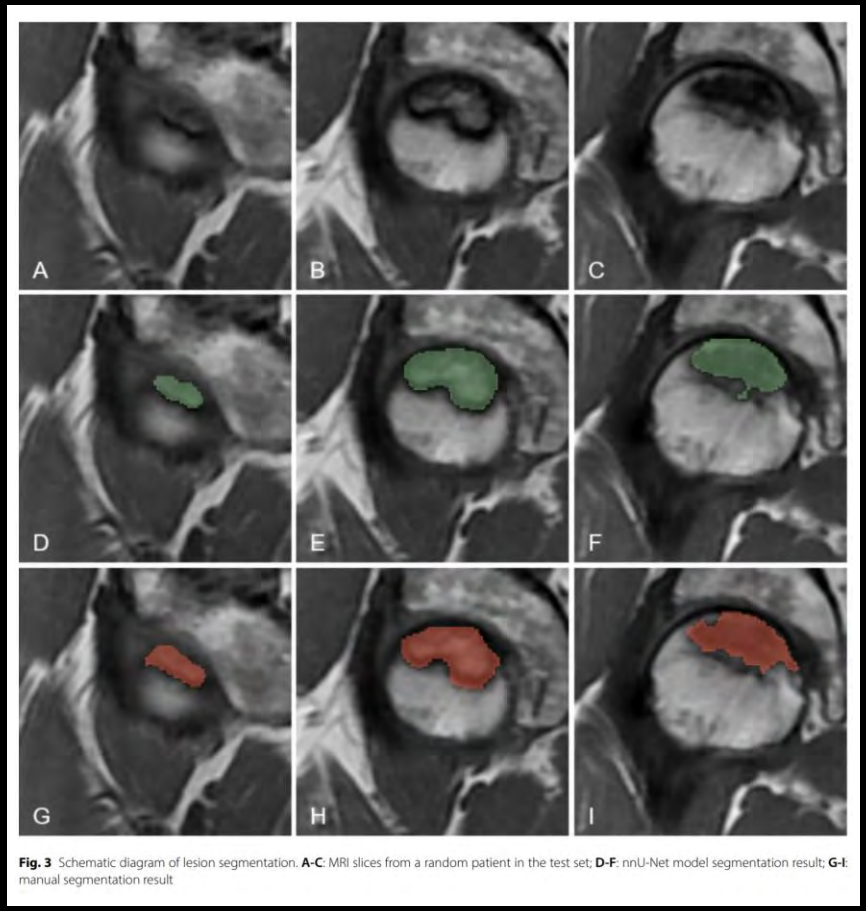

Fig. 3 Schematic diagram of lesion segmentation. **A-C**: MRI slices from a random patient in the test set; **D-F**: nnU-Net model segmentation result; **G-I**: manual segmentation result

DL vs manual segmentation

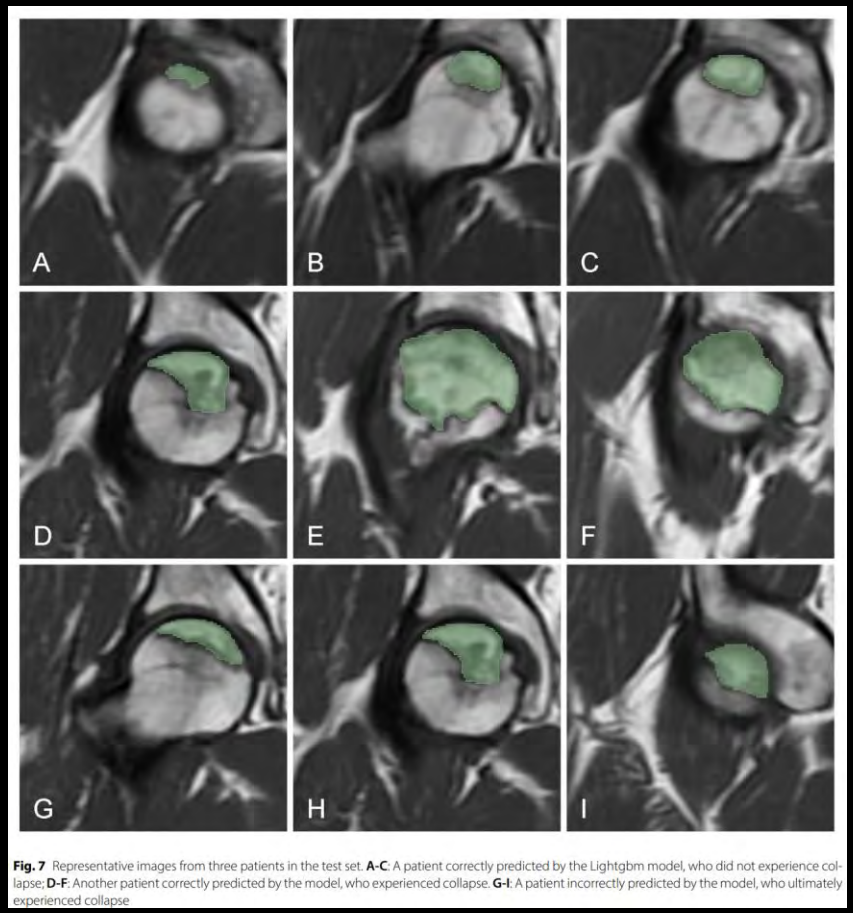

Fig. 7 Representative images from three patients in the test set. **A-C**: A patient correctly predicted by the Lightgbm model, who did not experience collapse; **D-F**: Another patient correctly predicted by the model, who experienced collapse. **G-I**: A patient incorrectly predicted by the model, who ultimately experienced collapse

True negative, true positive, false negative

From Gao *et al.*, *BMC Med Inform Dec Making* 2024; 24: 430.

MR DL Risk of Femoral Collapse

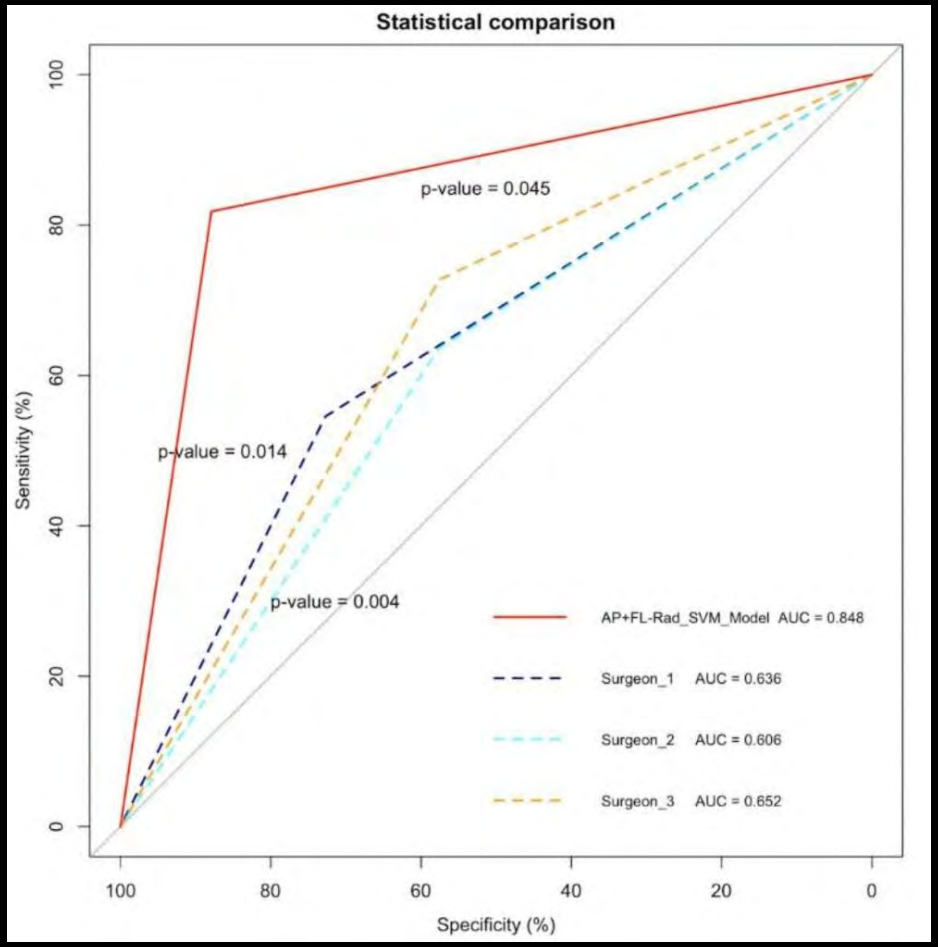

From Gao *et al.*, *BMC Med Inform Dec Making* 2024; 24: 430.

MR DL Risk of Femoral Collapse

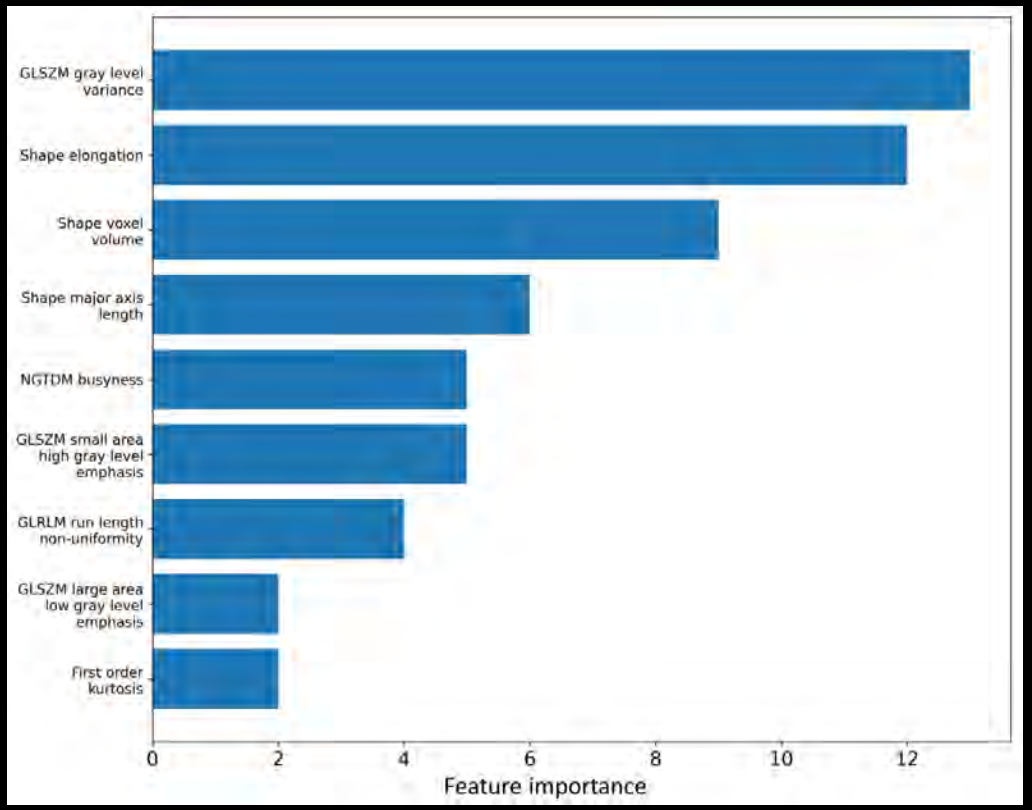

Radiomics features identified by DL: shaped-based, intensity, texture
GLSZM = grey level size zone matrix, GLRLM = grey level run length matrix,
NGTDM = neighboring grey tone difference matrix

From Gao *et al.*, *BMC Med Inform Dec Making* 2024; 24: 430.

Detection by AI:
Bone Lesions (XR & MR)

XR DL Detection of Bone Lesions

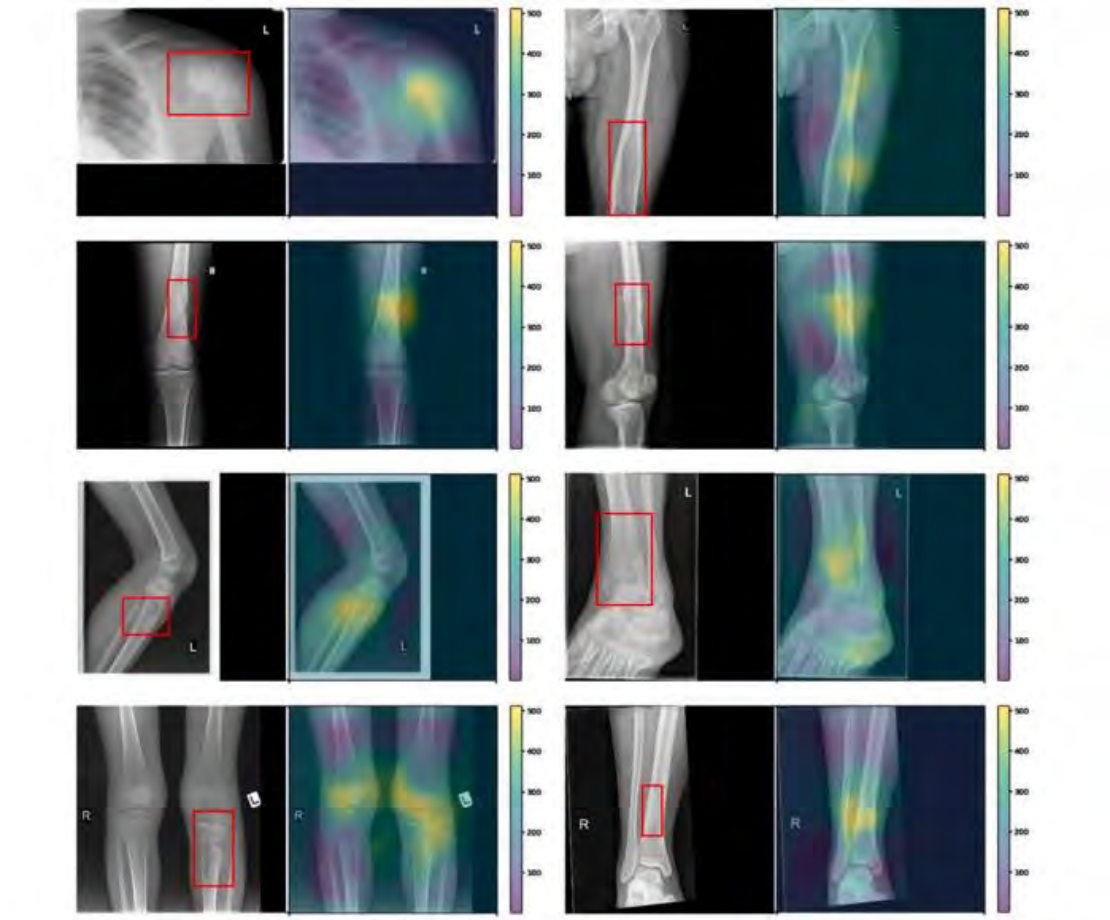

Figure 5 Representative attention map results for True Positive images from the test set, demonstrating abnormal cases correctly classified as abnormal. The color bar on the right side indicates regions of high model attention associated with abnormality. On the original image, the red rectangle represents the actual tumor.

From Rinott *et al.*, *Clin Radiol* 2025; 90: 107075.

XR DL Detection of Bone Lesions

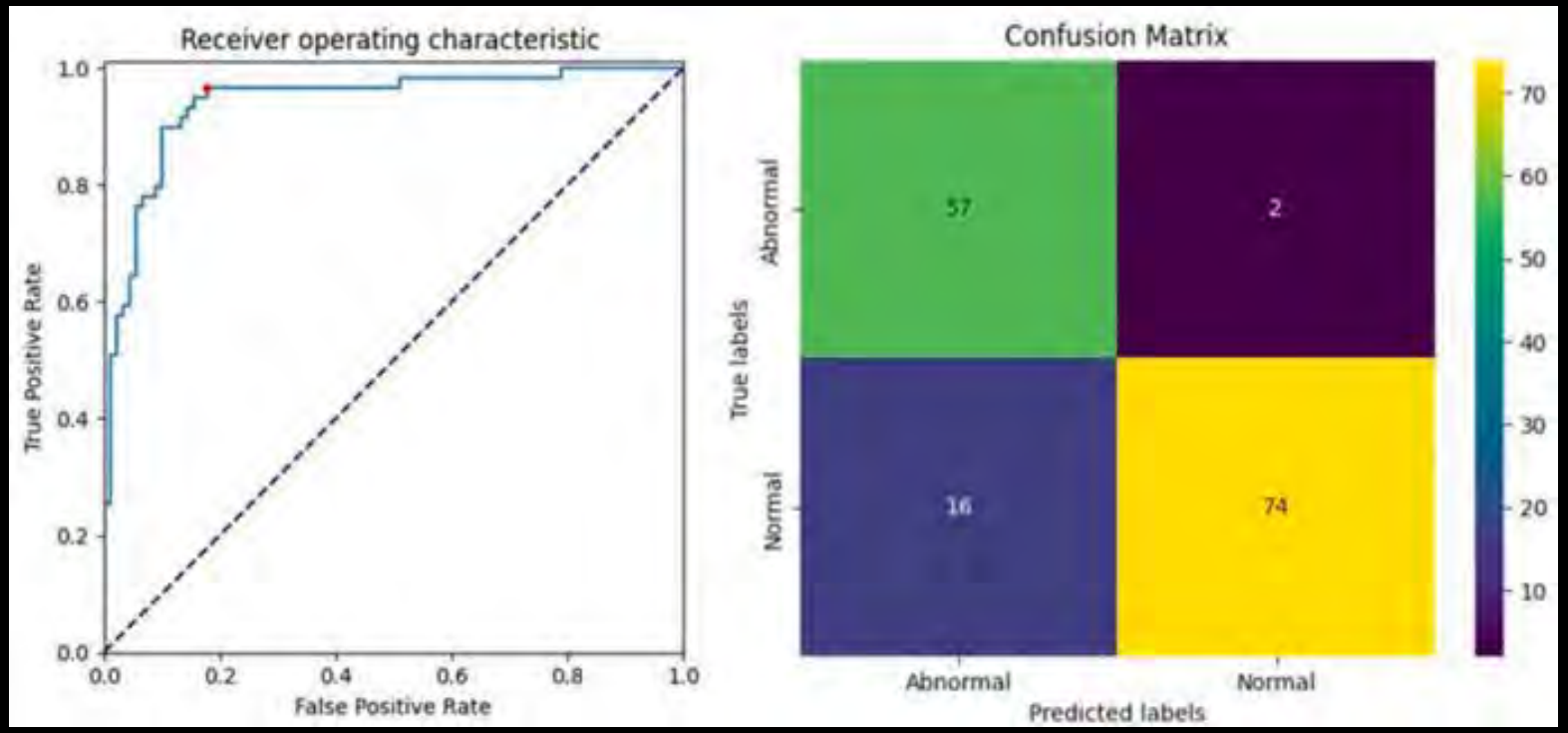

From Rinott *et al.*, *Clin Radiol* 2025; 90: 107075.

MR DL Detection of Bone Lesions

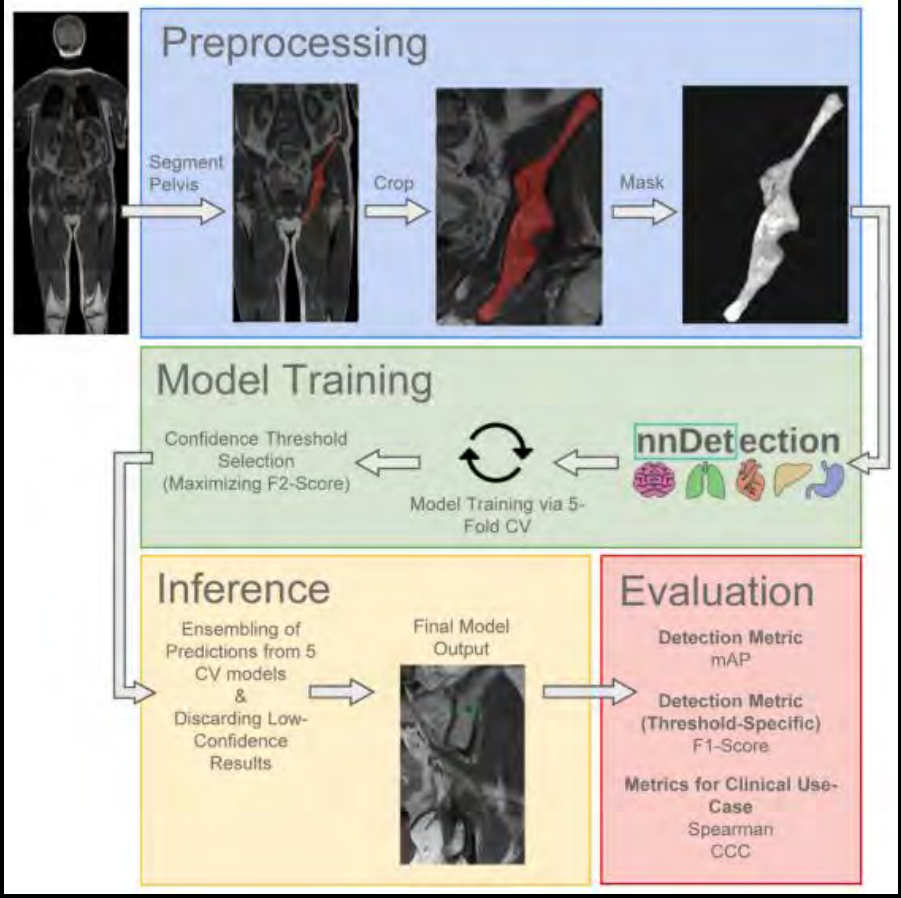

Detection of bone lesions in myeloma

From Wennmann *et al.*, *Acad Radiol* 2025; 32: 6012-6026.

MR DL Detection of Bone Lesions

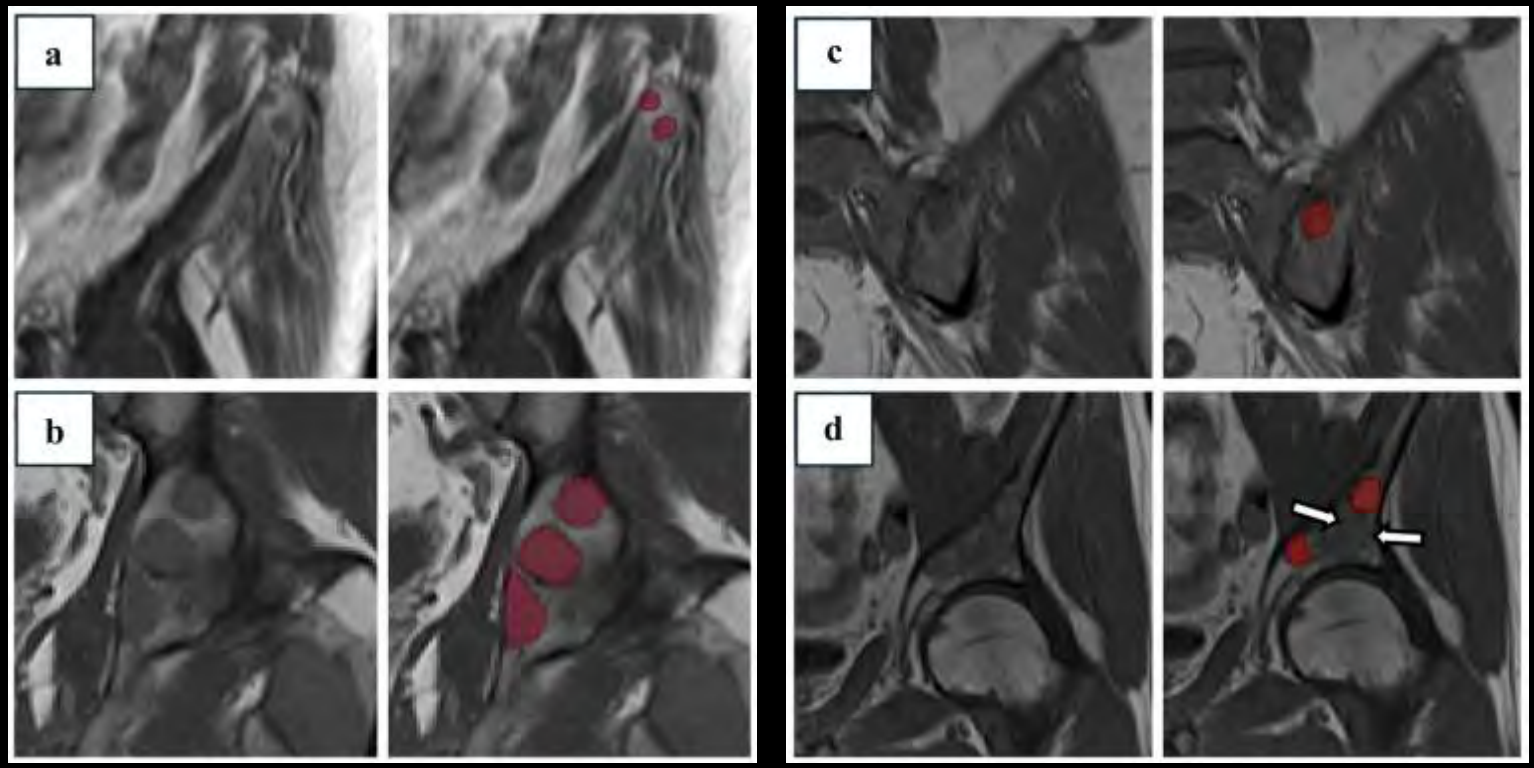

From Wennmann *et al.*, *Acad Radiol* 2025; 32: 6012-6026.

MR DL Detection of Bone Lesions

TABLE 2. Performance of the Detection Algorithm on Object Level

	Internal Test Set	External Multicentric Test Set	Subsets of External Multicentric Test Set		
			Subset 1	Subset 2	Subset 3
Algorithm					
mean average precision (mAP)	0.44 [0.27,0.59]	0.34 [0.25,0.45]	0.45 [0.26,0.65]	0.21 [0.07,0.37]	0.41 [0.29,0.66]
F1-Score	0.54 [0.30, 0.64]	0.44 [0.33, 0.53]	0.50 [0.28, 0.66]	0.30 [0.13, 0.46]	0.53 [0.38, 0.68]
sensitivity = recall	0.49 [0.34, 0.63]	0.34 [0.25, 0.45]	0.44 [0.23, 0.65]	0.21 [0.09, 0.34]	0.43 [0.30, 0.65]
positive predictive value = precision	0.61 [0.29, 0.74]	0.61 [0.46, 0.74]	0.60 [0.33, 0.78]	0.52 [0.21, 0.79]	0.71 [0.44, 0.86]
Interrater experiment					
F1-Score	/	0.58 [0.50, 0.65]	0.50 [0.38, 0.60]	0.58 [0.42, 0.70]	0.65 [0.52, 0.70]
sensitivity = recall	/	0.72 [0.61, 0.80]	0.56 [0.34, 0.53]	0.78 [0.59, 0.89]	0.78 [0.61, 0.85]
positive predictive value = precision	/	0.49 [0.41, 0.57]	0.45 [0.34, 0.53]	0.45 [0.30, 0.63]	0.55 [0.42, 0.62]

Reader 1 is considered the reference in comparison with the algorithm, and in comparison with rater 2 for the interrater experiment

From Wennmann *et al.*, *Acad Radiol* 2025; 32: 6012-6026.

Detection by AI:
Dark Marrow/Fat Fraction (MR)

MR DL Fat Fraction

- DL tool for high-throughput bone marrow fat fraction analysis
- Used dataset of 729 patients from UK Biobank
- Developed new lightweight attention-based U-Net model for segmentation
- Determined fat fraction using in- and out-of-phase images and measuring voxel intensity in areas of interest (based on different resonance frequencies of hydrogen atoms bound to fat and water)

From Morris *et al.*, *Comp Struct Biotech J* 2024; 24: 89-104.

MR DL Fat Fraction

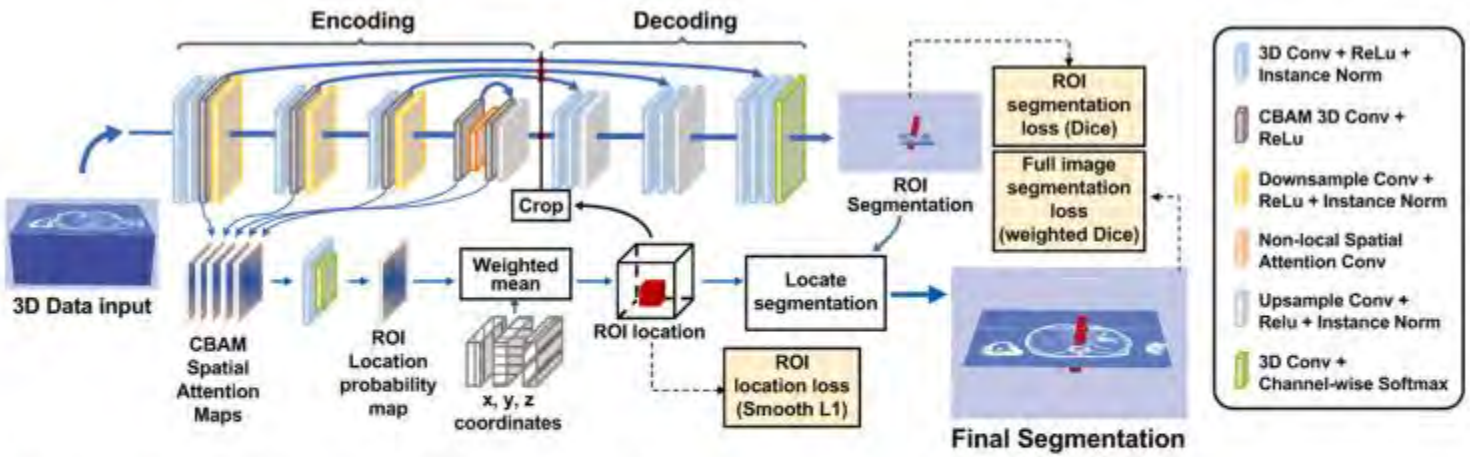

Fig. 2. Architecture of our CBAM Attention ROI U-Net for segmenting small structures from large 3D data. Each convolutional block in the U-Net encoding subnetwork (or contracting path) includes one or two CBAM (convolutional block attention module) layers. A fixed-size single channel spatial attention map is generated by each CBAM layer through 1X1X1 convolutions and trilinear interpolation. These attention maps are then combined to produce a probability map of object location with which a ROI is defined. The encoded features of all resolution-levels are then cropped to the ROI and input into the decoder which produces the segmentation results within the detected ROI. A non-local spatial attention layer is inserted in the final block to generate globally sensitive features. The final segmentation results are then generated by implanting the ROI back into the whole data volume.

From Morris *et al.*, *Comp Struct Biotech J* 2024; 24: 89-104.

MR DL Fat Fraction

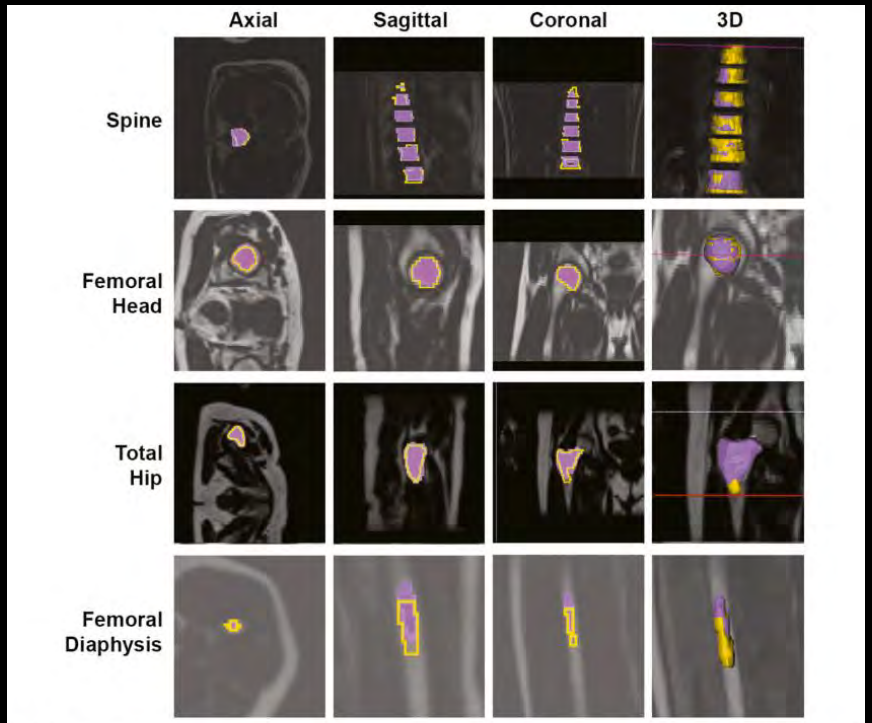

Fig. 3. Visual comparison of manual vs deep learning segmentations. Deep learning segmentation results (purple) are displayed on top of the ground-truth (manual) segmentations (yellow). Representative images from the axial, coronal and sagittal plane are shown, along with a 3D rendering. Note that the Total Hip includes the intertrochanteric region.

Segmentation Accuracy (dice scores) of the traditional U-Net and our CBAM-ROI-attention U-Net.

	Spine	Femoral head	Total Hip	Femoral Diaphysis
U-Net	0.925	0.951	0.904	0.69
ROI-Attention-U-Net	0.912	0.945	0.912	0.866

From Morris *et al.*, *Comp Struct Biotech J* 2024; 24: 89-104.

MR DL Fat Fraction

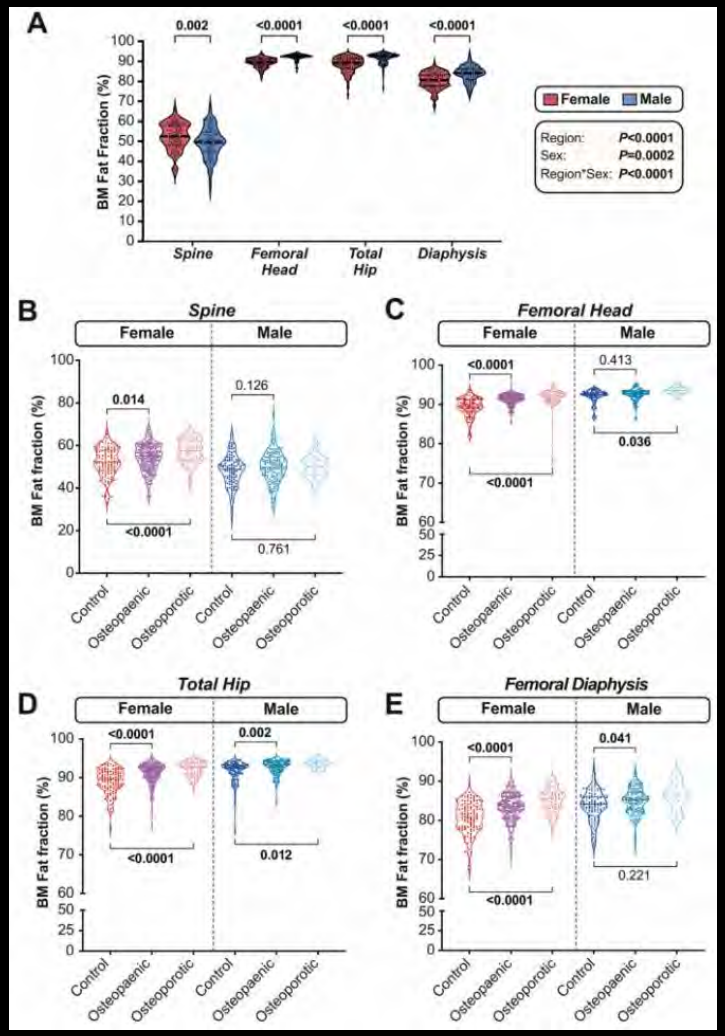

From Morris *et al.*, *Comp Struct Biotech J* 2024; 24: 89-104.

AI in Gaucher XR/MR

- Combined applications of DL to segment osteonecrosis and bone lesions from remaining bone, then determine fat fraction of background bone marrow

- This is potentially useful in clinical application:
  - Isolation of background dark marrow (most susceptible to treatment effect) from potentially irreversible bone lesions
  - Ability to quantify dark marrow in specific portions of bone (e.g. in the whole femur or in parts of the hip/femur)
  - Allows for more standardized assessment of MRI images and more useful quantitative analysis
  - Quantification of size of osteonecrosis and bone lesions to determine focal structural weakness of bone and risk of insufficiency or pathologic fracture

Summary

- Bone disease is present in most patients with Gaucher disease, with dark marrow, fractures, osteonecrosis, and bone lesions that can be seen on imaging including x-ray and MRI.

- AI/ML is a useful tool for assessing x-ray and MRI images in Gaucher disease, allowing segmentation of these imaging features, which can aid in interpretation, quantify severity of disease, and assess for more minute changes in disease severity or response to therapy.

- Radiomics offers the potential to characterize disease features by 'looking beyond' the images themselves.

Assessment of Bone Involvement in Gaucher Disease Using Advanced Imaging & AI

Ravi S. Kamath, MD, PhD
Fairfax Radiological Consultants & Inova Health System
University of Virginia School of Medicine
Fairfax, Virginia, USA

FAIRFAX RADIOLOGY CENTERS

INOVA®

UNIVERSITY of VIRGINIA